Editing Hematopoietic Stem Cells for HIV Treatment

Jack Michele Pietro Castelli

A dissertation

submitted in partial fulfillment of the

requirements for the degree of

Doctor of Philosophy

University of Washington

2025

Reading Committee:

Jennifer E. Adair, Chair

Rachel A. Bender Ignacio

Jay Shendure

Program Authorized to Offer Degree:

Molecular Medicine and Mechanisms of Disease

University of Washington

Abstract

Editing Hematopoietic Stem Cells for HIV Treatment

Jack Michele Pietro Castelli

Chair of the Supervisory Committee:

Jennifer E. Adair

Department of Laboratory Medicine and Pathology

Advances in genome editing technologies have opened the door to one-time treatments for previously incurable, chronic diseases. This has accelerated interest in delivering gene therapies and other biologic drugs with durable therapeutic effects. Hematopoietic stem and progenitor cells (HSPC) are a promising target for gene therapy as they provide a steady supply of cells throughout the body over long periods of time. In this dissertation, I explore the use of CRISPR/Cas systems in HSPC to achieve site-specific gene knock-in and to produce antibodies against HIV *in vivo*. The editing approach described here has been optimized to target the endogenous locus for antibody expression in primates and does not rely on viral vectors. Following transplantation in an animal model, edited HSPC are capable of self-renewal and development into mature hematopoietic cell types. Anti-HIV antibodies are detected in these animals, demonstrating productive knock-in of our gene encoding DNA template. These findings are a proof-of-concept for non-viral HSPC gene editing as a platform for durable biologics production in the treatment of chronic diseases.

Contents

Chapter 1: Gene Therapy in HIV Research

Gene Therapy

Gene therapy has undergone remarkable evolution since the first patient was treated nearly 35 years ago.[1] This initial attempt marked the beginning of a field seeking to harness genetic interventions for the treatment of human disease. Since then, numerous gene therapies have been developed and entered the clinic for a variety of different diseases.[2] In fact, the fraction of active clinical trials in the United States incorporating gene therapy has steadily risen over this period of time, reflecting growing scientific confidence in its potential to address previously untreatable conditions.[3]

Gene therapies have historically targeted disorders with known mechanisms, typically monogenic (i.e. Mendelian) diseases.[4] Early efforts focused on diseases such as adenosine deaminase (ADA) deficiency and X-linked severe combined immunodeficiency (SCID-X1), where a single gene encoding an enzyme or part of a cytokine receptor is deficient and addition of a wildtype gene sequence confers a natural selective advantage in cells.[5] The Online Mendelian Inheritance in Man (OMIM) database lists 4,608 genes implicated in Mendelian diseases, highlighting the vast potential for gene therapy to treat genetic conditions.[6]

Researchers have repurposed and engineered various viral particles—such as retroviruses, lentiviruses, and adeno-associated viruses (AAV)—as delivery vehicles for functional copies of genetic elements conferring therapeutic value.[7] Gene therapies leveraging these vectors aimed to achieve long-lasting expression of the therapeutic genetic element, ideally through a one-time administration. Some were successful and approved by the United States Food and Drug Administration (FDA), some were rejected by the FDA or withdrawn from the market for safety concerns, and many more failed to achieve desired therapeutic effects.[8] Gene therapies have also recently demonstrated an “economic valley of death”, wherein therapies receiving biologics licensing authorizations have been withdrawn post-approval owing to inability to manufacture cost

effectively combined with small patient populations.[9] These challenges underscore the need for continued innovation in gene therapy design and delivery.

As our understanding of disease mechanisms has deepened, so too has the scope of gene therapy applications. Initially focused on Mendelian diseases, the field has expanded to address conditions with complex etiologies.[4] Diseases caused by somatic mutations, such as cancer, have been treated using gene therapies delivering tumor suppressors or chimeric antigen receptors (CAR), among other approaches.[10,11] Chronic diseases, such as cardiovascular disease or arthritis, have been treated using gene therapies delivering growth factors and cytokines—to varying degrees of success.[12,13] Even Mendelian diseases for which the causative mutations cannot be fixed by simply delivering a functional copy of the gene, such as amyotrophic lateral sclerosis, or where the defective gene is too large for conventional viral delivery, such as different forms of muscular dystrophy, are being treated using clever workarounds enabled by the development of genome editing tools.[14,15]

Genome Editing Tools

Since the first generation of genome editors including zinc finger nucleases (ZFN) and transcription activator-like effector nucleases (TALEN), gene therapy has aimed to deliver tools capable of precisely modifying the genome.[16] The repurposing of clustered regularly interspaced short palindromic repeats (CRISPR) and CRISPR-associated proteins (Cas) for gene editing in 2012 transformed the field, enabling interventions for a broad range of diseases.[17,18] Subsequent advancements including base editing, prime editing, and prime-editing-assisted site-specific integrase gene editing (PASSIGE), have further diversified this toolkit.[19] Together, these tools have enabled researchers to reach unparalleled levels of genomic engineering efficiency and precision

and enabled advance of these strategies to the clinic with the first CRISPR-based gene therapy (exagamglogene autotemcel) authorized by the FDA in 2023.[20]

Unlike viral vectors, which integrate genetic material at fixed or random sites if at all, genome editors enable precise changes to be introduced at specific genomic loci.[7,21] This avoids risks associated with unintended insertions, such as oncogenic changes from tumor suppressor inactivation, or proximity-induced activation of oncogenes.[22] Additionally, gene editing introduces a new therapeutic strategy: disrupting gene function. Tools that create double-stranded breaks (DSB), such as CRISPR/Cas9, can knock-out disease-causing genes, an approach widely adopted in early clinical trials.[23,24] For transthyretin-mediated amyloidosis (ATTR), for example, *in vivo* delivery of CRISPR/Cas9 reduces the production of defective protein in the liver.[25] There is no shortage of targets for gene knock-out, with over 6,000 genes in the human genome known to tolerate loss-of-function mutations and an estimated 7,000 more for which impact remains unknown.[26]

However, gene disruption alone is not sufficient for many other diseases and conditions. Restoring gene function remains an important focus of gene therapy, whether by precise, nucleotide-level changes to DNA or by the insertion of large DNA sequences encoding entire genes (i.e. transgenes). To achieve this, engineered viruses have been used both to deliver genome editing tools and as DNA templates for transgene insertion.[27] Early approaches focused on genomic safe harbors—regions of the genome considered stable, functionally predictable and tolerant of large genomic changes.[28] This strategy has been validated in various cell types, demonstrating that insertion of new DNA occurs through a DNA repair pathway known as homology-directed repair (HDR).[29] By introducing a DSB at the target locus and providing homologous sequences within the viral template, it has been shown that transgenes can be knocked-in via HDR.[30] In addition, this approach holds promise for integrating genes at endogenous loci, allowing their expression to be regulated by native genomic elements, leading to physiologically relevant gene expression.

HSC Gene Therapy and Editing

Hematopoietic stem cells (HSC) are an attractive target for gene therapy due to their unique biological properties. As self-renewing cells capable of differentiating into different cell lineages, HSCs are responsible for maintaining hematopoiesis throughout life. Their ability to reconstitute the entire hematopoietic system following transplantation makes them an ideal target for treating blood disorders. Allogeneic HSC transplantation, in the absence of gene therapy, can be used to treat hemoglobinopathies, hematologic malignancies, immune deficiencies, and other inherited blood disorders, such as congenital cytopenia and metabolic diseases.[31] While advances in transplantation protocols have drastically improved outcomes, the procedure remains complex and high-risk, requiring donor matching, pre-transplantation conditioning with chemotherapy, radiotherapy, or immunotherapy, and persistent immune suppression to avoid transplant rejection and graft-versus-host disease (GVHD).[32]

Autologous HSC transplantation, in which a patient's own stem cells are collected, modified, and reinfused, offers a promising alternative by eliminating the risks associated with donor matching and immune rejection. Gene therapy can be used to correct disease-causing mutations within a patient's HSCs, allowing autologous transplantation to potentially treat many of the same conditions as allogeneic transplantation, without the need for immunosuppression.[33] The first clinical trial using genetically modified HSCs was conducted for the treatment of SCID.[34] Since then, various viral vectors have been developed to efficiently transduce HSCs and deliver therapeutic payloads.[35] Only integrating vectors provide durable therapeutic effects to this cell type, as transgene expression must persist through cell division and differentiation.[36] While this strategy has led to successful treatments, untargeted integration presents the risk of abnormal gene expression

and oncogenic mutations, as seen in early trials for SCID and another primary immunodeficiency called Wiskott-Aldrich syndrome wherein a subset of patients developed leukemia.[37,38]

The emergence of programmable nucleases has enabled targeted gene modification in HSCs, reducing the likelihood of unintended consequences. As a result, many groups have worked to apply CRISPR to genetically engineer HSC.[39-41] However, editing these cells presents unique challenges. Due to their largely quiescent nature, HSCs exhibit distinct DNA repair pathway preferences that influence editing outcomes.[42] HDR for instance, the pathway required for gene knock-in, is primarily active during S/G2 phases of the cell cycle, limiting its efficiency in quiescent (i.e. non-cycling) HSCs.[43,44] In contrast, non-homologous end joining (NHEJ) is active throughout the cell cycle and is the dominant repair mechanism in HSCs, making gene disruption more efficient than precise modifications or gene knock-in. As a result, early clinical trials have focused on gene knock-out strategies.[45] Beyond repair pathway limitations, tightly regulated levels of protein translation in HSCs hinder the expression of exogenous nucleases like Cas9, and the efficient delivery of nucleic acids remains a significant barrier.[46,47] Finally, HSCs display both intrinsic and extrinsic responses to pathogenic infection, meaning that both viral and bacterially-derived gene editing tools can impact HSC fitness.[48] Many groups have worked to optimize editing conditions, testing different delivery strategies to overcome these obstacles. Some approaches involve suppressing NHEJ or other DNA damage responses, while others focus on delivering Cas9 as a recombinant protein rather than as an mRNA or plasmid.[49-51] These refinements have improved editing efficiency, but challenges remain in achieving robust and consistent modifications across patient populations.

Despite these technical hurdles, exagamglogene autotemcel (Casgevy®), the first approved CRISPR-based gene therapy, is an autologous HSC therapy designed to treat sickle cell disease and beta-thalassemia by targeting regions of the genome relevant to activity of the B cell leukemia/lymphoma 11A gene (*BCL11A)*, a key regulator of fetal hemoglobin expression.[20] By

disrupting the *BCL11A* enhancer element, Casgevy® restores fetal hemoglobin production, effectively compensating for defective adult hemoglobin. Clinical trials have demonstrated that this approach leads to durable therapeutic effects, reducing disease symptoms and eliminating the need for frequent blood transfusions and other interventions.[52,53] However, accessibility remains a major concern. At $2.2 million USD per treatment, Casgevy®—alongside Lyfgenia, another HSC gene therapy for sickle cell disease priced at $3.1 million USD—are among the most expensive drugs ever developed. The high cost of these therapies poses serious challenges for widespread implementation, particularly for patient populations that are already medically underserved.[54] Nevertheless, the continued development of HSC gene therapies highlights their therapeutic potential and underscores the need for further innovation to improve accessibility and affordability. Of particular interest is simplification of the manufacturing process to streamline and scale the production of gene therapy products.[55]

Edited HSC in the Treatment of HIV

HSCs have also played a pivotal role in human immunodeficiency virus (HIV) cure-related research. To date, all confirmed cases of an eradicating cure—where replication-competent HIV is completely eliminated from the body—have been in individuals who received allogeneic HSC transplantations.[56] The nine confirmed cases arose in the context of transplantation for primary malignancies such as acute myeloid leukemia or Hodgkin's lymphoma.[57-65] In these individuals, the transplantation process involved high-risk, mostly intensive conditioning regimens (one case received reduced intensity conditioning), which depleted their viral reservoirs, followed by an infusion of donor-matched HSCs carrying mostly homozygous genetic resistance to HIV (one case received cells with heterozygous resistance, one case received cells without genetic resistance), allowing repopulation of HIV-resistant T cells in their immune system.[66-68] This resistance is conferred by a naturally

occurring deletion in the C-C chemokine receptor type 5 (*CCR5*) gene (*CCR5Δ32*), which prevents HIV-1 from entering T cells through its co-receptor activity. However, this mutation is rare, found in only about 1% of individuals of Northern European descent, and inappropriate in the setting of non-malignant HIV infection, making it an impractical solution for most people living with HIV.[69,70]

More recently, efforts have shifted toward using CRISPR-based gene editing to recreate this protective *CCR5Δ32* variant directly in autologous HSCs, offering a more accessible and scalable therapeutic strategy.[71] While clinical trials are ongoing, it remains to be seen whether individuals receiving *CCR5*-edited HSCs will achieve long-term remission.[72] Moreover, at least two studies suggest that individuals harboring the *CCR5Δ32* variant are more vulnerable to influenza and West Nile Virus.[73,74] Interestingly, a recent case has also suggested that HIV cure may be possible following allogeneic HSC transplantation from a wild-type *CCR5* donor, raising the possibility that factors beyond *CCR5* deletion may contribute to viral eradication.[62] While these cases offer proof-of-concept that HIV resistance can be transferred from donor to recipient, the approach remains impractical given the risks, costs, and logistical challenges of HSC transplantation.

Currently, combination antiretroviral therapy (ART) remains the gold standard for HIV treatment.[75] The widespread availability of ART has dramatically reduced HIV-related mortality, increased life expectancy, and prevented new infections.[76] However, ART does not eradicate HIV and requires lifelong adherence to maintain viral suppression. For those with access to these drugs who achieve adherence and who do not suffer from long-term toxicities, ART enables long-term health and viral suppression. Despite these successes, treatment gaps persist, particularly in resource-limited settings where ART is not available, where people are not able to afford out-of-pocket costs, or where accessing HIV treatment is stigmatized.[77,78] Adherence challenges, drug resistance, and logistical barriers also hinder effective disease management.[79-81] Viral control in the absence of ART

or with infrequent ART is viewed by the HIV community as the goal to achieve what is referred to as a "functional cure".[82] To address these issues, new long-acting therapies are being developed.[83-85]

One such class of emerging therapeutics is broadly neutralizing antibodies (bnAb). Most people living with HIV fail to mount an effective antibody response due to the virus's rapid mutation rate and evasion of antibody-mediated immunity.[86,87] Likewise, vaccine development has struggled to elicit antibodies capable of preventing infection, controlling viral replication, and limiting escape variants.[88,89] Unlike conventional antibodies, bnAbs target highly conserved epitopes on the HIV envelope protein, neutralizing a diverse array of viral strains.[90] These antibodies were initially discovered in a small subset of individuals known as elite controllers, who maintain undetectable viral loads without ART.[91,92] Studies have shown that viral control in these individuals is mediated by a combination of humoral immunity (bnAb production) and robust cell-mediated immunity, driven by strong cytotoxic T cell responses.[93,94] In addition, certain host genetic factors—such as protective human leukocyte antigen (HLA) alleles—and viral genetic features, such as defective or attenuated proviral genomes, contribute to their ability to suppress infection without treatment.[95]

Together, these observations suggest that a successful gene therapy-based HIV cure will require a multifaceted approach incorporating three key components: (1) conferring resistance to HIV infection, (2) inducing protective immunity (either humoral and/or cell-mediated), and (3) depleting the replication-competent viral reservoir. Until a single-shot curative strategy is realized, functional cures that address these pillars individually remain an attractive alternative. In this dissertation, I will primarily focus on the humoral component of HIV immunity and explore how HSC gene therapy and editing can be leveraged to engineer durable antibody-mediated protection.

NHP Models of HIV and Gene Therapy

Non-human primates (NHP) have long been used as an animal model for the study of HIV infection and for pre-clinical development of HIV treatments.[96] Their close genetic and physiological resemblance to humans has made them invaluable for understanding viral pathogenesis and testing interventions *in vivo*. NHP models have played a key role in understanding and optimizing vaccine strategies, combination ART, and bnAb-based treatments.[97-99] However, since HIV-1 is unable to productively infect most NHP species, those commonly used in research, such as rhesus or pig-tailed macaques, are infected with simian immunodeficiency virus (SIV) or simian/human immunodeficiency virus (SHIV) chimeras.[100] No alternative animal model has been developed to date that can validate proof-of-concept HIV therapies before moving to human clinical trials.

Beyond their role in HIV research, rhesus and pig-tailed macaques are a well-established model for HSC transplantation and hematopoiesis studies.[101,102] Transplantation protocols in NHPs closely mimic those used in humans, enabling researchers to evaluate long-term engraftment, multi-lineage differentiation, and immune system reconstitution over extended periods ranging from months to years. These models have been instrumental in defining the identity of HSC and HSPC populations, shedding light on their role in reconstituting hematopoietic lineages.[103,104] Furthermore, HSC gene therapies are commonly tested in NHPs prior to moving to the clinic.[102,105] For any HSC-based gene therapy aimed at treating HIV, rigorous preclinical validation in NHPs will be essential to assess safety, efficacy, and long-term engraftment before moving to human trials. However, successful translation requires careful consideration of host-specific factors.[106] When using gene editing, we need to consider genetic divergence between humans and NHPs as single base-pair changes can abrogate any function or result in unintended, off-target editing.[107] Thus, optimizing gene editing conditions and reagents is critical before undertaking expensive and time-intensive large-animal studies.

To address this, I have leveraged a recently developed small animal model that allows the study of NHP HSPC engraftment and differentiation.[108,109] By first testing our approach in this "pre-preclinical" setting, we aim to optimize editing conditions and establish proof-of-concept before advancing to large-animal studies in NHPs and, ultimately, human trials. This work is a necessary step in bridging the gap between *in vitro* development and clinical application, ensuring that our therapeutic strategy is both effective and translatable. The resulting study is presented Chapter 2, modified from a manuscript entitled "*In vivo* production of an anti-HIV antibody from primate hematopoietic cells by non-viral knock-in" at the time of its submission.[110] In this paper, my co-authors and I demonstrate that our editing approach achieves CRISPR-mediated bnAb transgene knock-in at the target genomic locus and results in productive antibody expression following hematopoiesis and antigen presentation. The results presented here establish a foundation for the use of edited HSPC as therapeutic modality for durable production of biologics to treat chronic disease.

Chapter 2: Targeted Gene Knock-In

Introduction

Anti-HIV bnAbs isolated from long-term non-progressors are capable of providing immune protection against diverse strains of HIV-1.[111] They have been demonstrated as viable treatment alternatives to controlling viral loads in NHP models and in human clinical trials.[99,112] As opposed to standard-of-care ART, bnAbs can be administered less frequently and sustain activity in circulation for up to 6 months, a key advantage for reaching vulnerable populations who cannot achieve daily adherence or suffer from ART-associated long-term toxicities.[113] Previous studies have explored the delivery of bnAb transgenes to various cell types using viral vectors.[114,115] When delivered into muscle tissues in animal models, AAV vectors can achieve bnAb expression and protect from viral challenges.[116,117] However, this indiscriminate production of antibody, combined with the immunogenicity of AAV, results in host anti-antibody and anti-AAV responses.[118-120] These responses curtail the sustained production of bnAbs and prevent re-treatment. Immunization strategies have also failed to induce endogenous bnAb expression, in part due to extensive somatic hypermutation required to attain high-affinity bnAb sequences, as well as poly- and auto-reactive precursor sequences that fall prey to negative selection during maturation of germinal center B cells.[121-124]

CRISPR/Cas technology has enabled precise targeting of the immunoglobulin heavy chain (*IGH*) locus to replace endogenous antibodies with transgenes delivered by viral vectors.[125-132] Edited B cells expressing engineered antibodies have conferred anti-viral protection in murine models.[125,126,129] It remains unclear how long such gene-edited B cells can sustain an immune response, though those that develop into long-lived plasma cells could confer immune memory.[128,129] Notably, one of the earliest cell types explored for bnAb transduction were HSPCs, the precursors to all B cells.[133] These lentivirally-transduced HSPCs could subsequentially differentiate into bnAb-producing plasma cells *in vitro* but antibody production was driven from proviral elements

semi-randomly integrated into the genome.[133] If the endogenous antibody-producing *IGH* locus of HSPC could be precisely edited non-virally and retain the ability to engraft and differentiate into antibody-producing B cells that retain the antibody transgene *in vivo*, this approach could provide a durable source of bnAb-producing B cells without viral vector-triggered immune responses. While *in vivo* delivery of CRISPR/Cas to HSPC with high specificity remains a challenge, animal models offer valuable insights into hematopoiesis and engraftment potential.

Here, we utilized the MISTRG mouse strain (*CSF1*$^{h/h}$ *IL-3/CSF2*$^{h/h}$*SIRPA*^{tg} *THPO*$^{h/h}$ *Rag2*$^{-/-}$ *Il2rg*$^{-/-}$), which supports the engraftment of NHP HSPC, to investigate the development of edited HSPC and transgene expression following non-viral knock-in.[108,109] The use of NHP cells enables the development of editing materials, dependent on genomic context, for a relevant pre-clinical model of HIV infection. Our findings in this primatized mouse model demonstrate the potential for durable bnAb production from hematopoietic cells as a strategy for controlling HIV.

Results

Optimized editing of *IGH* locus in primate HSPC

We first characterized and tested CRISPR guide RNA (gRNA) for targeted gene knock-in in NHP HSPC (CD34^{+}). Sequence data for the *IGH* locus was available for rhesus macaques (*Macaca mulatta*) but had not been documented for pigtail macaques (*M. nemestrina*), a closely related and larger species that has been used as a model for HIV-1 infection and long-term HSPC engraftment studies.[96,103] We sequence-verified the region of this locus spanning from the final J segment to the Eμ enhancer in *M. nemestrina*, an intronic region with low heterogeneity that is unchanged by variable (V), diversity (D) and joining (J) segment (VDJ) recombination (Figure 1A).[134] Using the verified sequence, we screened for all potential CRISPR/Cas9 and CRISPR/Cas12a guide RNA (gRNA) by identifying relevant protospacer-adjacent motif (PAM) sequences within this locus. Cas9 and Cas12a nucleases

generate site-specific DNA cuts but with different free DNA end configurations and with different PAM sequences, with the latter associated with higher specificity.[135] Chen *et al*. demonstrated that sequence context can influence the outcome of gene editing following CRISPR treatment, with Tatiossian *et al*. showing that larger deletions are associated with an increased likelihood of HDR at a specific locus.[136,137] For these reasons, a total of 120 Cas9 gRNA and 56 Cas12a gRNA were identified and ranked based on predicted efficiency and accuracy using the CRISPOR webtool (https://crispor.gi.ucsc.edu/, Table S1).[138] Lindel (logistic regression model to predict insertions and deletions) scores were included as a measure of HDR pathway preference following double-strand breaks induced by Cas9 to minimize the production of undesired mutations with these gRNA.[136] We then synthesized the top five gRNA for each CRISPR/Cas system for empirical testing.

To evaluate the performance of these guides, we isolated primary bone marrow-derived $CD34^+$ HSPCs from healthy adult NHP donors (Figure 1B). $CD34^+$ cells were purified from bone marrow aspirates, reaching 79-97% purity post-enrichment (Figure 1C, Table S2). Cells were electroporated with CRISPR ribonucleoproteins (RNP), and insertion and deletion (indel) formation at the target loci was assessed through high-throughput sequencing. Cas9 gRNA exhibited indels in up to 1.4% of sequence reads (Figure 1D). Cas12a gRNA demonstrated higher average editing levels, albeit without statistical significance (0.84% ± 0.38% vs. 0.46% ± 0.25%, unpaired two-tailed t-test, $p = 0.42$), with the most efficient gRNA achieving a 2.3% indel frequency (Figure 1E). This was statistically higher than other gRNA (ordinary one-way ANOVA, $p = 0.0026$), although overall editing efficiencies were low. These results demonstrate feasibility of gene editing in NHP HSPC, with Cas12a showing a slight advantage in editing efficiency over Cas9 at this locus.

Achieving HDR at *IGH* locus and transgene expression *in vitro*

In addition to sequence context which can influence HDR frequency, we assessed the ability of CRISPR/Cas9 and CRISPR/Cas12a systems to mediate the knock-in of a DNA template into the target *IGH* locus via HDR. Cas9 nuclease generates a blunt double-strand break, while Cas12a introduces staggered cuts with 5 base pair (bp) single-stranded overhangs.[139] These differences in DNA cleavage can also influence HDR outcomes, resulting in either productive insertion of the DNA template at the correct locus with proper transgene expression or non-productive insertions that are truncated, duplicated, or introduce additional indels that may compromise transgene expression (Figure 2A).

To quantify HDR efficiency and fidelity, we electroporated a NHP B cell line (LCL 8664) with ribonucleoproteins (RNP) and a small single-stranded oligodeoxynucleotide (ssODN) template. Sequencing of the edited cells allowed us to classify genotypes based on productive or non-productive HDR events. Cas9 gRNA achieved up to 5.9% total HDR, with nearly half of these events being non-productive (Figure 2B). In contrast, Cas12a gRNA exhibited a higher total HDR efficiency, reaching up to 8.0%, and showed a much lower fraction of non-productive HDR events (Figure 2C). Based on these findings, we selected a Cas12a gRNA that showed a favorable ratio of productive HDR to non-productive HDR and indels for further experiments (NHP *IGH* Cas12a guide #5: TTTAGAATTATGAGGTGCGC). To further optimize HDR efficiency, we designed and tested ssODN templates positioned at different distances from the predicted cut site of this optimal Cas12a gRNA (Figure 2D).[140] Among the tested configurations, HDR templates placed +10-20 bp downstream from the first gRNA base exhibited the highest HDR efficiency, along with the highest ratio of productive HDR to indels (Figure 2E). Subsequent templates were designed with insert sequences placed +15 bp from the Cas12a gRNA.

We next designed a large 2,250 bp DNA template encoding a green fluorescent protein (GFP) reporter transgene under the control of a constitutive cytomegalovirus (CMV) promoter, flanked by 450 bp homology arms aligned to the NHP *IGH* locus (Figure 2F). Three versions of this CMV-GFP^{Cas12a} template were tested for their ability to induce GFP expression when delivered by electroporation to LCL 8664 cells alongside Cas12a RNP including our optimal gRNA. GFP expression was monitored over several cell divisions. LCL 8664 cells electroporated with double-stranded DNA (dsDNA) or plasmid templates with Cas12a RNP showed durable GFP expression, indicating successful knock-in of the transgene (Figure 2G). The dsDNA template produced higher GFP expression than plasmid template alone or with Cas12a RNP, indicating greater efficiency for transgene knock-in. In contrast, co-delivery of ssODN template was not associated with significant GFP expression. Thus, we proceeded with dsDNA templates for our non-viral editing approach in mouse studies.

Engraftment and hematopoiesis of edited NHP HSPC in MISTRG mice

We next evaluated the potential for transgene knock-in, engraftment, and differentiation potential of primary CD34$^+$ NHP HSPC. To achieve this, we utilized the immunodeficient MISTRG mouse model, which supports NHP cell engraftment.[109] NHP HSPC were electroporated with Cas12a RNP and a 2,384 bp VH4-GFP^{Cas12a} construct expressing GFP under the control of a B cell-specific promoter derived from NHP variable heavy (VH) domain allele 4-38-2, the most conserved allele and most abundant VH transcript.[141] Electroporated HSPC were then transplanted into sub-lethally irradiated, neonatal MISTRG mice (Figure 3A). Engraftment and development of NHP cells were tracked through regular peripheral blood draws and in different tissues at necropsy.

Results showed that electroporated NHP HSPC were able to successfully engraft in immunodeficient MISTRG mice. Mean NHP-CD45$^+$ white blood cell (WBC) populations in peripheral blood reached up to 3.3% at peak engraftment (Figure 3B). Increased HSPC cell doses trended

towards higher engraftment (Figure S1). Engraftment persisted for over 16 weeks without visual signs of graft-versus-host disease (GVHD). To assess multilineage differentiation, mice injected with 1.4 × 10^5 VH4-GFP^{Cas12a} electroporated HSPC were monitored for white blood cell populations, including lymphocytes and monocytes. Early after transplantation, we observed mostly B cell populations, with T cell populations emerging around week 12, eventually surpassing B cells by week 16 (Figure 3C). Monocyte levels remained consistent and low throughout the study (Figure 3D). Hematopoietic NHP cells were detected in the bone marrow and liver at necropsy (Figure 3E). These trends were also observed in MISTRG mice receiving control (i.e., non-edited) HSPC (Figure S3).

GFP expression was detected in 50% of mice transplanted with edited HSPC, with four out of eight mice showing GFP$^+$ cells in peripheral blood. From weeks 10 to 14, 0.41% to 0.77% of NHP-derived cells expressed GFP (Figure 3F). However, a decline in GFP expression coincided with decreasing B cell populations and engraftment levels. Further sequencing confirmed the presence of edited cells *in vivo* (Figure 3G). Indels, including large insertions, were detected at the target NHP *IGH* locus in the early weeks post-transplantation but had drastically declined by week 16 when peripheral blood B cells also declined.

In vivo expression of a bnAb from the *IGH* locus in primate B cells

We next developed templates for expressing a bnAb transgene. Our 2,790 bp template design was based on previous efforts to engineer antibody knock-in at the human *IGH* locus.[134] Specifically, we constructed a sequence containing the VH4 B cell-specific promoter, along with a complete light chain and recombined heavy chain separated by a short linker, followed by a splice site allowing the integration of an endogenous heavy chain constant region (Figure 4A). The coding sequences for bnAb 10-1074, which targets the V3 glycan site on the HIV envelope protein, were optimized for NHP expression, resulting in the VH4-10-1074^{Cas12a} template.

To validate expression of VH4-10-1074^{Cas12a}, we transfected HEK 293E cells *in vitro* with plasmid and measured transgene surface expression levels (Figure 4B). Recombinant bnAb was isolated from cell culture supernatant and subsequently assessed for binding affinity to an HIV envelope protein antigen. Using gp120 monomers from various HIV strains, we observed that HIV strain CN97001 exhibited the highest affinity for recombinant 10-1074 (Figure 4C, Figure S3). These results confirmed that the transgene design permitted 10-1074 binding to its target antigen.

In addition to a dsDNA template amplified from the plasmid, we produced an AAV template to compare non-viral and viral knock-in strategies for NHP HSPC. We compared a panel of AAV serotypes to transduce NHP HSPC and selected AAV6.2 serotype for experiments (Figure S4). Subsequently, NHP HSPC edited with each of these VH4-10-1074^{Cas12a} templates were injected at a dose of 5.0×10^5 cells into MISTRG mice (Figure 4D). To promote clonal expansion of B cells with productive bnAb knock-in, beginning at 8 weeks of age, mice were immunized with HIV-CN97001 gp120 monomers. Peripheral blood and plasma samples were collected to monitor lymphocyte development and antibody production. Multiple tissues, including secondary lymphoid organs (lymph nodes, spleen), bone marrow, and liver, were collected at necropsy for further analysis.

As with previous experiments, edited NHP HSPC demonstrated successful engraftment and differentiation into mature cell types, including large B cell populations early in the study (Figure 4E, Figure S5). With CD34$^+$ doses of 5.0×10^5, up to 8.2% NHP-CD45$^+$ cells were observed at peak engraftment in peripheral blood of mice receiving dsDNA templates. Four weeks after immunization, anti-HIV antibody titers were detectable in a subset of primatized mice (Figure 4F). In the cohort receiving the dsDNA template, one of five (20%) mice developed antibody titers up to 2.4 μg/mL. 10-1074-expressing cells were identified in all primatized mice, although cell-surface expression was low, with less than 0.46% of NHP-derived cells observed in peripheral blood (Figure 4G). Interestingly, the mouse with detectable antibody titers in plasma had the highest NHP CD45$^+$ WBC

engraftment levels but did not show a significantly larger population of 10-1074-producing cells, suggesting that most antibody-expressing cells were likely not in circulation (Figure S6). Hematopoietic NHP cells were detected in all tissues analyzed at necropsy, including $CD34^+$ cells in the bone marrow (Figure S7).

Mean indel frequency peaked at 1.5% in peripheral blood at week 16 (Figure 4H). Sequencing of cells from bone marrow, liver, spleen, and lymph nodes confirmed the continued presence of edited cells in different tissues at necropsy (Figure S6). While antibody production was not significantly correlated with indel levels, large insertions (defined as ≥8bp, 0.20% of sequence reads) were observed in the mouse with detectable antibody titers. Lymphocyte populations followed the same trends as previously observed (Figure S5). B cell populations declined with similar kinetics as previous experiments despite immunization. The mouse with detectable antibody titers demonstrated a decline in B cell populations, with T cell populations taking over at week 12 (Figure S7). NHP-$CD19^+$ B cells were present in the lymph nodes of all mice, as well as the liver and the spleen of a subset of mice at necropsy, where B cell maturation occurs in germinal centers, of which up to 17% were 10-1074-producing cells (Figure 4I).

Antibody expression and B cell maturation in MISTRG6 mice

To further validate *in vivo* 10-1074 production, we repeated the injection of edited NHP HSPC in MISTRG6 mice, a strain derived from MISTRG with the additional knock-in of human interleukin-6 (IL-6).[142] Given IL-6's role in promoting B cell development and immunoglobulin G (IgG) production, we hypothesized that antibody titers would be detectable in a larger fraction of animals. To compare viral and non-viral editing conditions, seven mice were injected with HSPC receiving VH4-10-1074^{Cas12a} as either dsDNA or AAV6.2 template (Figure 5A). In addition, tissue analysis was performed

at an earlier timepoint closer to peak antibody expression to identify the location of antibody-producing cells.

Engraftment levels in the non-viral condition were no different than control, whereas mice in the AAV6.2 template group displayed significantly lower NHP-CD45$^+$ engraftment levels in the peripheral blood (Figure 5B). As anticipated, B cell populations remained high in MISTRG6 mice (Figure 5C). Anti-HIV antibody titers were detectable in five of seven mice at week 8, remained detectable in four of six mice at week 10, and were significantly above control mice receiving the same immunization regimen (Figure 5D). Plasma titers peaked at 4.0 μg/mL at 8 weeks post-transplantation. There was no significant difference in antibody titers between viral and non-viral conditions.

Cell surface expression levels of 10-1074 antibody remained very low in circulation, as did the number of NHP-IgG$^+$/CD138$^+$ antibody-producing cells (Figure S8). In contrast, 10-1074- and IgG-producing cells were present in the liver and spleen (Figure 5E-F). Plasma cells, as defined by CD20$^{low/-}$/CD31$^+$/CD138$^+$ cells in NHP, were also detected in the bone marrow and liver (Figure 5G). Of note, one mouse died in each condition, including experimental and control groups, prior to the endpoint. Deceased mice showed clear signs of GVHD. Of all 10-1074-producing cells detected across tissues, 27-34% were CD20$^+$ B cells and 5.3-13% were CD20$^{low/-}$/CD31$^+$/CD138$^+$ plasma cells (Figure 5H).

Sequencing once again confirmed editing at the target NHP *IGH* locus in different tissues of transplanted mice, with AAV-edited HSPC displaying a higher proportion of large insertions (Figure 5I). Editing at the target locus averaged 13.7% in the peripheral blood of dsDNA mice and 18.4% in that of AAV mice, remaining constant over 2 weeks. Edited NHP cells were also detected in all tissues analyzed at necropsy (Figure S9). To confirm productive knock-in of the template in the non-viral condition, long-read sequencing of the *IGH* locus was performed on CD34$^+$ cells. Amplicons of over 5.2 kb contained the full-length template at the expected insertion site, including an intact coding

region, single-base changes unique to the homology arms, such as the blocking mutation at the PAM, and an additional 2.6 kb of the *M. nemestrina* genome past the homology arms, matching unedited samples (Sequence S1).

Discussion

This study lays the foundation to address a gap in current HIV therapies, which lack the ability to produce drugs or antibodies for extended periods of time and potentially lasting years. Existing genome engineering approaches for durable biologic production primarily rely on viral vectors. While effective, these methods are costly and can induce immune responses that limit practicality. By contrast, non-viral gene knock-in strategies that leverage endogenous antibody-producing cells and genomic loci could offer a promising alternative for producing engineered antibodies against HIV over a lifetime. Here, we utilized a relevant pre-clinical model of HIV to demonstrate that non-viral HSPC editing at the *IGH* locus offers a viable pathway to achieve expression of therapeutic antibodies.

Our data demonstrate that both CRISPR/Cas9 and CRISPR/Cas12a systems can generate genetic edits at the *IGH* locus in pigtail macaque primary HSPC. We observed that the choice of nuclease and gRNA influenced knock-in efficiency, extending beyond total editing efficiency. This finding aligns with previous studies suggesting that HDR outcomes may be influenced by the sequence context surrounding the cut site.[136,137] Our data suggest that the staggered cuts produced by Cas12a, in contrast to the blunt double-strand breaks created by Cas9, may increase the likelihood of productive transgene knock-in or reduce off-target mutations at this locus. In addition to targeting a non-coding region, precise edits could minimize impacts on non-antibody producing cells derived from edited HSPC, improving the safety profile of this approach, but remain to be tested. We observed that the choice of template also impacted editing efficiency and productive

transgene knock-in. Although it produced perfect HDR events with small templates (<200 bp), ssODN was less effective for achieving knock-in of large sequences (>200 bp) at the *IGH* locus. This is in contrast to other studies where knock-in was achieved in HSPC using ssODN.[143,144] Though less efficient at gene knock-in at the human hemoglobin subunit beta (*HBB*) locus, ssODN templates did not impair engraftment as compared to viral templates with known genotoxic risks in humanized mouse models (NSG and NBSGW).[145] It is of note that knock-in of anti-HIV bnAbs was recently reported in human HSPC with high efficiency at the *CCR5* locus using AAV following transplantation in NSG and NBSGW mice.[146] Likely all of these factors together (choice of nuclease, target locus, DNA template, and mouse model) impact desired editing outcomes observed in primary cells. Our data in MISTRG/MISTRG6 mice suggest that HSPC edited *ex vivo* with long dsDNA templates at an endogenous antibody locus remain capable of engraftment without compromising productive knock-in efficiency and potential to differentiate into antibody-producing B cells.

The potential of gene-modified HSPC for treating chronic diseases is generating considerable interest, with authorization recently given for the first CRISPR-based gene therapy drug product including primary human HSPC for the treatment of sickle cell disease.[20] However, the ability of CRISPR-mediated gene knock-ins in HSPC at highly recombinatory loci to persist throughout differentiation remains uncertain. Our results show that non-viral knock-in edited NHP HSPC are capable of engrafting into an immunodeficient mouse model, where they successfully differentiated into B cells capable of expressing antibody transgenes. Moreover, we detected antibody titers in the circulation of these mice, confirming that edited HSPC could differentiate into functional immune cells producing detectable levels of antibodies in response to antigen. While edited cells could express the transgene, their populations diminished over time, even with continued immunization. While these declines aligned with a well-described switch from peripheral B cells to T cells in humanized and primatized mice,[109,147] it may also suggest selective pressure against edited cells,

contributing to their reduction over time. It was recently reported that HSPC edited with Cas9 nuclease and ssODN template for HDR *ex vivo* demonstrated impaired long-term engraftment in a NHP model.[148] This raises the question of whether dependence on the HDR pathway could impede clinical translation. One possible workaround could be the adoption of gene knock-in technologies that do not depend on endogenous repair machinery, such as systems based on engineered prime editors and recombinases.[149]

In initial experiments with MISTRG mice, the relatively low number of HSPC with large insertions transplanted, corresponding to approximately 1,000 cells (only 1 of which on average contains a perfect HDR event), likely failed to generate or spontaneously lost detectable bnAb levels due to the stochastic loss of HSPC clones during hematopoiesis. Although not a head-to-head comparison of the two strains, a change to MISTRG6 mice expressing human IL-6 was sufficient to increase the fraction of mice demonstrating plasma antibody titers from one of five mice to seven of seven mice. In addition, it has been shown that 10-1074 titers of 5 μg/mL, similar to those achieved here, are sufficient to reduce simian-HIV (SHIV) infection by ≥99.9% in NHP.[150] Of note, we validated bnAb expression in HEK 293E; expression levels could be further optimized in mature primary NHP B cells. It also remains unclear how NHP antibody-producing B cells are maturing in the primatized MISTRG6 mouse model. There is limited evidence for the formation of germinal centers and long-lived plasma cells in humanized MISTRG6 mice.[151,152] It remains unclear, however, whether optimization in mice to achieve higher numbers of antibody-producing animals is relevant to translation of this approach in the autologous setting in NHP. The use of better immunization regimens and the presence of fully functional germinal centers in an NHP model may produce biologically relevant antibody titers.

A non-viral approach to gene knock-in could have significant clinical value, particularly if adapted for *in vivo* delivery. HIV treatments such as ART can complicate viral transduction.[115] A vector capable of delivering a RNP and DNA template to specific cell types for targeted, transient

genome editing would offer a highly programmable platform for *in vivo* biologic production. In conclusion, this study provides foundational insights for the development of non-viral gene therapies aimed at achieving durable, *in vivo* antibody production by targeting HSPC. These findings could have broader implications for treating HIV and other chronic diseases through sustained biologic production, representing a significant advance in genome engineering and therapeutic development.

Materials and Methods

HSPC isolation and culture

The NHP HSPC isolation protocol was derived from published methods and adapted for non-mobilized, healthy adult NHP donors.[153] Bone marrow aspirates were obtained from the femur or humerus and hemolyzed (Pharm Lyse; BD Biosciences) the same day. White blood cells were enriched for $CD34^+$ by sequentially incubating with 12.8 IgM anti-NHP-CD34 antibody (obtained from Fred Hutchinson Cancer Center Therapeutics Products Program) for 30 minutes at 4°C, followed by anti-IgM microbeads (Miltenyi Biotec) for 30 minutes at 4°C, and then loading onto a magnetic column (Miltenyi Biotec).[154] NHP-$CD34^+$ cells were eluted from the column and prepared for flow cytometry to confirm purity (Table S2).

Immediately following isolation, NHP HSPC were transferred to HSPC medium (StemSpan Serum-Free Expansion Medium (SFEM) II (StemCell Technologies) with 100 ng/mL recombinant human thrombopoietin (TPO), stem cell factor (SCF), and flightless 3 (FLT-3) ligand, all from CellGenix) at 1.0×10^6 cells/mL in tissue culture (TC)-treated flasks, incubated at 37°C and 5% CO_2. Alternatively, NHP HSPC were cryopreserved in CS10 medium (StemCell Technologies) or in 90% heat-inactivated fetal bovine serum (FBS; Gibco) with 10% dimethyl sulfoxide (DMSO; Thermo Fisher Scientific).

IGH sequencing and gRNA selection

Sequencing primers for NHP *IGH* were designed based on the rhesus macaque genome (rheMac10 assembly, Table S3). Genomic DNA was isolated from pigtail macaque and used to amplify 1,024 bp segments, which were submitted for Sanger sequencing. Pigtail macaque sequences were aligned using MAFFT (v7)[155] to identify divergence from rhesus macaque and human sequences.

All possible CRISPR/Cas9 and CRISPR/Cas12a gRNA within this sequence were computationally screened using CRISPOR (v5.01).[138] These gRNA were ranked by predicted specificity scores, efficiency scores, and Lindel scores (logistic regression model to predict insertions and deletions) when available, in that order (Table S1). The top 5 gRNA for each nuclease with guide and protospacer-adjacent motif (PAM) sequences that had perfect homology to both rhesus and pigtail macaques were selected for synthesis. CRISPR/Cas9 were synthesized as CRISPR RNA (crRNA) for pairing with tracer RNA (trRNA), while CRISPR/Cas12a were synthesized as single gRNA (Integrated DNA Technologies (IDT)).

NHP B cell culture

B lymphocyte cell line (LCL) 8664 (American Type Culture Collection (ATCC)), a lymphoma-derived rhesus macaque cell line, were maintained in Roswell Park Memorial Institute (RPMI) medium 1640 containing 10% FBS and 1% penicillin/streptomycin (Gibco) at 37°C and 5% CO_2.[156] Cells were cultured in TC-treated flasks and passaged at 80-90% confluence approximately once every 4 days. Cell identity was authenticated by Sanger sequencing.

HDR template construction

Templates for measuring HDR efficiency in NHP B cells were synthesized as ssODN (IDT) of the non-template strand with 40-bp homology arms flanking an 8-bp insertion. Templates for each gRNA

were designed for insertion at the predicted cut site, namely -9 bp from Cas9 PAM or +15 bp from Cas12a PAM. Homology arms contained 2-bp blocking mutations in the PAM sequence for Cas9 gRNA and 1-bp blocking mutations for Cas12a gRNA to prevent cutting following HDR and multiple insertion events.

Templates for gene knock-in were cloned as bacterial plasmids containing ampicillin resistance. The 450-bp homology arms were amplified from pigtail macaque genomic DNA. As VH4 is the major expressed VH allele in rhesus macaque, alleles from the IgVH4 locus were aligned, the most conserved of which (VH4-38-2 allele) was selected for B cell-specific expression.[141] Expression was confirmed in NHP B cells. Transgene sequences, including linker and splice signals, and a compact CMV promoter were synthesized as gBlocks (IDT).[157] Cloning was performed by DNA ligation (Thermo Fisher Scientific), blocking mutations were introduced by site-directed mutagenesis, and all final products were confirmed by whole plasmid sequencing (Plasmidsaurus). Plasmids were used to PCR amplify gel-purified dsDNA templates and to synthesize long ssODN templates (GenScript). All templates will be made available through Addgene upon publication.

RNP electroporation

LCL 8664 cells were passaged to obtain a cell population of 1.0×10^6 cells per sample in the exponential growth phase on the day of electroporation. Cas9 RNP complex was prepared by combining 3 µL 200 µM crRNA, 3 µL 200 µM tracrRNA, and 6 µL of duplex buffer (IDT). The mixture was incubated at 95°C for 5 minutes, followed by cooling at room temperature for 15 minutes. Cas12a RNP complex was prepared by combining 3 µL 200 µM crRNA, 3 µL water, and 6 µL of duplex buffer. To each reaction, 4 µL 100 µM DNA template and 1 µL 10 mg/mL Cas9 or Cas12a nuclease (Aldevron) were added and incubated at room temperature for 5 minutes. For the control group,

templates were electroporated without nuclease. Cells were recovered in culture for 3 days prior to genomic DNA isolation for sequencing analysis.

Cryopreserved primary NHP HSPC were thawed in Iscove's Modified Dulbecco's Medium (IMDM), recovered for 24 hours in HSPC medium at 1.0 ×10^6 cells/mL in a TC-treated T25 flask, and washed twice with Dulbecco's phosphate-buffered saline (PBS; Gibco) prior to electroporation. For gRNA screening, HSPC were electroporated using an ECM 830 Electroporation System (Harvard Bioscience). In each reaction, 5.0 × 10^5 $CD34^+$ cells were combined with 10 nmol gRNA and 180 pmol nuclease in 50 µL BTX buffer (Harvard Bioscience), and electroporated at 125 V for 5 ms. Cells were recovered in 1.0 mL HSPC medium in a TC-treated 12-well plate for 3 days, after which genomic DNA was isolated for sequencing.

For the MISTRG mice receiving reporter edited cells, HSPC were electroporated using an Amaxa Nucleofector II Device (Lonza). In each reaction, 5.0 × 10^5 $CD34^+$ cells were combined with 10 nmol gRNA, 180 pmol nuclease, and 5 µg dsDNA template in 100 µL Nucleofector Solution V with Supplement 1 from Nucleofector Kit V (Lonza), and electroporated using program U-008. For MISTRG mice receiving antibody edited cells, HSPC were electroporated using a Neon Transfection System (Thermo Fisher Scientific). In each reaction, 5.0 × 10^5 $CD34^+$ cells were combined with 10 nmol gRNA, 180 pmol nuclease, and 5 µg dsDNA template or 5.0 × 10^{11} viral genomes (vg) AAV6.2 template in 100 µL buffer T (Thermo Fisher Scientific), and electroporated in a 100 µL tip at 1650 V for 3 pulses with a width of 10 ms. In both cases, cells were recovered in 1.5 mL HSPC medium in a TC-treated 6-well plate for 4 hours prior to injection or for 3 days prior to genomic DNA isolation for sequencing.

Indel and HDR analysis

Genomic DNA samples were prepared for high-throughput sequencing on a MiSeq platform (Illumina). PCR amplifications were performed to enrich the NHP *IGH* locus using target-specific

primers (Table S3), to then attach overhangs using P5 and P7 adapters, and finally to barcode each sample using Nextera indexes (Illumina), gel purifying amplicons of the desired length at each step. Indexed amplicons were quantified and pooled at 5 or 10 nM. Paired-end, 250-bp reads were sequenced using MiSeq Nano v2 according to the manufacturer's protocol.

Sequencing results were processed using an in-house algorithm and adapted to the target NHP reference sequence (GitHub: https://github.com/jack-cast/FredHutch_Gene_Edit_2).[158] Stitched reads are aligned to the reference sequence. Indels and HDR events are measured within a quantification window spanning 50-bp on either side of the gRNA and normalized to a control, non-edited sample. Due to heterogeneity at the *IGH* locus in LCL 8664 cells, indel and HDR percentages were calculated per target allele with perfect sequence identity for each gRNA.

AAV transduction

Based on previous literature, 4 serotypes were chosen for testing on NHP-CD34^{+} cells: AVV2, AAV6, AAV6.2, and AAV-DJ.[159] A standard *in vitro* grade panel with CMV-mediated GFP reporter expression (VectorBuilder) was transduced into 3.75×10^5 cells at multiplicities of infection (MOI) of 2.4×10^4 and 6.7×10^5 vector particles (vp). Cell viability and GFP expression were assessed by flow cytometry at days 1 and 3 post-transduction. Based on these results, the AAV6.2 serotype was selected for packaging of the VH4-10-1074^{Cas12a} template. For HSPC transduction prior to mouse transplantation, AAV6.2 was added at an MOI of 1.0×10^6 vp alongside RNP during electroporation.

Primatized mouse studies

For xenotransplantation experiments, cryopreserved NHP HSPC were slow thawed within 24 hours of MISTRG/MISTRG6 mouse birth and recovered in HSPC medium overnight. Within 48 hours (MISTRG) or 72 hours (MISTRG6) of birth and 4 hours prior to injection, pups are irradiated with 150 cGy γ-rays in a cesium-137 irradiator. NHP HSPC from different donors were pooled together, electroporated as described above, recovered for 4 hours in HSPC media, then resuspended in PBS with 1% heparin (Table S4). HSPC were injected intra-hepatically at variable cell doses in 40 µL. Control HSPC were transferred to the same 6-well plate without electroporation. When cell counts allowed, non-injected HSPC samples were set aside for 3-day recovery and genomic DNA isolation.

Peripheral blood from the retro-orbital sinus at various time points was collected into Vacutainer K2 EDTA coated tubes (BD Biosciences). When applicable, plasma samples were collected by centrifuging at 1,000 x g for 10 minutes and transferring the supernatant either to be stored at 4°C or in aliquots at -20°C. Without plasma collection, blood samples were centrifuged at 600-800 g for 3 minutes. Cell pellets were treated twice with 1.0 mL of ACK Lysis Buffer (Thermo Fisher Scientific), first for 5 minutes then for 3 minutes. Cells were washed and resuspended in 1.0 mL of PBS. Approximately half of the sample was pelleted and reserved for genomic DNA analysis, the other half of the sample was further processed for flow cytometry staining. During terminal cardiac puncture bleeds, blood was collected in test tubes and allowed to clot for 30 minutes. Serum from the supernatant was then stored at 4°C.

Liver, spleen, femurs, and, when available, thymus and lymph nodes of mice were harvested at necropsy. Livers and spleens were processed into single cell suspensions by grinding the tissue between the frosted edges of two microscope slides. Bone marrow was isolated from femurs by removing all excess tissue around the bone and snipping at the trochanter and epicondyle ends. A 27-gauge needle was inserted through the medullary cavity, and the cavity was flushed with 1.0 mL

of PBS twice. Thymus and lymph nodes were processed into single cell suspensions by using the back end of the plunger of a 3-mL syringe to pass the tissue through a 100 µm cell strainer placed in a dish with PBS. Cell suspensions were filtered through a 100 µm cell strainer and washed with PBS. Of each sample type, approximately 2.0×10^5 cells were reserved for flow cytometry, 2.0×10^5 cells were processed for genomic DNA extraction, and 2.0×10^5 cells were cryopreserved in 90% FBS and 10% DMSO.

Recombinant bnAb production

The transgene for 10-1074 bnAb was cloned into a mammalian expression plasmid (pTT3) containing a NHP IgG constant heavy chain with a 6x His-Avi-Tag using In-Fusion (Takara Bio[160]). The resulting plasmid (pTT3 10-1074 NHP-IgG) expressed full length antibody and was confirmed by whole plasmid sequencing (Plasmidsaurus).

Human embryonic kidney (HEK) 293E cells, which are engineered for enhanced protein expression, were maintained in RPMI media containing 10% FBS and 1% penicillin/streptomycin at 37°C and 5% CO_2.[160] One day prior to transfection, 1.6×10^7 cells were seeded in a TC-treated T150 flask with Freestyle 293 Expression Medium (Gibco) at a density of 5.0×10^7 cells/mL. 10 µg of pTT3 10-1074 NHP-IgG was transfected using 40 µL 293-Free Transfection Reagent (MilliporeSigma). Cell cultures were grown out for 7 days, after which recombinant protein was isolated from the supernatant using Protein A IgG Purification Kit (Thermo Fisher Scientific).

Bio-layer interferometry

HIV gp120 monomers from various clade C strains – including 16055-2 (accession ABL67444.1, Abcam), Du172.17 (accession DQ411853), ZA.1197MB (accession AY463234), CN97001 (accession G4XFJ5-1 with E46G, T396A, A497T), and ZM249M.PL1 (accession DQ388514, Thermo Fisher) – were

screened for kinetic interactions with recombinant 10-1074 using the Octet RED96 Instrument (Sartorius). Anti-Human Fc Capture (AHC) Biosensors (Sartorius) were soaked for 15 minutes in Kinetics Buffer consisting of 1% Bovine Serum Albumin (BSA; Thermo Fisher Scientific), 0.05% sodium azide (MilliporeSigma), and 0.02% polysorbate 20 (Tween20; MilliporeSigma) in PBS. 1 μM of antigen and 40 μg/mL of antibody were loaded onto a non-treated, clear bottom 96-well plate. A non-specific antibody (MxR01, courtesy of Matthew Gray) was used as a negative control. AHC probes were loaded onto the instrument and allowed to equilibrate in the kinetics buffer. Once confirmed, 10-1074 was loaded onto the probe, and a baseline with the loaded antibody was confirmed. The association of the antibody to various antigens was then measured. To determine dissociation, probes were dipped into analyte free kinetics buffer. Association Rate Constant (K_a), Dissociation Rate Constant (K_d), and Affinity Constant (K_D) were calculated, and the control antibody sample was adjusted to be the baseline standard for all antigens using the Octet Software (Sartorius, version 3.43).

Flow cytometry

Flow cytometry samples were first stained for dead cells by incubating in Zombie-NIR Live/Dead Stain (BioLegend) diluted 1:250 in PBS for 15-20 minutes. Cells were washed with 1.0 mL FACS buffer (1mM EDTA (Thermo Fisher Scientific) and 0.5% FBS in PBS), and mouse samples were incubated in Fc block (anti-mouse CD16/CD32, clone 2.4G2, BD Biosciences) diluted 1:25 in FACS buffer for 10 minutes. Antibodies used in the various flow panels were combined in FACS buffer and added to cells for 20-30 minutes (Tables S5-6). Samples were washed and resuspended in FACS buffer and run on a FACSCelesta for cell cultures or a FACSymphony A5 for mouse samples (BD Biosciences). Results were analyzed to exclude dead cells and debris, and to sort live cells by a standard gating strategy using FlowJo (TreeStar, version 10.8.0, Figures S10-11).

Kinetic colorimetric ELISA

Nunc immuno clear bottom 96-well plates (Thermo Fisher Scientific) were coated with 100 ng per well of HIV gp120 (426c Core with biotin, courtesy of Matthew Gray) in 100 µL PBS. Freshly coated plates were sealed and shaken at 250 rpm for 5-10 minutes to evenly distribute antigen and then incubated overnight at 4°C. Post-incubation, all wells were washed three times with wash buffer (0.05% Tween20 in PBS). Plates were blocked by incubating in 150 µL blocking buffer (wash buffer with 3.0% BSA) and shaking at 250 rpm for 1 hour at room temperature. Excess blocking buffer was removed and 100 µL of recombinant 10-1074 was loaded onto the plate in serial dilutions ranging in concentrations from 1-2,048 ng/mL as standards. Plasma samples were loaded onto the plate at a 1:50 dilution in blocking buffer. The plate was shaken at 250 rpm for 90 minutes at room temperature. The plate was washed 3 times with wash buffer, and goat anti-rhesus IgG(H+L)-horseradish peroxidase (HRP, SouthernBiotech) at a 1:6,000 dilution (MISTRG plasma) or a 1:3,000 dilution (MISTRG6 plasma) in blocking buffer was added to the wells and incubated for 1 hour. The plate was washed 3 times with wash buffer, and 100 µL of 3,3',5,5'-tetramethylbenzidine (TMB) solution (Thermo Fisher Scientific) was added to each well. Samples and standards were then analyzed at 2.5-minute increments up to 30 minutes using a BioTek Synergy H4 Hybrid Multi-Mode Microplate Reader (Marshall Scientific) set at a 405 nm absorbance wavelength.

Figures

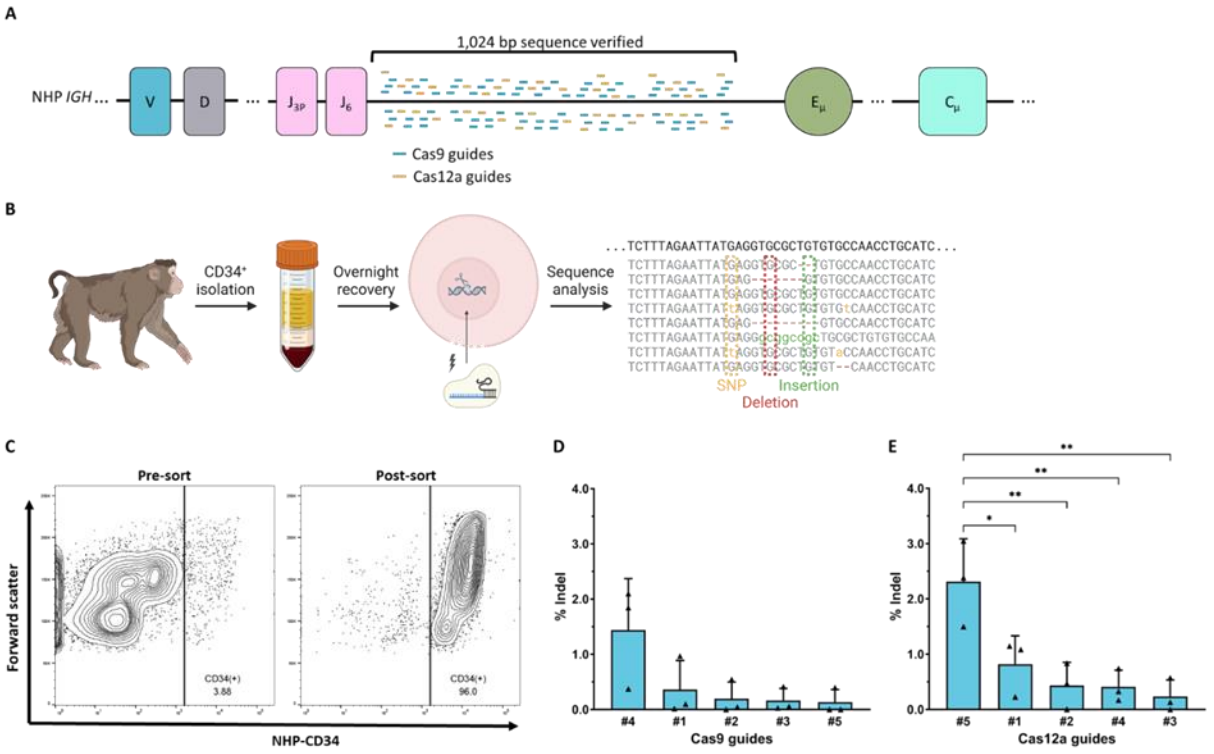

Figure 1. CRISPR/Cas guides capable of editing of IGH locus in NHP HSPC.

(A) Target genomic site within the NHP *IGH* locus, between the *VDJ* genes and the constant regions, sequence verified in two NHP species, *M. mulatta* and *M. nemestrina*. All possible Cas9 and Cas12a guides were screened within this sequence. (B) $CD34^+$ HSPC were isolated from *M. nemestrina* bone marrow aspirates and electroporated with RNP. Target locus was analyzed for genetic edits, including single nucleotide polymorphisms (SNP), insertions, and deletions (indel). (C) $CD34^+$ purity following immunomagnetic separation as measured by flow cytometry. (D, E) Indel frequency of selected Cas9 (D) and Cas12a (E) guides 3 days after electroporation of 10^6 $CD34^+$ cells (n = 3 biological replicates, 3 donors). Data are presented as mean ± standard deviation (SD). Significance was calculated with an ordinary one-way ANOVA with *p<0.05, and **p<0.01.

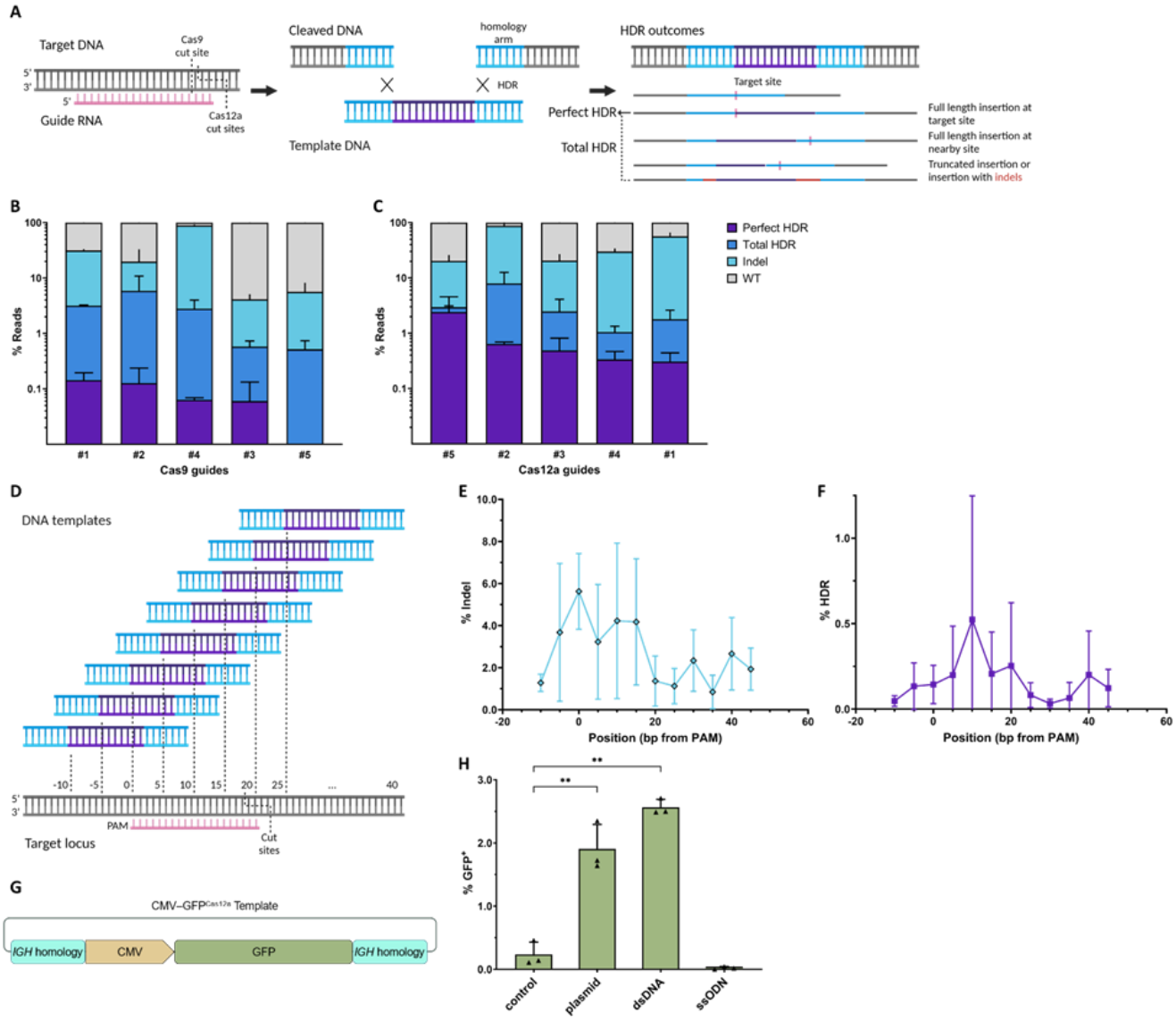

Figure 2. Guides associated with HDR events using short templates enable knock-in and expression of transgene encoding cassettes.

(A) Cas9 and Cas12a guides produce distinct cuts, allowing knock-in of template with homology to cut site, and result in different HDR outcomes. (B, C) HDR frequency with Cas9 (B) and Cas12a (C) guides following electroporation in 10^6 LCL 8664 cells, a cell line derived from *M. mulatta* lymphocytes (n=3 experimental replicates). Reads were classified by editing outcomes. (D) ssODN templates positioned for insertion at different distances from PAM, varying from -10 bp to +40 bp. (E, F) Fraction of reads containing indel and perfect HDR events following electroporation in 10^6 LCL

8664 cells (n = 3 experimental replicates). (G) GFP template was constructed for knock-in and genomic expression. Homology arms were designed for insertion at cut site of optimal Cas12a guide. (H) Stable GFP expression 15 days following electroporation in 10^6 LCL 8664 cells using different templates: plasmid without RNP (control), plasmid, dsDNA, or ssODN with RNP (n = 3 experimental replicates). Data are presented as mean ± SD, significance calculated with an ordinary one-way ANOVA.

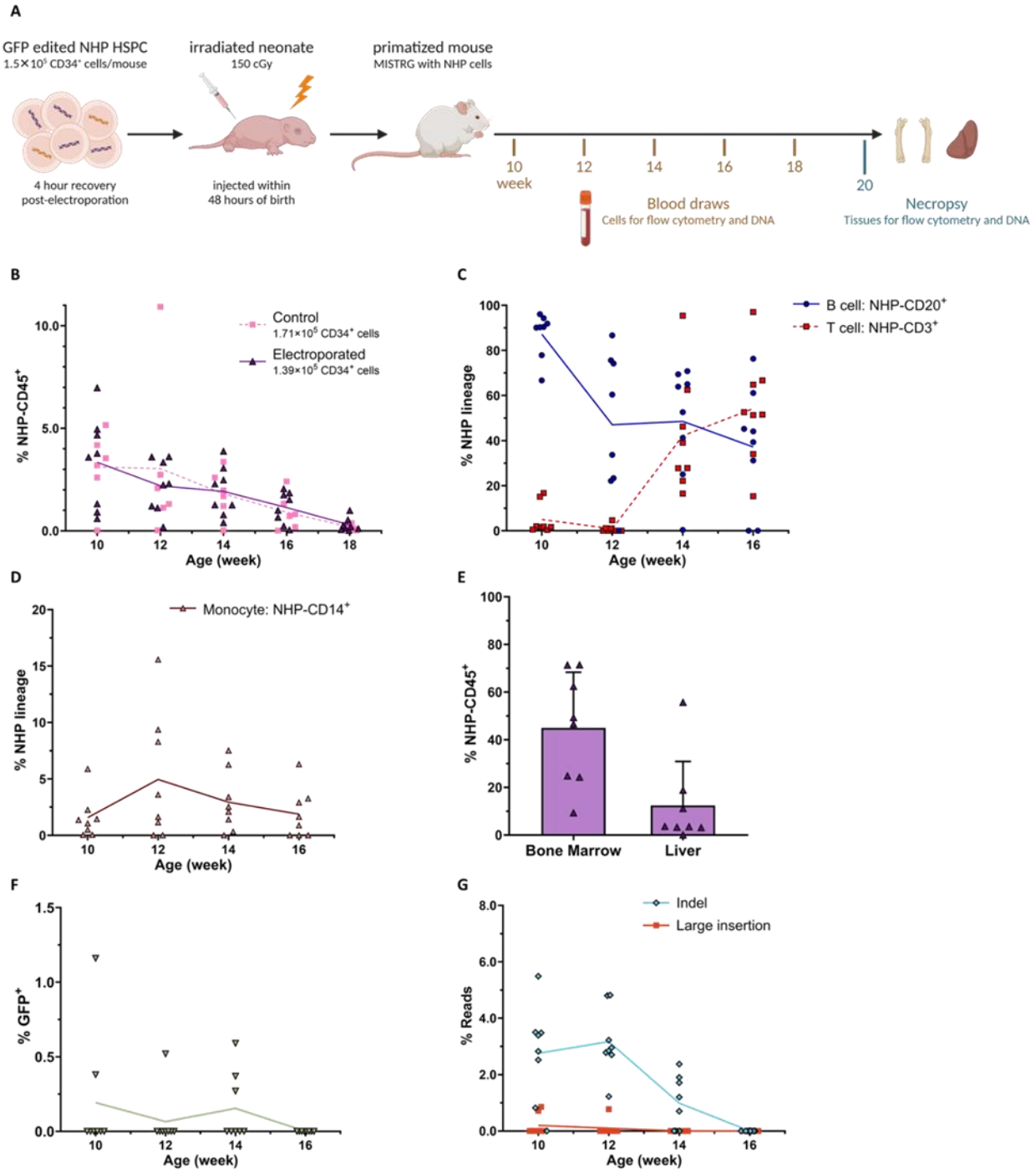

Figure 3. Edited HSPC engraft in MISTRG model and express inserted transgene.

(A) NHP HSPC electroporated with VH4-GFP^{Cas12a} were injected into sub-lethally irradiated, neonatal MISTRG mice. Hematopoietic lineages in the primatized mice were monitored over time and at necropsy. (B) Engraftment levels in peripheral blood over time as measured by flow cytometry on

NHP-CD45$^+$ cells from mice injected with electroporated or control HSPC. n = 8 mice, n = 2 NHP donors (electroporated group, 1.39 × 10^5 CD34$^+$ cells/mouse). n = 6 mice, n = 2 NHP donors (control group, 1.71 × 10^5 CD34$^+$ cells/mouse). (C, D) Multilineage engraftment in peripheral blood over time as measured by frequency of B cells (CD3$^-$ CD20$^+$), T cells (CD3$^+$ CD20$^-$), and monocytes (CD3$^-$ CD20$^-$ CD14$^+$) in NHP-derived populations (NHP-CD45$^+$). (E) Engraftment levels in the bone marrow (femur) and the liver at necropsy, performed at week 20. Error bars represent SD. (F) *In vivo* transgene expression as measured by frequency of GFP$^+$ cells in NHP-derived populations (NHP-CD45$^+$), as compared to total B cell frequency in peripheral blood over time. (G) Editing levels at the NHP *IGH* locus in peripheral blood as measured by high-throughput sequencing on MiSeq platform. Large insertions represented by insertions >8 bp. Lines represent means in (B, C, D, F, and G). n = 8 mice, n = 2 NHP donors (electroporated group, week 18 omitted for low engraftment levels, C-G).

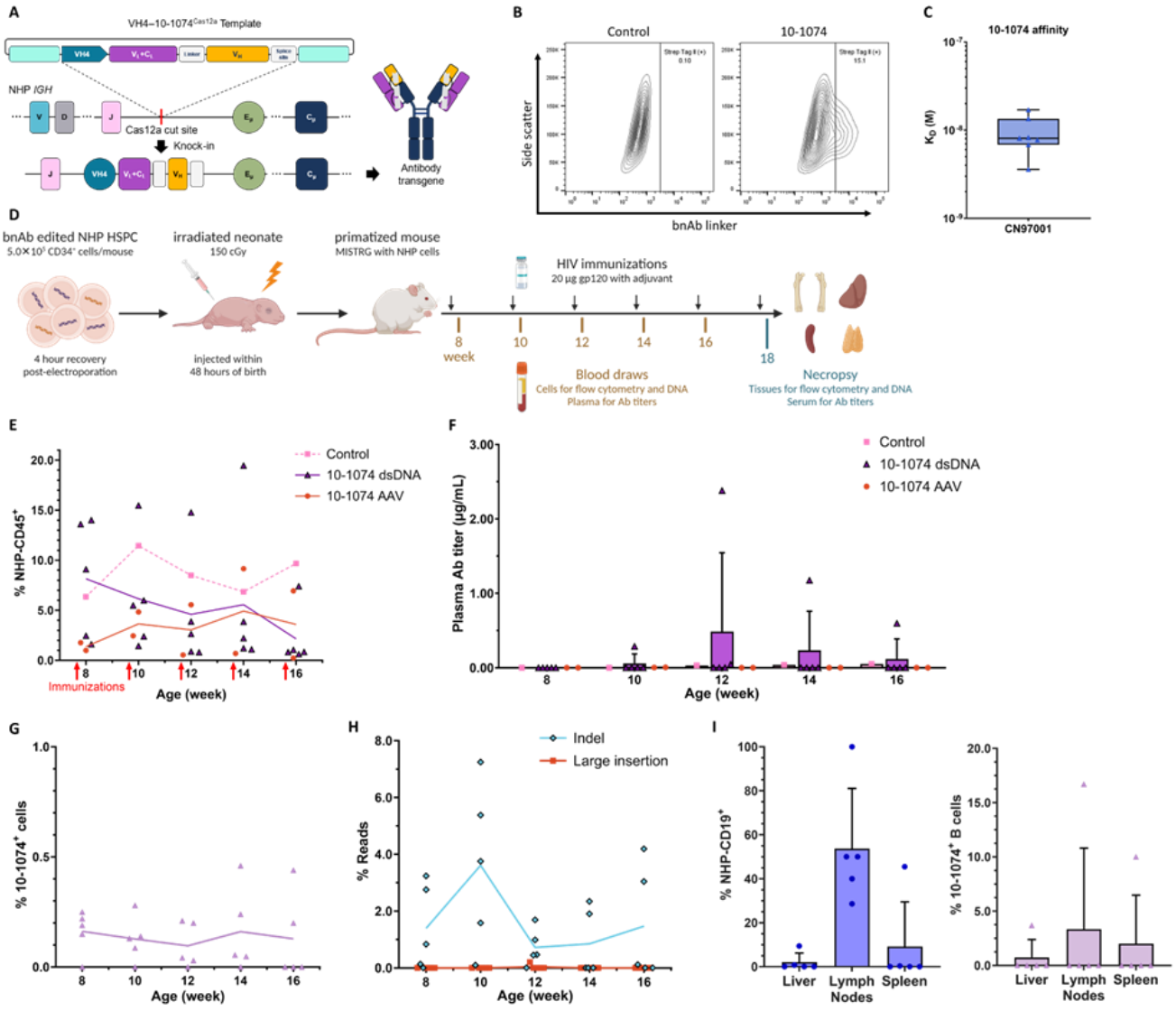

Figure 4. bnAb transgene expression and immunization in MISTRG mice.

(A) bnAb template was designed for expressing the full light chain and the variable heavy chain fragment of 10-1074. Following productive knock-in at the target locus, bnAb expression replaces endogenous antibody production, bypassing VDJ recombination and forming a full-length transcript via splicing with a constant heavy chain. (B) *In vitro* 10-1074 production as confirmed by staining of cell surface transgene linker. Flow cytometry was performed on HEK 293E cells following transduction with an expression vector containing an IgG constant heavy chain. (C) Binding of recombinant bnAb to HIV antigen, the gp120 protein of strain CN97001, as measured by bio-layer

interferometry (BLI) and quantified as the dissociation constant (K_D). n = 6 technical replicates. (D) NHP HSPC were electroporated with VH4-10-1074^{Cas12a}, either as dsDNA or AAV, and transplanted into MISTRG mice as before. Beginning at week 8, mice were immunized with CN97001 gp120 injections once every two weeks until necropsy. Control mice were injected with unedited HSPC. (E) Engraftment levels in peripheral blood over time as measured by flow cytometry on NHP-CD45$^+$ cells in mice injected with edited HSPC using different templates. (F) *In vivo* anti-HIV antibody titers were measured by ELISA with a biotinylated gp120 on diluted plasma samples. dsDNA: n = 5 mice, n = 2 NHP donors. AAV: n = 2 mice, n = 2 NHP donors. Control: n = 1 mouse, n = 2 NHP donors. n = 2 technical replicates per sample. (G) Cell surface expression of 10-1074 in peripheral blood as measured by flow cytometry with antibody against its linker. (H) Editing levels at the NHP *IGH* locus in peripheral blood as measured by high-throughput sequencing (MiSeq). Large insertions represent insertions >8 bp. (I) B cell populations and fraction of B cell population expressing 10-1074 at necropsy, week 18, as measured by flow cytometry on NHP-CD19$^+$. n = 5 mice, n = 2 NHP donors (10-1074 dsDNA group, G-J). Error bars represent SD.

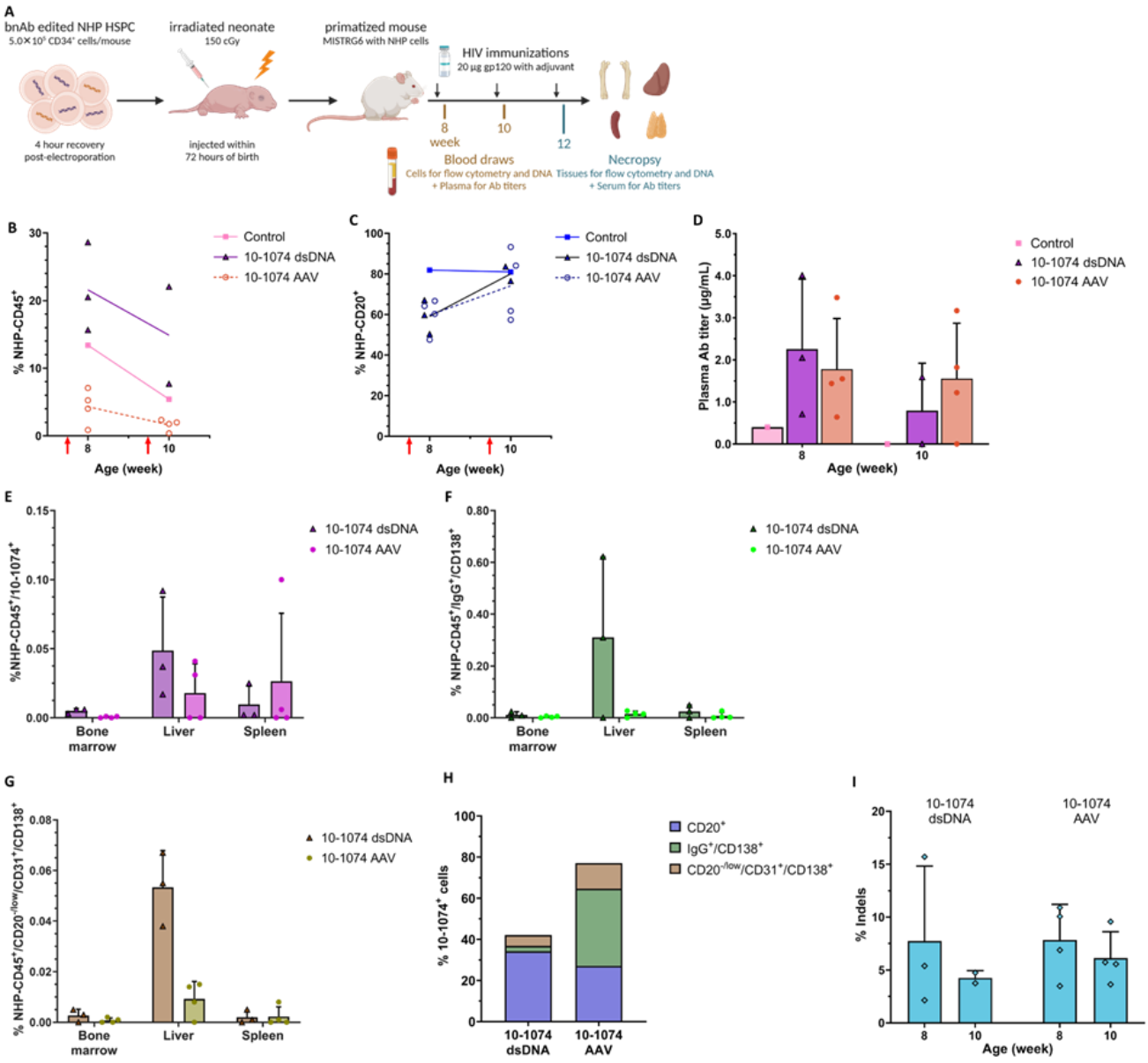

Figure 5. MISTRG6 mice support more robust NHP HSPC engraftment and antibody production from liver and spleen.

(A) MISTRG6 mice were xenotransplanted using the same protocol applied in MISTRG mice, this time allowing up to 72 hours from birth for HSPC injections. Necropsy was performed at an earlier timepoint to allow the detection of 10-1074-producing cells while antibody titers were still detectable. Control mice received unedited $CD34^+$ cells. (B) NHP engraftment levels in the peripheral blood of MISTRG6 mice over time. (C) B cells (NHP-$CD4^-$/$CD8a^-$/$CD20^+$) as a fraction of

NHP lineage in the peripheral blood of MISTRG6 mice. (D) Anti-HIV antibody titers in the plasma of MISTRG6 mice as measured by ELISA. (E-G) 10-1074-expressing cells (Strep Tag II^{+}), IgG-producing cells (NHP-IgG^{+}/CD138^{+}), and plasma cells (NHP-CD20$^{-/low}$/CD31^{+}/CD138^{+}) in different tissues of MISTRG6 mice at necropsy. (H) Fraction of total 10-1074-expressing cells found across all tissues that are either B cells, antibody-producing cells, or plasma cells. (I) Editing levels at the target locus in peripheral blood. n = 8 mice, n = 3 NHP donors. Error bars represent SD. Red lines in (B-C) represent immunizations.

Supplemental Information

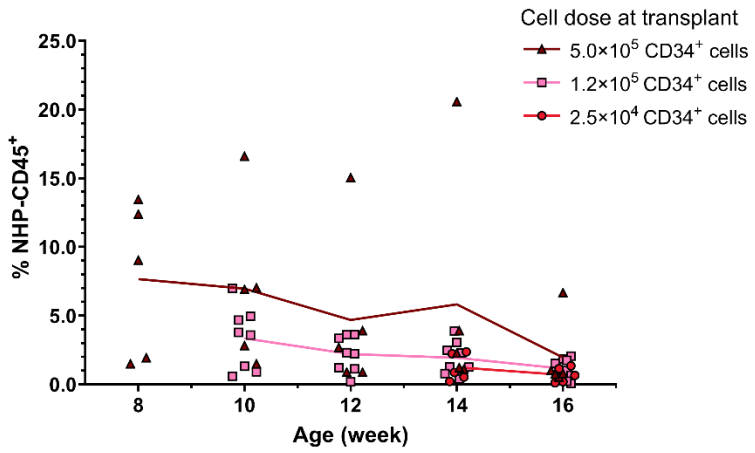

Figure S1. NHP HSPC engraftment in MISTRG mice at escalating cell doses.

Engraftment levels in peripheral blood over time as measured by flow cytometry on NHP-CD45$^+$ cells in mice injected with different doses of electroporated HSPC. n = 5 mice, n = 1 NHP donor (2.5 × 10^4 cell dose group). n = 8 mice, n = 2 NHP donors (1.2 × 10^5 cell dose group). n = 5 mice, n = 2 NHP donors (5.0 × 10^5 cell dose group).

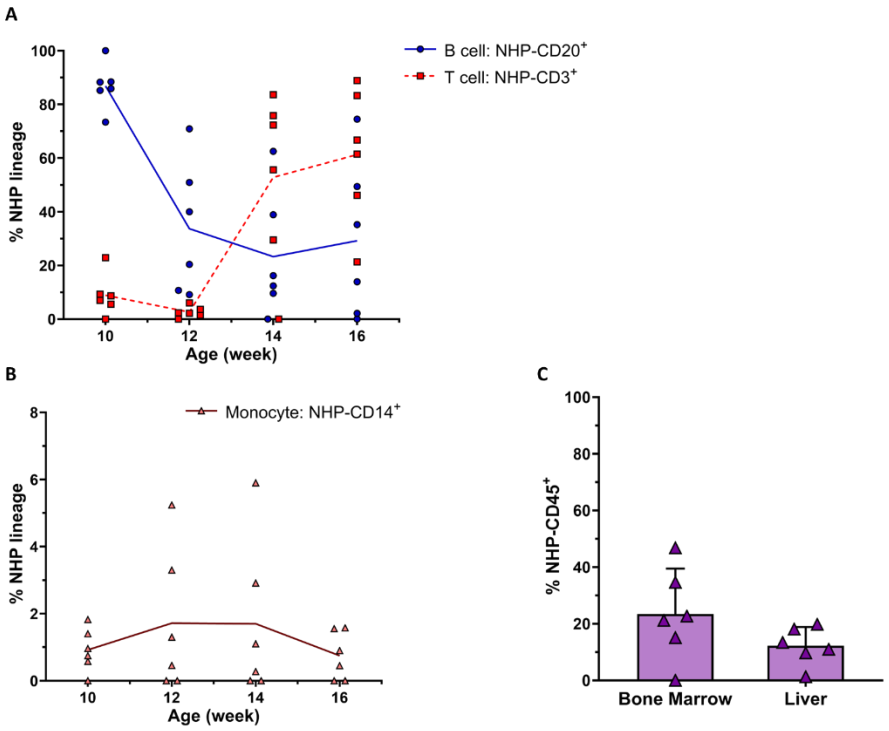

Figure S2. Control NHP HSPC differentiate into mature cell types in MISTRG model.

(A, B) Multilineage engraftment in peripheral blood over time as measured by frequency of B cells ($CD3^-$ $CD20^+$), T cells ($CD3^+$ $CD20^-$), and monocytes ($CD3^-$ $CD20^-$ $CD14^+$) in NHP-derived populations. (C) Engraftment levels in the bone marrow (femur) and the liver at necropsy, performed at week 20. n = 6 mice, n = 2 NHP donors (control group, week 18 omitted for low engraftment levels, A-B). Error bars represent SD (C).

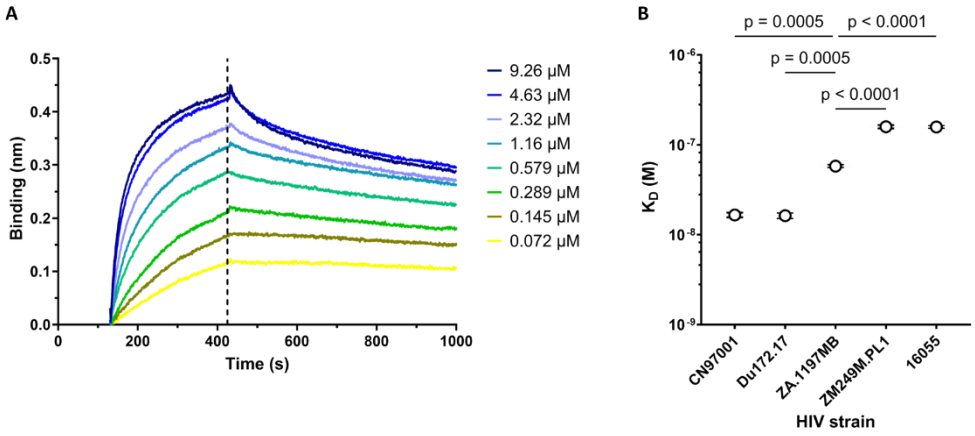

Figure S3. Recombinant 10-1074 antibody binds to HIV antigen.

(A) Binding of 1 µM gp120 monomer from HIV CN97001 to recombinant 10-1074 at varying antibody concentrations as measured by wavelength shift using bio-layer interferometry (BLI). Binding and dissociation phase, separated by dotted line, are shown here. Samples were aligned at beginning of binding phase. Lines represent mean. (B) Dissociation constant (K_D) calculated from BLI measurements for binding of recombinant 10-1074 to gp120 monomer from different HIV strains. Data are presented as mean ± SD. Significance was calculated with an ordinary one-way ANOVA. n = 2 technical replicates.

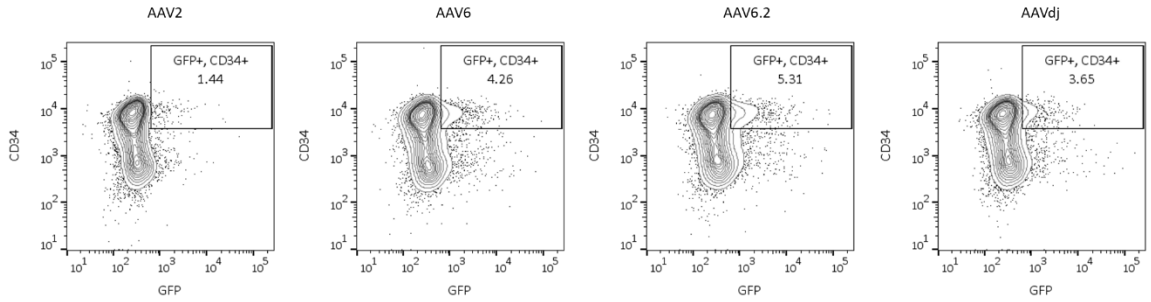

Figure S4. AAV6.2 transduces NHP HSPC and leads to GFP expression.

$CD34^+$ cells were transduced with AAV from 4 different serotypes containing a CMV-mediated GFP reporter at an MOI of 6.67×10^5. GFP expression was measured by flow cytometry 24 hours later. Transduction at an MOI of 2.40×10^4 did not produce significant GFP expression.

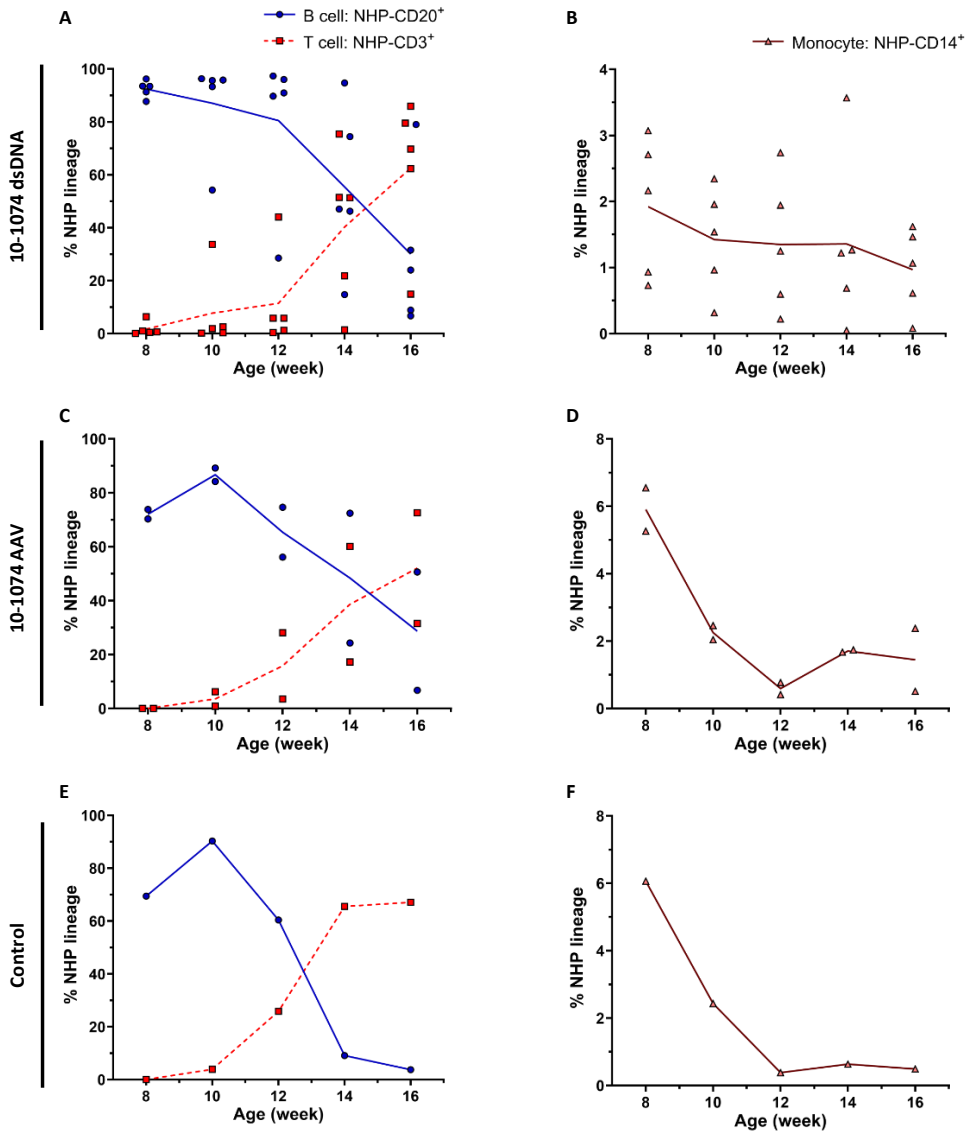

Figure S5. Hematopoietic lineages form in MISTRG mice injected with HSPC with or without different DNA templates.

Multilineage engraftment in peripheral blood over time as measured by frequency of B cells ($CD3^-$ $CD20^+$), T cells ($CD3^+$ $CD20^-$), and monocytes ($CD3^-$ $CD20^-$ $CD14^+$) in NHP-derived populations for mice receiving NHP HSPC electroporated with dsDNA (A, B) or AAV (C, D), as compared to mice receiving control NHP HSPC (E, F).

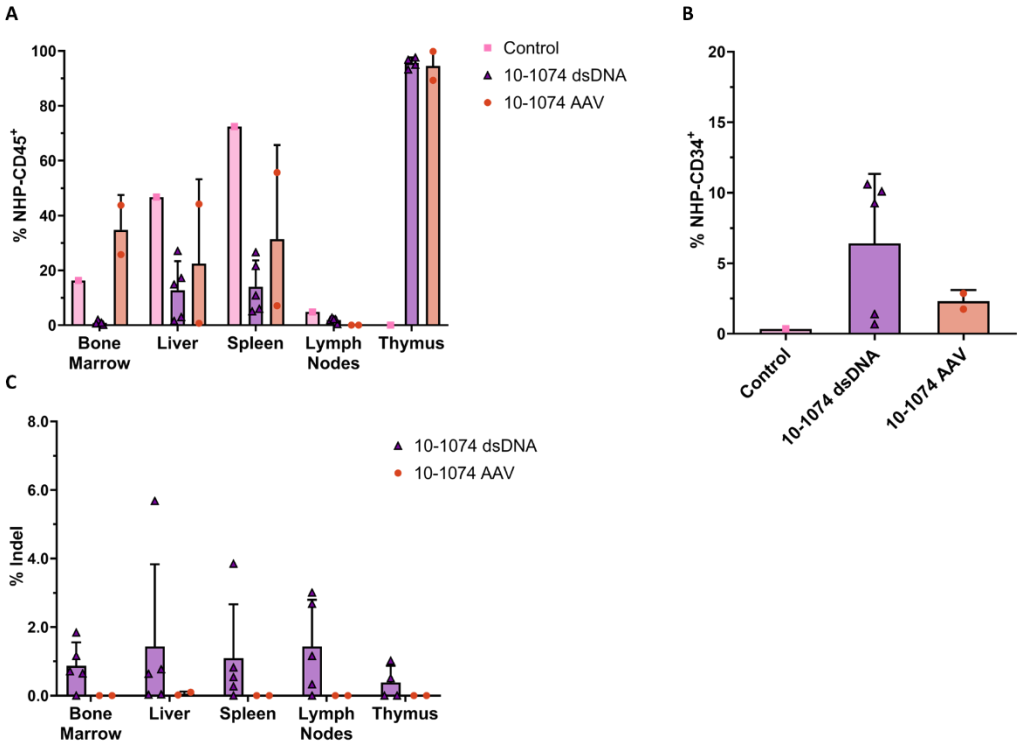

Figure S6. Engraftment and editing levels in various tissues at necropsy for MISTRG mice receiving different DNA templates.

(A) Fraction of NHP-CD45$^+$ in single cell suspensions from the bone marrow (femur), liver, spleen, lymph nodes, and thymus at necropsy, performed week 18. (B) Fraction of NHP lineage that is CD34$^+$ in the bone marrow. (C) Editing levels at the NHP *IGH* locus in the bone marrow, liver, spleen, lymph nodes, and thymus, as measured by fraction of MiSeq reads containing indels. n = 5 mice, n = 2 NHP donors (10-1074 dsDNA group). n = 2 mice, n = 2 NHP donors (10-1074 AAV group). n = 1 mouse, n = 2 NHP donors (control group). Error bars represent SD.

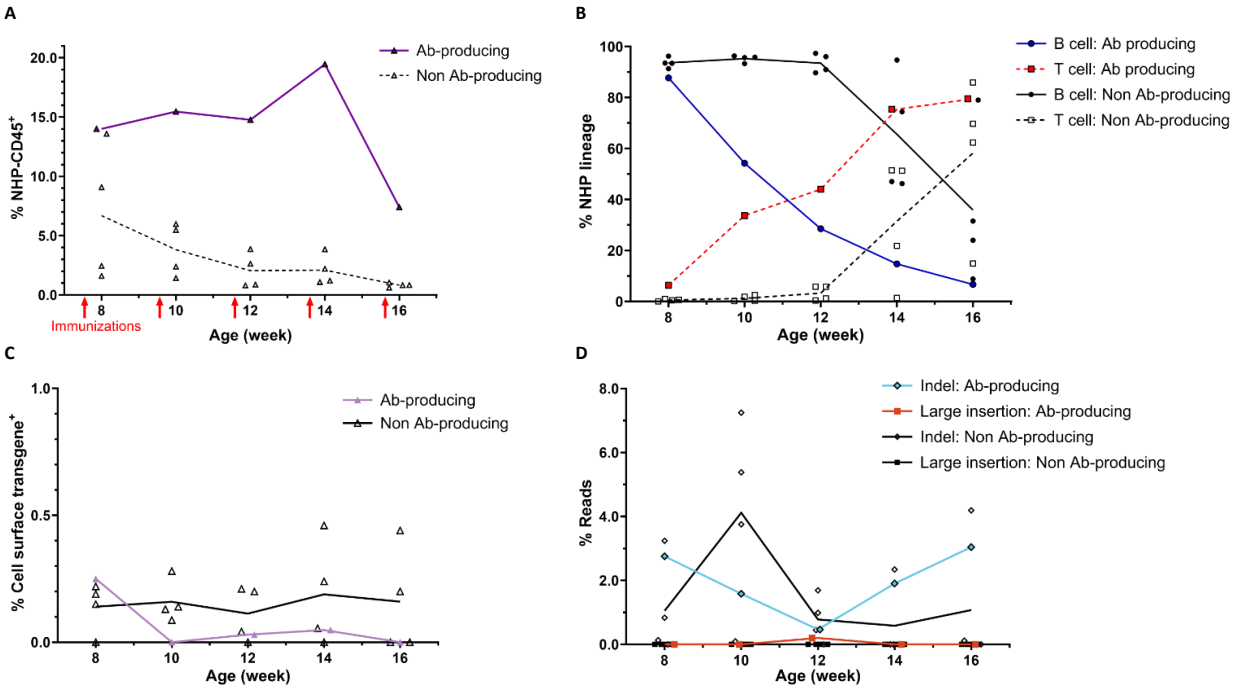

Figure S7. Engraftment, cell lineage, and editing in antibody-producing MISTRG mouse.

(A) Engraftment levels in peripheral blood over time as measured by flow cytometry on NHP-CD45$^+$ cells in 10-1074-producing mouse and non 10-1074-producing mice. (B) Lymphocyte populations in peripheral blood over time as measured by frequency of B cells (CD3$^-$ CD20$^+$) and T cells (CD3$^+$ CD20$^-$) in NHP-derived populations for 10-1074-producing mouse and non 10-1074-producing mice. (C) Cell surface expression of transgene in peripheral blood as measured by flow cytometry with antibody against its linker for 10-1074-producing mouse and non 10-1074-producing mice. (D) Editing levels at the NHP *IGH* locus in peripheral blood of 10-1074-producing mouse and non 10-1074-producing mice. Large insertions representing insertions >8 bp. The MISTRG mouse (n = 1 of 5, 20%) with detectable anti-HIV antibody titers has been singled out in each graph.

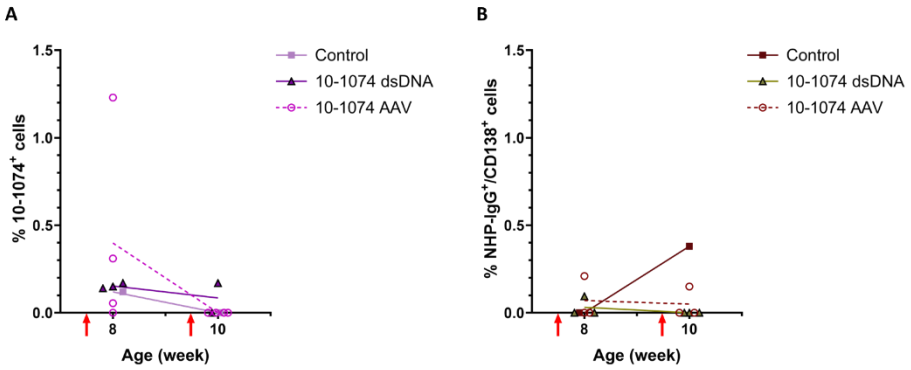

Figure S8. 10-1074-expressing and IgG-producing cells in circulation in MISTRG6.

(A) Cell surface expression of 10-1074 transgene in peripheral blood as measured by flow cytometry with antibody against its linker. (B) IgG-producing cells as measured by frequency of NHP-IgG$^+$/CD138$^+$ cells in NHP-derived populations (NHP-CD45$^+$). Red lines in represent immunizations.

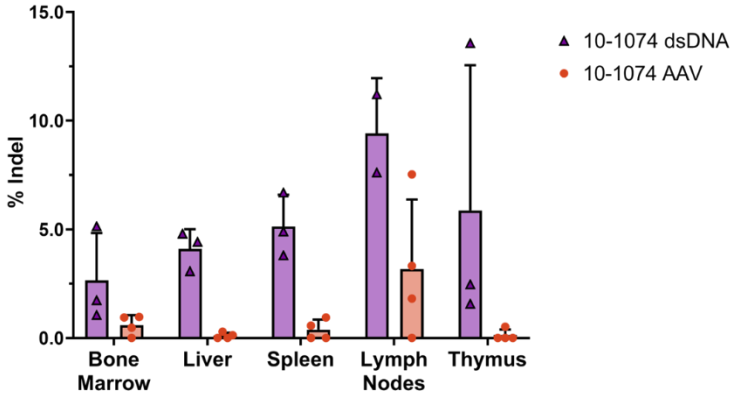

Figure S9. Editing levels in various tissues at necropsy for MISTRG6 mice.

Editing levels at the NHP *IGH* locus in the bone marrow, liver, spleen, lymph nodes, and thymus, as measured by fraction of MiSeq reads containing indels.

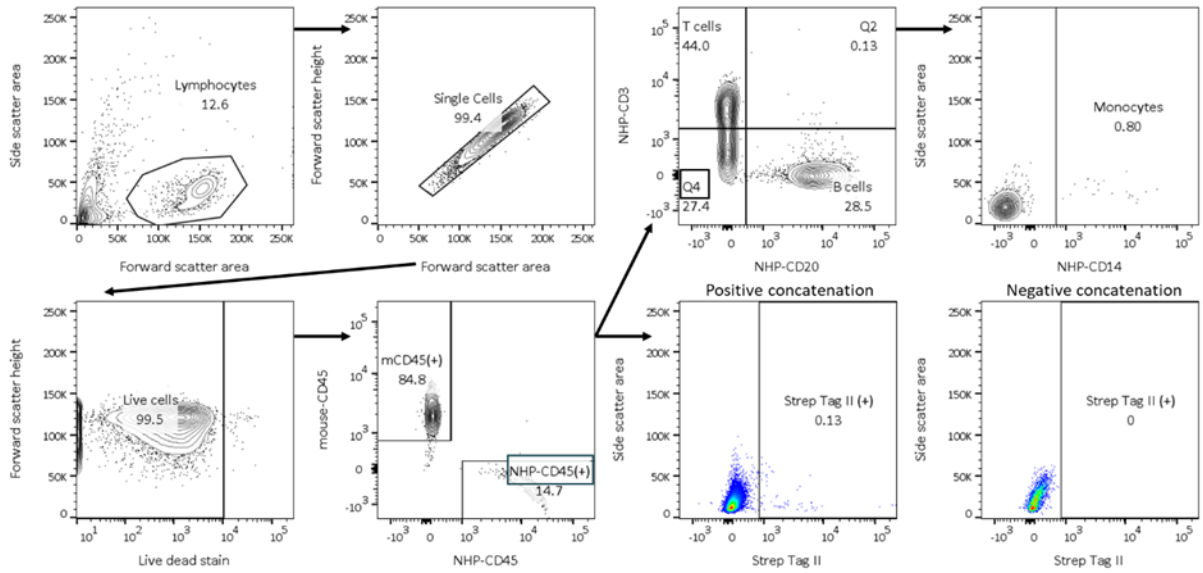

Figure S10. Flow cytometry gating strategy for MISTRG samples.

Example of gating strategy for flow cytometry of peripheral blood from antibody-producing mouse at week 12. Compensation was calculated for every fluorophore and each sample. For CD34 enriched samples, live cells were only gated on CD34 levels. For necropsy samples, B cells were gated as NHP-CD19^{+}/CD4^{-}/CD8a^{-}. Strep Tag II gates shown as concatenation of positive or negative samples due to low event counts.

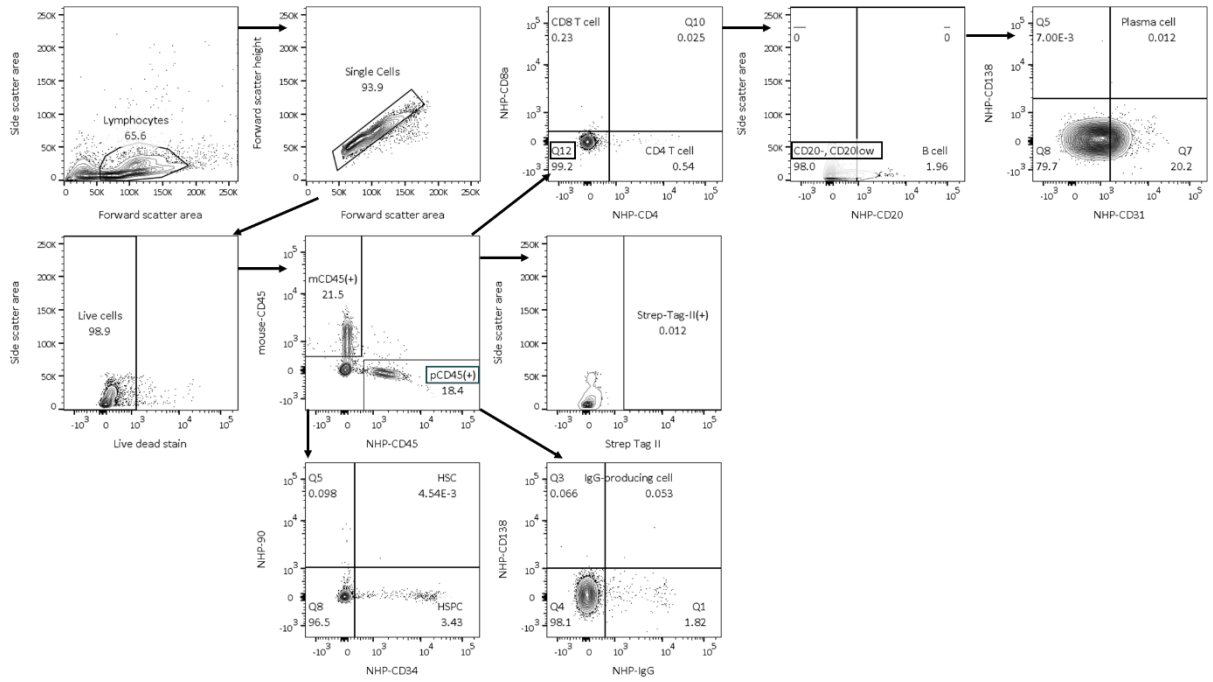

Figure S11. Flow cytometry gating strategy for MISTRG6 samples.

Example of gating strategy for flow cytometry of bone marrow from mouse injected with HSPC electroporated with dsDNA. Peripheral blood samples were gated using the same strategy. Compensation was calculated for every fluorophore and each sample.

Sequence S1. Template knock-in at *M. nemestrina IGH*

Upstream homology arm (PAM blocking mutation) : Site for barcode integration : VH4 promoter including Kozak sequence : Recombinant 10-1074 including splice site : Site for barcode integration : Downstream homology arm (Mutation for synthesis) : Reference sequence

TTGGAAAATGGGACTTAGGTTGGATGTGTCTGATGGAGTAACTGAGCCTGGGGGCTTGGGGAGCCACA

TTTGGACGAGATGCCAGAGCAAACCAGGGGTCTTAGTGATGGCTGAGGAATGTGTCTCAGGTGCGGTG

TCTGTAGGACTGCAAGATCGCTGCACACACAGCGAATCATGAAACATTATCTTTAGAATTATGAGGGATC

CTCGGACGAATTCCACACTCTCCGGGACAGATATATTCCCTCTAACCATGATGGATATTCTGAATTACAA

TAAACATTGCACGGATGTAGGTTTATATAAATTCACTGTGACGAATATATTTAGCTGCTGCCCTAATGTTTT

GAATGGAGATTTGACAATTTAGATAACCTGGATGTTTGGTTGGTTTCATATAAATCTTCAAGGGTACAACA

GCATTGAACCTATTCCAAAATCTATCCCTGATCCATGATCATACTCATCTCCCAGACCAGCTCCTTCAG

CACATCTCCCTACCTGGAAGAAGAGGAGTCTGGGCTTGGTGAGGGGAGGCCCCAGGAAGAGAACTG

GGTTCTCAGAGGGCACAGCCAGCATCCTCCTCTCAGGGTGAGCCCCAAAGACTGAGGCCTCCCTCA

TCCCTTTTCACCTCTCCATACAAAGGCACCACCCACATGCAAATCCTCACTTAGGCACCCACAGGAAA

CCACCACACATTTCCTTAAATTCAGGGTCCAGCTCACATGGGAAATGCTCTCTGAGAGTCACGGACCT

CCTGTGCAAGAACATGAAGCACCTGTGGTTCTTCCTCCTCCTGGTGGCAGCTCCCAGATGTGAGTGTA

GCTACGTTCGACCTCTCAGCGTTGCATTGGGAGAAACTGCTCGGATATCCTGCGGCAGGCAGGCCTT

GGGGAGTCGGGCAGTACAATGGTACCAACATAGACCAGGCCAGGCTCCAATCTTGTTGATTTATAATAA

TCAGGATAGGCCAAGCGGAATCCCCGAGAGGTTTTCTGGCACACCAGATATAAACTTTGGGACCCGA

GCAACACTCACTATCTCTGGGGTCGAGGCCGGAGACGAGGCTGACTACTATTGCCATATGTGGGATTC

AAGGTCCGGTTTCTCTTGGTCCTTTGGAGGTGCCACACGACTCACAGTGCTGGGCGGGCAGCCAAAA

GCATCTCCTTCCGTAACACTCTTTCCTCCATCATCTGAAGAATTGCAAGCCAATAAGGCTACCCTCGTTT

GCCTCATATCTGATTTTTATCCAGGCGCAGTCGAAGTGGCCTGGAAAGCTGATGGGTCTGCAGTCAATG

CAGGTGTCGAGACAACAAAGCCTTCAAAGCAGTCCAACAACAAGTACGCCGCCTCTTCCTACTTGTCT

CTCACATCTGATCAATGGAAAAGCCATAAGTCTTACAGCTGCCAGGTGACTCACGAAGGGAGCACTGT

AGAGAAGACCGTCGCTCCCGCTGAATGTTCTGGAGGCAGTTCTGGATCTGGGTCCGGAAGCAACTGG

TCTCATCCACAGTTCGAAAAAGGAGGGGGTGGATCAAATTGGTCACACCCACAGTTTGAAAAAGGAGG

TGGAGGTTCCAATTGGAGCCACCCACAATTCGAGAAAGGCTCAGGAGGCGGAGGGAGCGCAGGTGG

GCAGGTGCAGTTGCAAGAGTCCGGTCCTGGACTCGTTAAGCCATCTGAAACTCTTAGCGTCACCTGCT

CTGTCTCCGGAGACTCCATGAACAACTACTACTGGACTTGGATTCGGCAATCACCCGGCAAGGGACTT

GAATGGATCGGCTATATCTCAGACCGCGAATCTGCAACATACAATCCATCTCTCAATAGCAGAGTTGTT

ATTTCACGAGATACTTCAAAAAATCAGTTGTCCTTGAAGCTTAATTCAGTAACCCCCGCTGACACAGCCG

TGTACTATTGTGCTACTGCCAGACGCGGACAACGGATCTATGGTGTTGTAAGTTTCGGGGAGTTTTTTTA

CTATTATTCAATGGATGTCTGGGGGAAGGGAACTACTGTCACAGTGAGCAGCGGTGAGTCCTCACAAC

CTCTCTCCTGCTTTAACTCTGAGGGGTTTTGCTGCATTTTTGGGGGAAAACAAGTGTGGCGGCCGCTAC

GTAACTAGTGTGCGCTGTGTGCCAACCTGCATCTTAAATTCTTTGTTGGCTGGAAAGAGAACTGTCAGAG

TGGGTGAATCCAGCCAGGACGGATGCGTAGCCTTGGTCTTGATGAGAGCAGGGTCGGGGCACGGGT

AGTCCAGAAAGGGTGGCTGCTGTCCTGACAGAGGCTTAGGGAGGCCACAGGAGCTCAGTGCCCTGA

AGTTGGTTTCCAAGAGAAAAGGATTGTTCATCTTAAGAGGCGTGCTTATTAAATGTTAAAAGACAGGATAT

GTTTGAAGTGGCTCCAGAGAAAAATGGTTAAGACAATTATGACTTAAAAATGTGAAAGATTTTGAAGTATAT

TAATTTTTTTAACTGTCTAAGTATTTGAAATTCTTATCATTTGATTAACACCCATGAGTGGTATGTCTCTGGAA

TTAGGGCCAAAGTAAGTTTAGCTAAGAAATACTAGCACAGTGCTGTCGGCTCTGATGCAGGACTGAGTT

TTGAGCATCATAAATCAAGTTTATTTTTTTAATTAATTGAGTGAAGCTGGGAGCGGATGATGAGTTAGAGTC

AAGATGGCTGCATGGGGGTCTTGGGCACCCACAGCAGGTGGCAGGAAGCAGGTCACCGCAAGAGTC

TATTTTAGGAAGCAAAAAAACACAATTGGTAAATTTATCACTTCTGGTTGTGAAGAGGTGGTTTCGCCTGG

GCCCAGATCTGAAAGTGCTCTACTGAGCAAAACAACACCTGGACGATTTGCGTTTCTAAAATAAGGCAA

GGCTGACCGAAACTGGAAAGGCTCTTTTTTTTTTAACTATCAGAATTTCATTTCCAATCTTAGCTTATCAAC

TGCTAGTTTGTGCAAACAGGATATCAACTTCTAAACTGCATTCATTTTTACAGTAAGATGTTTAAGAAATTAA

AGAGTCTTAGGGAGAGTTTATGACTGCATTCAAAAAACTTTTAAAATTAGTCTGTTATCCCTTCATGTGATA

ATTAATCTCAAACACGTTTTCAATACCTCAGAGCATTATTTTTATAATAACTATGTTCACAATCTTTTTAGGTT

AACTCGTTTTCTCTTTGTGATTAAGGAGAAACACTTTGATATTCTGATAGAGTGGCCTTCATTTTAGTTGTTT

TTCAAGACCACTTTTCAACTACTCACTTTAGGATAAGTTTTAGGTAAAATATGCATCATTATCCTGAATTATT

TCAGTTAAACATGTTAGTTTGTGGCTTAAGAGAAAACTCAGTCAGATAGTGCTGAAGACAGGACTGTGGA

GACACCTTAGAAGGACGGGTTCTGTTCGGAATCACCGATTCGGCTTCAGCCAGACTGGCCTAGCGGA

GGCTCTGGGAGGCTGCCTGCCAGGCCCGGGCTGGGCTTTGGGTCTCCCCGGACTACCCAGAGCTG

GGATGCGTGGCTTCTGCCACCAGACCAACTGGCTGCTCAGGACCCAGCCCTTGTTAATGGACTTGGA

GGAATGATTCCATGCCAAAGCCTTGCAAGGCTCGCAGTGACTACACACACCGACATGGTAAGAGACA

GGCAGCCGCCGCTGCTGCATTCGCTTCTCTTAAACCTTTGTATTTGATGTCTTATTTGCACTAGAAGGGG

AATTGGTCTTTGCTTGATGAAGAGCAGGAGACTCATTCGTGTGAGTCTTTTGACTGACCATTGTCTGGGT

CACTCCCATTTAACTTTCCCTAAAGCCCATTTGAAGGAGAGGTCACCCGAGCTCTTTCGCAACCTCTGA

ATGCGGATGGCATGAGTCATGATGCTTCAGCCCCACTGGCATCGCCCTTGTCTAAATCATTGACTTAGG

TCATCGCGCCCTTGAAAGTAGCCCATGCCTTCCAAAGCGATTTGCGGTAAATGGCAGAATTTTAAGTGG

CAAATTCAGATAAAATGCATTTCTTGGTTGTTTCCAATGATGACTGTTATCTAGAGGGAATTTAAAGGCAG

GGGTTTATTTCAGACTCAGAAGGGAGGAGATGCTCTGAGAAGGTGGAGGCTTTGAGCATTTCAGTACCC

TCCTCTCGGTGCAGAAGCTATGCTGCCGATTCTAGAGCAAGGGGAGCTCCTCATTTTTATCACAGTACA

GGCTCCTAAATTCTCGGTCTAATTCTGAAGATGTTCTAATAACTTTAAAGCAGCAAAGAAATATTCCACCC

AGGTAGTGGAGGGTGGTAATGATTGGTACTGCTTTGGAACCAAAACCCAGGTGGTGCTAGGGCAGGAC

TGCAGGAAACTGGGGTATCAAGTAGAGGGAGACAAAAGATGAAAGCCGGCCTGTGCAGGAACCTAGC

AATGAGACGGCCTTAGCTGAGACAAGCAGGTCTGGTGGGCTGACCGTTTCCAGCCATGACAACTCCA

TCCAGCTTTCAGAAATGGCCTTGGATGGGCAAAACTGACCTAAGCTGACCTAGACTAAACAAGGCTGA

ACTGCGCTGAGCTGAGCTGGGTTGAGCTGAGC

Table S1. Cas9 and Cas12a gRNA sequences and scores.

All possible gRNA sequences at the NHP *IGH* locus identified for Cas9 and Cas12a. Protospacer adjacent motifs (PAM) are included for each sequence. Specificity scores, efficiency scores, and Lindel scores were included where available. Sequences were included for both *Macaca nemestrina* (pigtail macaque, PM), and *M. mulatta* (rhesus macaque, RM). gRNAs were sorted by specificity score first, and the top 5 for each nuclease with homology to both PM and RM were synthesized. NHP_IGH_Cas12a_5 is referred to as the optimal Cas12a gRNA in text.

Table S1. Cas9 and Cas12a gRNA sequences and scores.							
Sequence (including PAM)	**Nuclease**	**Specificity score (MIT)**	**Efficiency score (Doench '16 for Cas9, DeepCpf1 for Cas12a)**	**Lindel score**	**PM**	**RM**	**Synthesized as**
TTTTTTTAACTGTCTAAGTATTTG	Cas12a	75.5	1.4		TRUE		
TTTGGATTCCTGGGGCCAAGGGGC	Cas12a	64.0	51.4		TRUE		
TTTTTTAACTGTCTAAGTATTTGA	Cas12a	57.7	1.4		TRUE		
TTTTTAACTGTCTAAGTATTTGAA	Cas12a	56.5	9.7		TRUE		
GACATGTTCCAAGGGCACCTGGG	Cas9	56.4	62.4	88.0	TRUE		
TTTAACTGTCTAAGTATTTGAAAT	Cas12a	55.6	9.7		TRUE		
TTTTAACTGTCTAAGTATTTGAAA	Cas12a	55.1	28.4		TRUE		
TTTCAAATACTTAGACAGTTAAAA	Cas12a	54.6	46.5		TRUE		
AGAAAACAAAGGCTCTAGAGTGG	Cas9	52.8	61.4	81.0	TRUE	TRUE	NHP_IGH_Cas9_1
CCAGTCCGCCCAGGTGCCCTTGG	Cas9	51.6	37.6	68.0	TRUE		
TTTCTGGACTACCCGTGCCCCGAC	Cas12a	49.9	29.8		TRUE	TRUE	NHP_IGH_Cas12a_1
TTTGGACGAGATGCCAGAGCAAAC	Cas12a	49.7	73.9		TRUE	TRUE	NHP_IGH_Cas12a_2
TTTAGAATTATGAGGTGCGCTGTG	Cas12a	49.5	30.5		TRUE	TRUE	NHP_IGH_Cas12a_3
TTTTGAAGTATATTAATTTTTTTA	Cas12a	49.2	1.1		TRUE		
TTTAATAAGCACGCCTCTTAAGAT	Cas12a	49.2	33.5		TRUE	TRUE	NHP_IGH_Cas12a_4

Table S1. Cas9 and Cas12a gRNA sequences and scores.

Sequence (including PAM)	Nuclease	Specificity score (MIT)	Efficiency score (Doench '16 for Cas9, DeepCpf1 for Cas12a)	Lindel score	PM	RM	Synthesized as
TTTCTTTAGAATTATGAGGTGCGC	Cas12a	49.1	2.1		TRUE	TRUE	NHP_IGH_Cas12a_5
TTTGCTCTGGCATCTCGTCCAAAT	Cas12a	49.0	51.5		TRUE	TRUE	
TTTGTGGGGTGAGGATGGACATTC	Cas12a	48.9	31.8		TRUE	TRUE	
TTTTGTGGGGTGAGGATGGACATT	Cas12a	48.9	55.0		TRUE		
TTTAACATTTAATAAGCACGCCTC	Cas12a	48.8	14.5		TRUE	TRUE	
TTTGATTAACACCCATGAGTGGTA	Cas12a	48.7	34.4		TRUE	TRUE	
TTTTCCAAAGGCATCGGAAAATCC	Cas12a	48.7	54.7		TRUE	TRUE	
TTTGGAAAATGGGACTTAGGTTGG	Cas12a	48.7	57.1		TRUE	TRUE	
TTTTCTGAGCATTGCAGGCTGGTC	Cas12a	48.6	36.8		TRUE	TRUE	
TTTTCTGCTATTGCCTGTGGGGTT	Cas12a	48.6	27.6		TRUE	TRUE	
TTTTCTTTAGAATTATGAGGTGCG	Cas12a	48.6	2.4		TRUE	TRUE	
TTTCTGAGCATTGCAGGCTGGTCC	Cas12a	48.5	16.7		TRUE	TRUE	
TTTTTGTGGGGTGAGGATGGACAT	Cas12a	48.5	31.8		TRUE		
TTTCATGATTCGCTGTGTGTGCAG	Cas12a	48.5	27.6		TRUE	TRUE	
GGACATGTTCCAAGGGCACCTGG	Cas9	48.4	37.9	76.0	TRUE		
TTTCCGATGCCTTTGGAAAATGGG	Cas12a	48.4	43.2		TRUE	TRUE	
TTTTCTCTGGAGCCACTTCAAACA	Cas12a	48.4	46.0		TRUE	TRUE	
TTTGGCCCTAATTCCAGAGACATA	Cas12a	48.3	78.7		TRUE	TRUE	
CCAGGACGGATGCGTAGCCTTGG	Cas9	48.2	49.4	78.0	TRUE	TRUE	NHP_IGH_Cas9_2
TTTCTCTGGAGCCACTTCAAACAT	Cas12a	48.1	28.5		TRUE	TRUE	
TTTCTCTTGGAAACCAACTTCAGG	Cas12a	48.1	21.0		TRUE	TRUE	
TTTTTCTCTGGAGCCACTTCAAAC	Cas12a	48.1	28.5		TRUE	TRUE	
TTTAAGATGCAGGTTGGCACACAG	Cas12a	48.1	45.0		TRUE	TRUE	
TTTTAACATTTAATAAGCACGCCT	Cas12a	48.0	19.4		TRUE	TRUE	
GGCTACGCATCCGTCCTGGCTGG	Cas9	47.9	46.4	77.0	TRUE	TRUE	NHP_IGH_Cas9_3
TTTTCCGATGCCTTTGGAAAATGG	Cas12a	47.9	48.0		TRUE	TRUE	
TTTCCAAAGGCATCGGAAAATCCA	Cas12a	47.9	39.9		TRUE	TRUE	
CCAAGGCTACGCATCCGTCCTGG	Cas9	47.7	52.2	85.0	TRUE	TRUE	NHP_IGH_Cas9_4

Table S1. Cas9 and Cas12a gRNA sequences and scores.

Sequence (including PAM)	Nuclease	Specificity score (MIT)	Efficiency score (Doench '16 for Cas9, DeepCpf1 for Cas12a)	Lindel score	PM	RM	Synthesized as
TTTCTGCTATTGCCTGTGGGGTTT	Cas12a	47.6	4.7		TRUE	TRUE	
TTTGTTGGCTGGAAAGAGAACTGT	Cas12a	47.2	19.4		TRUE	TRUE	
TTTTAAGTCATAATTGTCTTAACC	Cas12a	47.0	41.0		TRUE	TRUE	
TTTTCTCTTGGAAACCAACTTCAG	Cas12a	46.9	35.3		TRUE	TRUE	
TTTAAGTCATAATTGTCTTAACCA	Cas12a	46.4	11.5		TRUE	TRUE	
TGCCCTTGGAACATGTCCCGAGG	Cas9	46.3	64.0	85.0	TRUE		
TTTGTTTTCTGCTATTGCCTGTGG	Cas12a	46.2	2.5		TRUE	TRUE	
TTTGAAGTGGCTCCAGAGAAAAAT	Cas12a	46.1	60.1		TRUE	TRUE	
TTTCCAGCCAACAAAGAATTTAAG	Cas12a	46.0	60.9		TRUE	TRUE	
TTTTTTAACTGTCCAAGTATTTGA	Cas12a	45.9	1.5			TRUE	
ACCCATGAGTGGTATGTCTCTGG	Cas9	45.7	41.4	81.0	TRUE	TRUE	NHP_IGH_Cas9_5
TTTTTAAGTCATAATTGTCTTAAC	Cas12a	45.4	11.5		TRUE	TRUE	
TTTCCAAGAGAAAAGGATTGTTCA	Cas12a	44.8	57.1		TRUE	TRUE	
GTCCTCGGGACATGTTCCAAGGG	Cas9	44.8	62.1	71.0	TRUE	TRUE	
TCCCCTTGGAACATGTCCCGAGG	Cas9	44.7	65.2	86.0		TRUE	
TTTTTAACTGTCCAAGTATTTGAA	Cas12a	44.2	14.4			TRUE	
ATGTTCCAAGGGCACCTGGGCGG	Cas9	44.1	69.3	82.0	TRUE		
TCCTCGGGACATGTTCCAAGGGG	Cas9	43.8	65.8	78.0		TRUE	
TTTAACTGTCCAAGTATTTGAAAT	Cas12a	43.8	14.4			TRUE	
GGGGCACGGGTAGTCCAGAAAGG	Cas9	43.7	54.8	83.0	TRUE	TRUE	
GTCTCAGGTGCGGTGTCTGTAGG	Cas9	43.5	55.8	78.0	TRUE	TRUE	
CCAAGGGGACCTGGGCGGACTGG	Cas9	43.5	40.5	53.0		TRUE	
CCAAGGGCACCTGGGCGGACTGG	Cas9	43.4	44.8	55.0	TRUE		
CTAAGACCCCTGGTTTGCTCTGG	Cas9	43.2	47.0	87.0	TRUE	TRUE	
GGTCCTCGGGACATGTTCCAAGG	Cas9	42.8	52.2	73.0	TRUE	TRUE	
TCCAGAGACATACCACTCATGGG	Cas9	42.8	59.7	84.0	TRUE	TRUE	
CAAACCAGGGGTCTTAGTGATGG	Cas9	42.8	54.6	76.0	TRUE	TRUE	
TTTCAAATACTTGGACAGTTAAAA	Cas12a	42.5	47.4			TRUE	

Table S1. Cas9 and Cas12a gRNA sequences and scores.

Sequence (including PAM)	Nuclease	Specificity score (MIT)	Efficiency score (Doench '16 for Cas9, DeepCpf1 for Cas12a)	Lindel score	PM	RM	Synthesized as
TGTGGATTTTCCGATGCCTTTGG	Cas9	42.3	33.4	70.0	TRUE	TRUE	
TTTTAACTGTCCAAGTATTTGAAA	Cas12a	42.2	31.2			TRUE	
TCTTGATGAGAGCAGGGTCGGGG	Cas9	42.2	53.5	76.0	TRUE	TRUE	
TTTCACATTTTTAAGTCATAATTG	Cas12a	42.0	7.5		TRUE	TRUE	
CCTTCCTGGCCAGTCCGCCCAGG	Cas9	41.9	45.8	70.0	TRUE	TRUE	
GGGCACGGGTAGTCCAGAAAGGG	Cas9	41.6	49.7	75.0	TRUE	TRUE	
TCTGGCATCTCGTCCAAATGTGG	Cas9	41.6	61.9	82.0	TRUE	TRUE	
TTTGAAATTCTTATCATTTGATTA	Cas12a	41.1	42.0		TRUE	TRUE	
TTTTGAAGTATATTAACTTTTTTA	Cas12a	40.9	3.1			TRUE	
TTCCAGAGACATACCACTCATGG	Cas9	40.9	54.7	80.0	TRUE	TRUE	
GGCACCTGGGCGGACTGGCCAGG	Cas9	40.7	42.3	81.0	TRUE		
GCCTTGGTCTTGATGAGAGCAGG	Cas9	40.7	45.2	84.0	TRUE	TRUE	
ATTTGATTAACACCCATGAGTGG	Cas9	40.6	64.1	85.0	TRUE	TRUE	
TCAGCCATCACTAAGACCCCTGG	Cas9	40.4	56.0	79.0	TRUE	TRUE	
GGACATGTTCCAAGGGGACCTGG	Cas9	40.4	34.6	68.0		TRUE	
ACGAGATGCCAGAGCAAACCAGG	Cas9	40.3	48.1	87.0	TRUE	TRUE	
CTTAGGTTGGATGTGTCTGATGG	Cas9	39.7	54.3	74.0	TRUE	TRUE	
GTTTTCTGAGCATTGCAGGCTGG	Cas9	39.6	48.6	85.0	TRUE	TRUE	
GACGGGCACTGGGGTGCCTTGGG	Cas9	39.6	32.1	66.0	TRUE	TRUE	
TGGGGTTTTCTGAGCATTGCAGG	Cas9	39.5	23.6	84.0	TRUE	TRUE	
CAGAGTGGGTGAATCCAGCCAGG	Cas9	39.5	58.0	79.0	TRUE	TRUE	
CACGGGTAGTCCAGAAAGGGTGG	Cas9	39.4	60.5	78.0	TRUE	TRUE	
GGGACCTGGGCGGACTGGCCAGG	Cas9	39.4	41.8	81.0		TRUE	
GCTGTCCTGACAGAGGCTTAGGG	Cas9	39.4	58.5	80.0	TRUE	TRUE	
CGAGATGCCAGAGCAAACCAGGG	Cas9	39.2	73.3	85.0	TRUE	TRUE	
AGCATTGCAGGCTGGTCCTCGGG	Cas9	39.1	47.7	62.0	TRUE	TRUE	
TTTGAAGTATATTAACTTTTTTAA	Cas12a	39.0	21.8			TRUE	
GGGGCTTGGGGAGCCACATTTGG	Cas9	38.9	25.5	70.0	TRUE	TRUE	

Table S1. Cas9 and Cas12a gRNA sequences and scores.

Sequence (including PAM)	Nuclease	Specificity score (MIT)	Efficiency score (Doench '16 for Cas9, DeepCpf1 for Cas12a)	Lindel score	PM	RM	Synthesized as
TTCTCTTGGAAACCAACTTCAGG	Cas9	38.7	25.9	69.0	TRUE	TRUE	
CCTTGGTCTTGATGAGAGCAGGG	Cas9	38.4	62.4	88.0	TRUE	TRUE	
ACGGGCACTGGGGTGCCTTGGGG	Cas9	38.4	44.8	73.0	TRUE	TRUE	
GGCCAGGAAGGGACGGGCACTGG	Cas9	38.2	35.7	72.0	TRUE	TRUE	
GCCAGGAAGGGACGGGCACTGGG	Cas9	38.0	38.4	62.0	TRUE	TRUE	
CTGGGCGGACTGGCCAGGAAGGG	Cas9	37.7	53.0	74.0	TRUE	TRUE	
TTGGAAAATGGGACTTAGGTTGG	Cas9	37.7	39.7	80.0	TRUE	TRUE	
GTCCTGACAGAGGCTTAGGGAGG	Cas9	37.6	61.7	76.0	TRUE	TRUE	
CCAGGAAGGGACGGGCACTGGGG	Cas9	37.4	53.4	81.0	TRUE	TRUE	
ATGTGGCTCCCCAAGCCCCCAGG	Cas9	37.3	46.7	81.0	TRUE	TRUE	
GAGCATTGCAGGCTGGTCCTCGG	Cas9	37.3	40.1	80.0	TRUE	TRUE	
GGCCTCCCTAAGCCTCTGTCAGG	Cas9	37.2	50.7	83.0	TRUE	TRUE	
ATGAGAGCAGGGTCGGGGCACGG	Cas9	37.2	43.5	77.0	TRUE	TRUE	
TGAGGAATGTGTCTCAGGTGCGG	Cas9	37.1	70.7	69.0	TRUE	TRUE	
GTCTTGATGAGAGCAGGGTCGGG	Cas9	37.1	45.4	85.0	TRUE	TRUE	
TTTGAAGTATATTAATTTTTTTAA	Cas12a	37.0	2.3		TRUE		
ATCTTAAATTCTTTGTTGGCTGG	Cas9	37.0	44.1	81.0	TRUE	TRUE	
AGGGGTCTTAGTGATGGCTGAGG	Cas9	37.0	62.1	80.0	TRUE	TRUE	
AAAGGATTGTTCATCTTAAGAGG	Cas9	37.0	50.0	78.0	TRUE	TRUE	
GTTTTCTGCTATTGCCTGTGGGG	Cas9	36.8	54.5	90.0	TRUE	TRUE	
TAACTGAGCCTGGGGGCTTGGGG	Cas9	36.7	41.7	81.0	TRUE	TRUE	
GTAACTGAGCCTGGGGGCTTGGG	Cas9	36.7	21.3	80.0	TRUE	TRUE	
ACTGGGGTGCCTTGGGGATCTGG	Cas9	36.5	14.0	74.0	TRUE	TRUE	
AGGACAGCAGCCACCCTTTCTGG	Cas9	36.3	19.7	75.0	TRUE	TRUE	
TCTGATGGAGTAACTGAGCCTGG	Cas9	36.3	41.8	74.0	TRUE	TRUE	
GAGATGCCAGAGCAAACCAGGGG	Cas9	36.1	75.0	86.0	TRUE	TRUE	
CTGGGGTGCCTTGGGGATCTGGG	Cas9	36.0	25.5	78.0	TRUE	TRUE	
TGAGAGCAGGGTCGGGGCACGGG	Cas9	35.9	38.8	71.0	TRUE	TRUE	

Table S1. Cas9 and Cas12a gRNA sequences and scores.

Sequence (including PAM)	Nuclease	Specificity score (MIT)	Efficiency score (Doench '16 for Cas9, DeepCpf1 for Cas12a)	Lindel score	PM	RM	Synthesized as
TTGTTTTCTGCTATTGCCTGTGG	Cas9	35.7	45.8	81.0	TRUE	TRUE	
GGACGGGCACTGGGGTGCCTTGG	Cas9	35.6	32.6	76.0	TRUE	TRUE	
AGGCATCGGAAAATCCACAGAGG	Cas9	35.6	76.9	86.0	TRUE	TRUE	
CCAGTCCGCCCAGGTCCCCTTGG	Cas9	35.5	42.9	74.0		TRUE	
CCCCAGTGCCCGTCCCTTCCTGG	Cas9	35.4	31.6	83.0	TRUE	TRUE	
CAATGCTCAGAAAACCCCACAGG	Cas9	35.4	66.2	70.0	TRUE	TRUE	
GGAGCTCAGTGCCCTGAAGTTGG	Cas9	35.3	50.2	73.0	TRUE	TRUE	
AAAGAATTTAAGATGCAGGTTGG	Cas9	35.1	56.0	79.0	TRUE	TRUE	
ACTTCAGGGCACTGAGCTCCTGG	Cas9	34.7	35.4	75.0	TRUE	TRUE	
CCTGGGCGGACTGGCCAGGAAGG	Cas9	34.7	46.5	80.0	TRUE	TRUE	
TCTCTTGGAAACCAACTTCAGGG	Cas9	34.6	45.3	78.0	TRUE	TRUE	
GTCCCATTTTCCAAAGGCATCGG	Cas9	34.6	53.3	55.0	TRUE	TRUE	
GCCTTTGGAAAATGGGACTTAGG	Cas9	34.6	56.5	77.0	TRUE	TRUE	
GGTGGCTGCTGTCCTGACAGAGG	Cas9	34.6	64.4	79.0	TRUE	TRUE	
CGGACTGGCCAGGAAGGGACGGG	Cas9	34.5	49.7	81.0	TRUE	TRUE	
ACCTAAGTCCCATTTTCCAAAGG	Cas9	34.4	60.8	81.0	TRUE	TRUE	
TGTTTTCTGCTATTGCCTGTGGG	Cas9	34.4	44.4	83.0	TRUE	TRUE	
CTGATGGAGTAACTGAGCCTGGG	Cas9	34.3	53.4	70.0	TRUE	TRUE	
GGAAAGAGAACTGTCAGAGTGGG	Cas9	33.7	59.0	77.0	TRUE	TRUE	
AGTAACTGAGCCTGGGGGCTTGG	Cas9	33.6	26.0	79.0	TRUE	TRUE	
GATGGAGTAACTGAGCCTGGGGG	Cas9	33.6	72.6	76.0	TRUE	TRUE	
TTTCCGATGCCTTTGGAAAATGG	Cas9	33.5	30.6	81.0	TRUE	TRUE	
GGTCTTGATGAGAGCAGGGTCGG	Cas9	33.4	52.4	81.0	TRUE	TRUE	
ATGTTCCAAGGGGACCTGGGCGG	Cas9	33.3	67.5	82.0		TRUE	
GATGAACAATCCTTTTCTCTTGG	Cas9	33.3	34.2	85.0	TRUE	TRUE	
CAACAAAGAATTTAAGATGCAGG	Cas9	32.9	44.5	74.0	TRUE	TRUE	
GTGGGTGAATCCAGCCAGGACGG	Cas9	32.8	64.1	80.0	TRUE	TRUE	
TTCAGGGCACTGAGCTCCTGGGG	Cas9	32.7	51.5	70.0	TRUE	TRUE	

Table S1. Cas9 and Cas12a gRNA sequences and scores.

Sequence (including PAM)	Nuclease	Specificity score (MIT)	Efficiency score (Doench '16 for Cas9, DeepCpf1 for Cas12a)	Lindel score	PM	RM	Synthesized as
CTGCATCTTAAATTCTTTGTTGG	Cas9	32.5	29.4	79.0	TRUE	TRUE	
TTCCGATGCCTTTGGAAAATGGG	Cas9	32.5	27.7	87.0	TRUE	TRUE	
GACATGTTCCAAGGGGACCTGGG	Cas9	32.4	59.7	76.0		TRUE	
TGGAAAGAGAACTGTCAGAGTGG	Cas9	31.8	63.0	86.0	TRUE	TRUE	
TGATGGAGTAACTGAGCCTGGGG	Cas9	31.2	59.9	61.0	TRUE	TRUE	
CTTCAGGGCACTGAGCTCCTGGG	Cas9	31.2	44.2	75.0	TRUE	TRUE	
TGCTGTCCTGACAGAGGCTTAGG	Cas9	31.0	34.7	73.0	TRUE	TRUE	
TGATAAGAATTTCAAATACTTGG	Cas9	29.7	41.3	76.0		TRUE	
CTTATTAAATGTTAAAAGACAGG	Cas9	29.6	45.5	81.0	TRUE	TRUE	
GAAGTGGCTCCAGAGAAAAATGG	Cas9	29.0	43.5	77.0	TRUE	TRUE	
ATGGCTGAGGAATGTGTCTCAGG	Cas9	28.8	52.7	78.0	TRUE	TRUE	
TGGGGATCTGGGAGCCTCTGTGG	Cas9	28.8	50.0	82.0	TRUE	TRUE	
GCGGACTGGCCAGGAAGGGACGG	Cas9	28.5	48.4	82.0	TRUE	TRUE	
CAGGCAATAGCAGAAAACAAAGG	Cas9	28.5	66.9	83.0	TRUE	TRUE	
TTGTCTTAACCATTTTTCTCTGG	Cas9	28.4	34.5	78.0	TRUE	TRUE	
AAGTTGGTTTCCAAGAGAAAAGG	Cas9	28.3	41.7	81.0	TRUE	TRUE	
CCCTGCTCTCATCAAGACCAAGG	Cas9	28.0	66.6	64.0	TRUE	TRUE	
CAGAGGCTTAGGGAGGCCCCAGG	Cas9	27.2	48.9	86.0	TRUE	TRUE	
CAGAGGCTCCCAGATCCCCAAGG	Cas9	24.8	62.4	82.0	TRUE	TRUE	
AAGACAGGATATGTTTGAAGTGG	Cas9	24.2	58.1	76.0	TRUE	TRUE	
ACATTTTCTTTAGAATTATGAGG	Cas9	22.3	53.4	71.0	TRUE	TRUE	

Table S2. NHP CD34 purity and yield following enrichment.

Donor information for all *M. nemestrina* animals from which bone marrow aspirates (BMA) were collected for $CD34^+$ enrichment. Viable cell counts were obtained by trypan blue dye exclusion staining pre- and post-enrichment. The percentage of $CD34^+$ cells was measured by flow cytometry, prior to cryopreservation.

Animal	Sex	Age (years)	Weight (kg)	Volume of bone marrow draw (mL)	Pre-enrichment count (viable cells)	Pre-enrichment viability	$CD34^+$ fraction count (viable cells)	$CD34^+$ fraction viability	% $CD34^+$ post-enrichment
M03312	Female	18.8	8.83	70.0	2.06E+09	92.0%	3.59E+07	69.0%	83.9%
Z12214	Male	10.1	13.34	87.5	7.28E+08	95.0%	8.72E+06	80.5%	95.2%
Z09133	Female	13.5	8.94	90.0	1.00E+09	91.5%	8.00E+06	85.5%	97.1%
Z14020	Male	8.9	18.27	100.0	1.05E+09	94.0%	7.28E+06	71.5%	87.9%
Z18090	Male	5.7	11.86	50.0	7.75E+08	89.0%	1.82E+07	79.0%	95.8%
Z14378	Female	8.7	8.56	75.0	5.02E+08	95.5%	7.95E+06	78.5%	79.4%
Z16134	Male	7.6	18.32	120.0	1.55E+09	94.0%	9.95E+06	74.0%	86.0%
Z14122	Male	9.8	11.86	60.0	8.86E+08	94.0%	7.08E+06	75.0%	84.3%
Z15386	Female	8.2	7.8	70.0	2.88E+09	90.0%	3.29E+07	87.5%	91.6%

Table S3. Primers for sequencing and template amplification.

Primer sequences used for amplifying the NHP *IGH* locus and associated transgene templates by PCR. Sanger sequencing of amplicons was performed in both the forward and reverse primer direction. MiSeq primers include Illumina adapter sequences, PacBio primers include M13 adapters. MiSeq library preparation was performed using primer pair 1 for Cas9 gRNA #1, primer pair 2 for Cas9 gRNA #2-4 and Cas12a gRNA #2, 3 and 5, and primer pair 3 for Cas9 gRNA #5 and Cas12a gRNA #1 and 4. Template amplification was performed using primer pair 1 for CMV-GFP^{Cas12a}, and primer pair 2 for VH4-GFP^{Cas12a} and VH4-10-1074^{Cas12a}. 5AmMC6: 5' Amino Modifier C6 (IDT).

Primer use	Name	Sequence
Sanger sequencing	NHP_IGH_F1	CCACTCTAGAGCCTTTGTTTTCTGC
	NHP_IGH_R1	CTTGGAAACCAACTTCAGGGCACTG
	NHP_IGH_F2	CTGGTCCTCGGGACATGTTCCAAGG
	NHP_IGH_R2	GGCCTCCCTAAGCCTCTGTCAGGAC
	NHP_IGH_F3	ATGCCTTTGGAAAATGGGACTTAGG
	NHP_IGH_R3	GACCCTGCTCTCATCAAGACCAAGG
MiSeq library	MiSeq_NHP_IgH_F1	TCGTCGGCAGCGTCAGATGTGTATAAGAGACAGGACATTCTGCCATTGTGATTACT
	MiSeq_NHP_IgH_R1	GTCTCGTGGGCTCGGAGATGTGTATAAGAGACAGAGGCTCAGTTACTCCATCAG
	MiSeq_NHP_IgH_F2	TCGTCGGCAGCGTCAGATGTGTATAAGAGACAGCTGATGGAGTAACTGAGCCT
	MiSeq_NHP_IgH_R2	GTCTCGTGGGCTCGGAGATGTGTATAAGAGACAGCACCCTTTCTGGACTACCC
	MiSeq_NHP_IgH_F3	TCGTCGGCAGCGTCAGATGTGTATAAGAGACAGGCCTTGGTCTTGATGAGAGC
	MiSeq_NHP_IgH_R3	GTCTCGTGGGCTCGGAGATGTGTATAAGAGACAGAGCACTGTGCTAGTATTTCTTAG
PacBio library	M13_IGH_HDR_F10	/5AmMC6/GTAAAACGACGGCCAGTTGGAAAATGGGACTTAGGTTGG

Primer use	Name	Sequence
PacBio library	M13_IGH_HDR_R11	/5AmMC6/CAGGAAACAGCTATGACGTTCTCTAGCAGGCTTAGGTCT
Template amplification	IGH_HDT_F1	GACATTCTGCCATTGTGATTACT
	IGH_HDT_R1	AGCACTGTGCTAGTATTTCTTAG
	IGH_HDT_F2	GATGGACATTCTGCCATTGTGAT
	IGH_HDT_R2	CTGTGCTAGTATTTCTTAGCTAA

Table S4. Primatized MISTRG and MISTRG6 cohort conditions.

MISTRG or MISTRG6 mice born on the same day were grouped into cohorts, each of which was injected with NHP HSPC from different donors and conditions as shown here. Results from cohort #1 were not included in the main text due to low engraftment and lack of GFP expression. All deceased MISTRG mice died prior to week 8 from causes seemingly unrelated to injection (no apparent signs of GVHD). Deceased MISTRG6 mice showed clear signs of GVHD. Mice that died prior to week 8 were not included in our analysis.

Cohort	Strain	NHP Donor(s)	Condition	Template	n (injected)	n (deceased)	$CD34^+$ cell dose
1	MISTRG	Z14020	CMV-GFP	dsDNA	6	1	2.54E+04
2	MISTRG	Z09133; Z14020	VH4-GFP	dsDNA	8	0	1.39E+05
			Control	NA	7	1	1.71E+05
3	MISTRG	Z16134; Z18090	VH4-10-1074	dsDNA	5	0	5.00E+05
4	MISTRG	Z15386; Z16134	VH4-10-1074	AAV6.2	2	0	5.00E+05
			Control	NA	2	1	5.00E+05
5	MISTRG6	Z15386; Z16134	VH4-10-1074	dsDNA	4	1	5.00E+05
			VH4-10-1074	AAV6.2	4	1	5.00E+05
			Control		2	1	5.00E+05

Table S5. Antibodies for flow cytometry on MISTRG samples.

Anti-mouse (m) and anti-primate (p) antibodies used for flow cytometry analysis in MISTRG studies. Cross-reactivity of clones in target species were confirmed on the Non-Human Primate Reagent Resource (NHPRR).

Marker	Fluor	Clone	Dilution	Peripheral Blood Panel	Necropsy Panel
mCD45	V500	30-F11	1/100	TRUE	TRUE
pCD45	V450	D058-1283	1/50	TRUE	TRUE
Anti-Strep Tag II	FITC	5A9F9	1/50	TRUE	TRUE
pCD138	BUV737	MI15	1/50	TRUE	TRUE
pCD20	APC	2H7	1/50	TRUE	
pCD3	BV650	SP34-2	1/50	TRUE	
pCD14	PE-Cy7	61D3	1/50	TRUE	
pCD34	PE	563	1/50		TRUE
pCD19	PE-eFluor610	HIB-19	1/50		TRUE
pCD4	PE-Cy7	SK3	1/50		TRUE
pCD8a	AF 647	RPA-T8	1/50		TRUE

Table S6. Antibodies for flow cytometry on MISTRG6 samples.

Anti-mouse (m) and anti-primate (p) antibodies used for flow cytometry analysis in MISTRG6 studies. Cross-reactivity of clones in target species were confirmed on the Non-Human Primate Reagent Resource (NHPRR). Peripheral blood and necropsy panels were identical.

Marker	Fluor	Clone	Dilution
mCD45	V500	30-F11	1/100
pCD45	V450	D058-1283	1/50
Anti-Strep Tag II	FITC	5A9F9	1/50
pCD138	BUV737	MI15	1/50
pCD31	BV650	WM59	1/50
pIgG	BV786	G18-145	1/50
pCD20	BUV395	2H7	1/50
pCD34	PE	563	1/50
pCD90	PerCP-Cy5.5	5E10	1/50
pCD4	PE-Cy7	SK3	1/50
pCD8a	AF 647	RPA-T8	1/50

Chapter 3: Translation to the Clinic

Summary of Advances in Non-Viral Editing

Targeted gene knock-in represents a promising therapeutic approach for chronic diseases such as HIV. While current ART regimens have significantly improved quality of life, the future of HIV treatment is shifting toward long-acting therapies that reduce the burden of lifelong medication adherence.[161,162] For those whom ARTs are contraindicated or unavailable, a gene therapy strategy capable of engineering humoral immunity could offer a durable alternative to conventional ART or even sustained HIV remission.

Here, we have demonstrated that non-viral, *ex vivo* genetic engineering of NHP HSPCs can result in biologically relevant expression of anti-HIV antibodies *in vivo*. This work establishes the foundation for a technology platform designed to engineer the body to produce therapeutic biologic drugs of choice. By achieving targeted knock-in without the use of viral vectors, we provide a strategy that avoids some of the risks and costs associated with traditional gene delivery methods, such as insertional mutagenesis and high manufacturing costs.

A key advancement of this study is the improved editing efficiency of primary cells using large DNA templates while minimizing manipulation of HSPC state. Efficient gene knock-in remains one of the primary challenges in HSC gene therapy, as these cells exhibit limited HDR activity.[163] By optimizing our approach, we have increased the likelihood of achieving therapeutically relevant expression levels while preserving HSPC engraftment levels in an immunodeficient model.

As outlined in the introduction, we envision this gene-editing approach as one component of a broader therapeutic strategy designed to achieve a functional cure for HIV. This strategy consists of three elements: (1) genetic resistance to HIV infection, (2) induction of protective immunity, and (3) depletion of the replication-competent viral reservoir. Ideally, this would be administered as a one-time treatment akin to vaccination. Until *in vivo* HSC gene therapy capable of delivering large cargos

becomes a reality, people living with HIV receiving the type of gene therapy presented here would need to undergo autologous HSC transplantation.

In this setting, they would receive mobilization to harvest their HSCs, and conditioning to reduce HIV reservoir cell populations and to allow room for uptake of gene-edited cells. It remains unclear whether complete myeloablation will be necessary for engraftment of modified HSCs in the bone marrow. The *IGH* locus would serve as the knock-in site for different bnAb templates, ideally targeting multiple conserved epitopes on the HIV envelope to minimize the risk of viral escape.[164,165] Additionally, the strategy would incorporate a gRNA for *CCR5* knock-out, preferably using the same nuclease to reduce payload size.[166,167] Lastly, additional components could be introduced to engineer cell-mediated immunity, such as producing CAR T cells targeting HIV reservoirs.[168,169]

Path Forward to Global Gene Therapy Access

As currently designed, this type of gene therapy would remain inaccessible to the vast majority of the more than 39 million people living with HIV globally. Most individuals would not meet the eligibility criteria for autologous HSC transplantation, lack the financial resources to afford the procedure, or live in regions where the specialized infrastructure required to perform such a therapy is unavailable.[170] Not to mention, there are ethical and medical risks in immunosuppressing people who are not sick, especially in the context of people living with HIV in low- and middle-income countries. Presently, clinical trials for gene therapy are largely confined to North America, Western Europe, and Eastern Asia, despite the fact that over 77% of all people living with HIV reside outside these regions.[171,172] Groups such as the Global Gene Therapy Initiative are actively working to address these disparities and to expand access to gene therapies.[173]

To develop an HIV gene therapy that can reach global populations, the field must continue advancing toward a single-shot cure.[174] One promising path forward is the direct *in vivo* targeting of

HSCs, which could eliminate the need for transplantation and significantly expand accessibility.[175] By refining *in vivo* gene delivery methods, it may become possible to achieve durable immune modification without the logistical and financial barriers associated with *ex vivo* manipulation and transplantation, while also addressing many of the ethical and medical risks that are involved. A variety of delivery platforms are currently being developed to facilitate targeted gene therapy, including viral vectors, engineered virus-like particles (eVLP), lipid-based nanoparticles (LNP), and metal-based nanoparticles such as gold nanoparticles (AuNP).[158,176,177] Each of these platforms presents distinct advantages and challenges, particularly in their payload capacity and ability to selectively target specific cell types. Additionally, for any of these platforms to reach clinical application, they must meet stringent safety criteria, minimizing *in vivo* toxicity, uptake and editing in off-target cell types, and genomic off-target effects. That said, there is significant movement to increase the use of nanomedicines in clinical practice, with regulatory guidance published by the FDA and the European Medicines Agency (EMA).[178,179]

The choice of payload is equally critical, as demonstrated through our experiments. Whether selecting a DNA template or a genome editing system, each component must be optimized to minimize immune activation and off-target effects. For instance, dsDNA and AAV can activate innate immune pathways, requiring encapsulation to evade detection, as well as various cellular responses in HSCs, which in turn can affect hematopoietic reconstitution.[180] Additionally, CRISPR/Cas systems should be delivered transiently to the cell nucleus to minimize the risk of off-target editing. RNP complexes are often preferred over plasmid or mRNA delivery for this reason.[181] However, this presents a significant challenge for *in vivo* applications, as most existing delivery vectors are unable to efficiently package and transport Cas9-like proteins with high molecular weight.[182]

HSC targeting remains a major obstacle for *in vivo* gene therapy. To achieve selective delivery, vectors must recognize and bind to a cell surface moiety that is both distinct to HSCs and capable

of mediating intracellular uptake. CD34, while a well-known HSC marker, does not efficiently mediate vector internalization, limiting its utility for targeted delivery.[183] In contrast, viral vectors engineered with anti-CD90 antibody fragments have demonstrated specificity for long-term HSC populations.[184] CD117 and CD133 have also emerged as promising targets for *in vivo* HSC gene therapy.[185,186] Similarly, LNPs and AuNPs have been modified to selectively bind HSC surface markers.[158,177] Careful consideration must be given to off-target populations that express these markers, as well as the density of these markers on the target cells. Additionally, the rarity of HSCs and their primary niche in the bone marrow pose further challenges for effective delivery. Whether these targeting strategies will succeed in a therapeutic context remains an open question, but it has been demonstrated that *in vivo* HSC editing is possible.[177] Continued optimization of delivery platforms and targeting mechanisms will be essential for advancing *in vivo* HSC gene therapy toward clinical translation.

Other strategies to enhance delivery could focus on optimizing clinical procedures to make HSC populations more accessible. One potential approach is the use of intraosseous (IO) injections, a technique in which a specialized needle is used to pierce the bone and access the marrow's vasculature. This method could increase vector exposure to HSCs before clearance, thereby improving targeting efficiency.[158,187] Although there is a nearly 1% risk of complications with IO access, it is most commonly used in emergency trauma settings, and not in a controlled setting such as a planned therapy.[188] Alternatively, mobilization regimens commonly used for HSC collection could be leveraged to increase the accessibility of HSCs prior to gene therapy delivery.[189] Agents such as granulocyte-colony-stimulating factor (G-CSF) and plerixafor (AMD3100) are well-characterized drugs that induce HSC mobilization into circulation, allowing for easier targeting through intravenous administration of gene therapy vectors.[190] Since these mobilization regimens are already clinically approved and well tolerated, they could serve as a practical method to enhance

in vivo HSC gene therapy efficiency. However, not all HSCs mobilize, and those that do are exposed to factors in circulation which they would otherwise not see in the bone marrow niche. Research is ongoing to determine the optimal combination of mobilization and delivery strategies to maximize gene transfer while maintaining safety and efficacy.[191]

Much work remains before a single-shot gene therapy cure for HIV can become a reality. One key implication is that if *in vivo* gene therapy can achieve efficient knock-in of transgenes, its applications will extend far beyond HIV treatment. The editing strategies presented in this dissertation have broad potential for treating a variety of diseases. Monoclonal antibodies, small peptides, and recombinant proteins are already widely used in medicine, yet often require repeated injections and are expensive to produce. Durable *in vivo* production of biologic drugs by targeting specific cell populations presents a compelling alternative to traditional manufacturing and delivery methods. Gene therapy could provide long-term expression of therapeutic proteins, reducing both cost and logistical barriers to treatment. If successfully developed, this approach has the potential to serve as a universal platform for biologic drug production, transforming the way chronic and infectious diseases are treated on a global scale.

NHP Model of Autologous HSPC Transplantation

This study serves as a foundation for future NHP research aimed at addressing critical questions that cannot be fully answered using primatized mouse models. A key objective will be to determine whether the *in vivo* production of bnAbs is sufficient to neutralize SHIV and maintain undetectable viral titers. Long-term studies in an immunocompetent model are needed to assess the durability of edited HSPCs and the persistence of the immune response they generate. The gene editing reagents and conditions optimized in this study can be directly applied to autologous HSPC transplantation in NHPs, though certain refinements could further improve their efficacy.

One such refinement involves the generation of multiple bnAb templates to enhance antiviral efficacy. A single bnAb is unlikely to provide complete protection against HIV, making a cocktail of bnAbs targeting different epitopes a more promising approach. To this end, we can edit HSPCs with equal amounts of templates encoding bnAbs such as 3BNC117 (targeting the CD4 binding site), VRC26.25 (targeting the V1/V2 loop), and 10E8v4-5R+100cF (targeting the gp120-gp41 interface) in addition to 10-1074 (targeting the V3 glycan). To ensure optimal expression in macaques, coding sequences will need to be adapted accordingly. We have constructed expression plasmids for 10-1074 and 3BNC117, highlighting the feasibility of this approach. Further optimization of the promoter used in our knock-in template could enhance bnAb expression levels in primary NHP B cells, which is crucial for achieving biologically relevant antibody titers. The more effectively these B cells express bnAbs, the greater the likelihood of achieving durable humoral immunity similar to that achieved by current immunization approaches.

Once the editing conditions have been refined, studies can proceed using one of two NHP models: prevention and treatment. The first model involves an uninfected pig-tailed macaque undergoing HSPC mobilization and collection. $CD34^+$ cells isolated from the animal would be edited *ex vivo* and reinfused following conditioning with busulfan. To evaluate bnAb expression, the animal would subsequently receive SHIV immunization with relevant antigens. The second model consists of a SHIV-C-infected pig-tailed macaque placed on ART until viral suppression is achieved. This animal would then undergo an autologous HSC transplantation following infection as described above. Once stable, analytical treatment interruption (ATI) would be performed to assess whether bnAb expression is sufficient to control viral rebound in the absence of ART. The prevention model would offer a lower level of difficulty than the treatment model from a research perspective, benefiting from a negative immune status at time of harvest and a lower barrier to preventing infection than to controlling viremia control.

A NHP model of autologous transplantation will facilitate the longitudinal evaluation of transgene expression, multilineage engraftment, and SHIV neutralization. ELISA using gp120 from various viral strains will allow for the detection of each bnAb in NHP serum. In the prevention model, adjustments to the immunization regimen could be made to fine-tune expression levels. Flow cytometry and barcode sequencing will be used to monitor the development of hematopoietic cell lineages, including the emergence of bnAb-expressing B cells and plasma cells. The knock-in templates used in this study contain restriction sites flanked by each homology arm, enabling the cloning of a diverse pool of barcoded templates. This strategy will allow for the tracking of clonal expansions in bnAb-expressing B cells. Additionally, bone marrow aspirates will provide insight into whether plasma cells derived from edited HSPCs persist long-term. Viral titers in the treatment model will indicate whether viral rebound occurs after ATI, and sequencing of proviral genomes will help determine whether viral escape mutations arise. In the prevention model, plasma samples could be tested using TZM-bl neutralization assays against a panel of viral strains. If bnAb titers are sufficient, a subsequent SHIV challenge could be performed to assess protective immunity.

The use of a large-animal model also presents an opportunity to thoroughly evaluate the distribution of edited cells *in vivo*, quantify the total number of cells expressing each transgene over time, and isolate bnAb-expressing cells for further characterization. The development of bnAb responses through immunization is an emerging field. Without a preventative or therapeutic vaccine, it remains challenging to study bnAb responses over time with different types and schedules of immunogens.[192] Long-term studies could reveal how clonal diversity evolves over time and whether memory B cell responses are achieved, an important consideration for the durability of gene therapy-based immunity.

It is also possible that targeting HSPCs alone may not be sufficient for robust immune protection. NHP studies could indicate that long-lived plasma cells are the primary contributors to circulating

bnAb titers, as these cells are responsible for the majority of IgG production in human serum. Given that IgG concentrations reach approximately 10 mg/mL at steady-state levels, editing as few as 0.05% of plasma cells could theoretically generate therapeutically relevant bnAb titers. Current efforts by other research groups are focused on *ex vivo* differentiation and editing of plasma cells, which may provide an alternative or complementary approach to HSC gene therapy.

In summary, this work represents an early step toward developing HSC-based gene therapies for HIV. Many challenges remain, but the potential for clinical translation is within reach. As research progresses, it is imperative to consider accessibility on a global scale. An ideal gene therapy platform would not only achieve durable immune protection but also be deliverable in regions most affected by HIV. Development of place-of-care manufacturing and local infrastructure will be critical for bridging the existing divide in gene therapy availability. It remains my personal hope that these advancements will pave the way for equitable access to transformative medicines in the near future.

Appendix 1

Lack of NHP Engraftment in NBSGW Mice

The mouse strains leveraged for the study in Chapter 2, MISTRG and MISTRG6, are excellent models for the hematopoiesis of NHP HSPCs, largely due to the presence of human cytokines and immune receptors with high homology to NHP. These factors support the engraftment of NHP HSPCs and the maturation of lymphocytes while evading innate immune responses. However, at present, MISTRG/MISTRG6 mice are difficult for many researchers to obtain. These xenotransplantation studies also require irradiation, which presents a significant barrier in low-resource research settings. To address these limitations, I pursued the development of a low-cost primatized mouse model that could enable future side-by-side studies on different continents.

The NSG mouse strain (NOD.Cg-*Prkdc*^{scid}*Il2rg*^{tm1Wjl}/SzJ) is a well-established model for human HSPC development.[193] When irradiated, neonatal NSG mice support high levels of engraftment (~70%) following the injection of human cord blood (CB) HSPCs at a dose of 1.0×10^5 CD34$^+$ cells per mouse.[194] A more recently developed strain, NBSGW (NOD,B6.SCID *Il2rγ*$^{-/-}$*Kit*$^{W41/W41}$), was derived from NSG mice and shows enhanced humanization without requiring irradiation.[195] In addition to the mutations found in NSG that inhibit the mouse immune system, NBSGW harbors a mutation in the stem cell factor receptor that provides a competitive advantage to wild-type cells without compromising viability. Humanized NBSGW mice, receiving 1.0×10^5 CB CD34$^+$ cells per mouse as adults, display high levels of engraftment in circulation (~60%) and very high engraftment in the spleen and bone marrow (>90%). Furthermore, gene therapy has been successfully applied to modify CD34$^+$ cells in humanized NBSGW mice using viral vectors.[196]

It has previously been shown that neonatal and adult NSG mice do not support the engraftment of NHP cells following irradiation, whether from rhesus or pig-tailed macaques.[109] Our group sought to determine whether NBSGW might support NHP engraftment. To this end, we performed tail vein

injections of NHP CD34$^+$ cells from adult pig-tailed macaques into adult, non-irradiated NBSGW. One group received 3.1×10^5 non-electroporated CD34$^+$ cells, while another group received 2.3×10^5 electroporated CD34$^+$ cells, edited using a dsDNA GFP template, as described in Chapter 2 (Figure 6A). Throughout the 12-week study, significant engraftment was only observed 8 weeks post-transplantation in mice receiving non-electroporated NHP HSPC (Figure 6B). By the following timepoint, circulating NHP-CD45$^+$ cell populations had dropped from 15.2% to 1.65%. Mice receiving electroporated NHP-CD34$^+$ cells exhibited a 30-fold reduction in engraftment at 8 weeks post-transplantation (15.2% vs 0.45%, $p = 0.0396$, unpaired two-tailed t-test), despite receiving similar doses of live cells. 12 weeks post-transplantation at necropsy, control mice had 18.4% engraftment in the bone marrow and 14.6% in the liver, whereas mice receiving electroporated HSPC had 30.2% engraftment in the bone marrow and 5.0% in the liver.

Next, we investigated whether conditioning NBSGW mice could improve NHP engraftment. Busulfan, a widely available and low-cost conditioning agent, had previously been used to prepare NBSGW mice for transplantation.[196] 48 hours pre-transplantation, 10-week-old mice were administered 10 mg/kg of busulfan and subsequently injected with 2.3×10^5 electroporated CD34$^+$ cells, using a dsDNA bnAb template. To ensure that procedures were properly performed, human CB HSPC were injected into conditioned mice as a positive control, at a dose of 1.0×10^6 human-CD34$^+$ cells per mouse (Figure 7A). Human-CD45$^+$ cells became detectable in circulation starting at 4 weeks post-transplantation and continued to rise, reaching 52.4% at the last timepoint, 8 weeks post-transplantation. In contrast, NHP-CD45$^+$ cells did not surpass 0.18% in circulation (Figure 7B). 12 weeks post-transplantation at necropsy, mice receiving electroporated NHP HSPC had 0.05% engraftment in the bone marrow and 0.99% in the liver. Humanized NBSGW were transferred to another study before necropsy.

Based on these results, we conclude that NBSGW mice are unlikely to be a viable model for NHP HSPC engraftment. Our non-viral editing approach did not yield detectable primate hematopoietic populations in the peripheral blood or bone marrow of these mice. We cannot, however, rule out the possibility that non-electroporated NHP HSPC might engraft in conditioned NBSGW or that engraftment could be achieved at higher cell doses. Following these experiments, an independent study reported that NBSGW mice do not support the engraftment of CB HSPCs from NHP (rhesus macaque).[197]

Figures

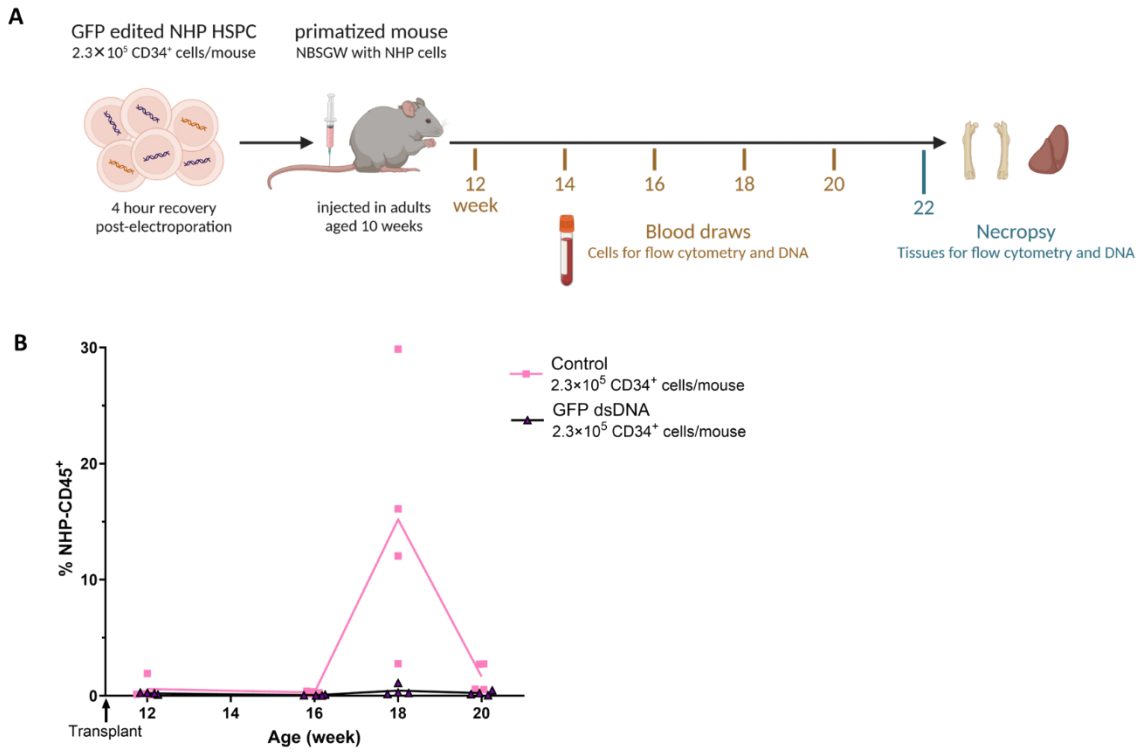

Figure 6. Low and transient NHP engraftment in NBSGW mice without conditioning.

(A) NHP HSPC electroporated with CMV-GFP^{Cas12a} are injected into non-irradiated, adult NBSGW mice. Hematopoietic lineages in the mice are monitored over time and at necropsy. Non-electroporated NHP HSPC are injected as a control. (B) Engraftment levels in peripheral blood over time as measured by flow cytometry on NHP-CD45^{+} cells. n = 8 mice, n = 1 NHP donor (Z18090). Lines represents mean.

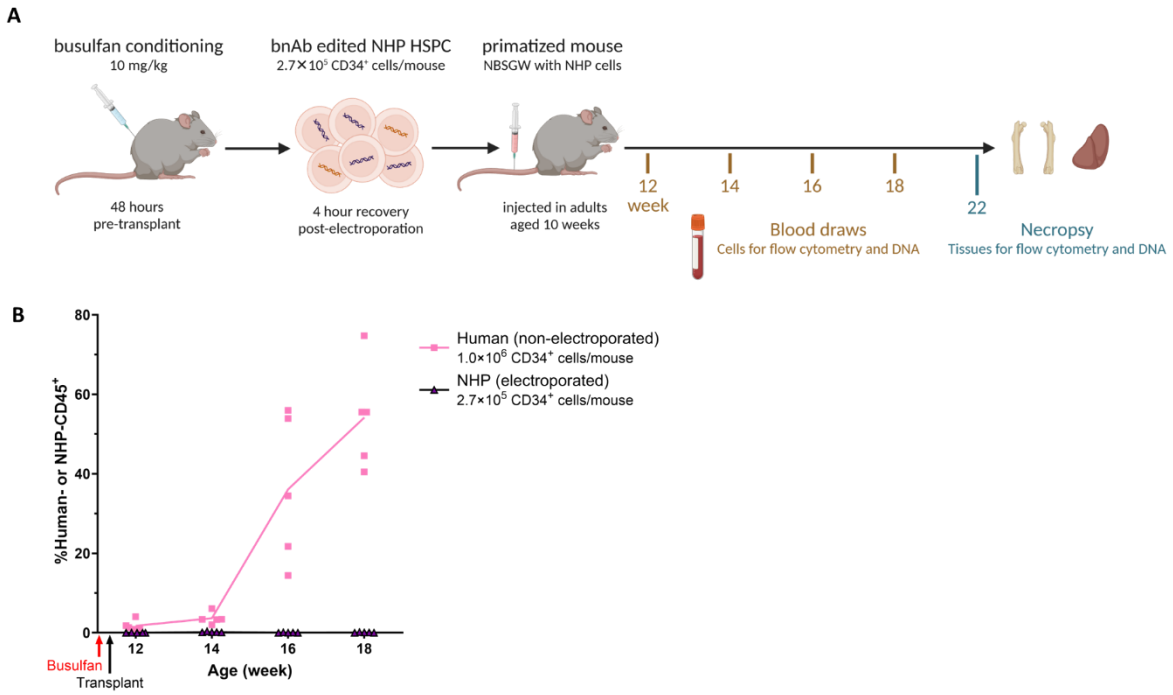

Figure 7. Electroporated NHP HSPC do not engraft in busulfan-conditioned NBSGW mice.

(A) Adult NBSGW mice were administered busulfan via intraperitoneal injection and then injected with NHP HSPC electroporated with VH4-10-1074^{Cas12a}. Hematopoietic lineages in the mice were monitored over time and at necropsy. Non-electroporated, human CB HSPC were injected as a positive control for the model. (B) Engraftment levels in peripheral blood over time as measured by flow cytometry on NHP-CD45$^+$ or human-CD45$^+$ cells. n = 10 mice, n = 1 NHP donor (Z14122), n = 2 human donors (StemCell). Lines represents mean.

Appendix 2

Targeted Gene Knock-In by eePASSIGE

As mentioned in the Discussion of Chapter 2, there is published evidence in NHPs suggesting that HDR-edited HSPCs might have impaired long-term engraftment and reduced clonal diversity.[148] These data suggest that HDR either alters the state of long-term HSCs or that editing does not occur in long-term HSCs. It is of note that this study was performed using a 220 nucleotide (nt) ssODN template, Cas9 RNP, and in the presence of a p53 inhibitor, conditions that vary from the approach presented in this dissertation. In contrast, there are reports that base editing does not impede long-term engraftment and clonal dynamics as much as HDR. Base editors are engineered fusions of catalytically inactive Cas9 with deaminase enzymes. They can programmably modify single nucleotides without genomic DNA cleavage, although final base pair conversion requires DNA replication or repair pathways that are distinct from HDR.[198]

Similarly, prime editing can programmably insert or delete sequences without producing DSBs.[199] Prime editors (PE) are engineered fusions of catalytically inactive Cas9 with reverse transcriptases. These technologies have garnered much interest and are currently being tested in the clinic. More recently, it was shown that large DNA transgenes could be knocked-in with high efficiency using evolved and engineered prime-editing-assisted site-specific integrase gene editing (eePASSIGE).[149] In addition to a PE, eePASSIGE includes a site-specific recombinase capable of recognizing an attachment sequence that catalyzes insertion of a DNA template with cognate attachment sequence. This role is fulfilled by an evolved and engineered variant of the recombinases Bxb1, called eeBxb1. Prime editing introduces Bxb1's 40-50 bp attachment sequence (*attB* or *attP*) into the genome, which then induces site-specific recombination of a DNA template with the opposite attachment sequence (*attP* or *attB*).

We hypothesize that eePASSIGE could achieve the same desired editing outcomes presented here, namely transgene knock-in at the NHP *IGH* locus, without impairing long-term engraftment of HSPCs in a large-animal model. This approach would not rely on HDR or any other endogenous repair machinery while potentially improving knock-in efficiency. In fact, prime editing has already been demonstrated in human HSPC, inserting the *attP* sequence in up to 64% of alleles when PEmax—an enhanced PE—is delivered as mRNA.[200] We sought to demonstrate proof-of-concept that eePASSIGE could achieve knock-in at the NHP *IGH* locus while delivering PE as an RNP complex with its engineered prime editing guide RNA (epegRNA). epegRNA is composed of a spacer sequence, a primer binding site (PBS) adjacent to the reverse transcriptase template (RTT), and structural motifs. eePASSIGE requires two epegRNAs that face each other and are separated by approximately 30-100 bp. The attachment sequence is encoded by the RTT on either epegRNA. Inserting *attP* into the genome results in higher knock-in levels than inserting *attB*.

To this end, we computationally screened all possible epegRNA sequences within a 240-bp window and synthesized the top 5 pairs within 60-80 bp of each other with the highest sum of predicted efficiency and specificity scores (Table 1). Two of these pairs were discarded due to SNP within the spacer (Table 2). We tested *attP* insertion in the NHP B cell line LCL 8664 by electroporation. epegRNAs were synthesized as synthetic RNA by GenScript, with either 9 bp or 12 bp PBS, and delivered at a dose of 200 pmol per 2.0×10^5 live cells. PEmax was synthesized as protein by GenScript and delivered at a dose of 50 pmol per 2.0×10^5 live cells. RNP complexes were allowed to form at room temperature for 5 minutes before being added to cells and electroporated using a Neon system. After recovering for 3 days, LCL 8664 cells were sequenced at the target locus using the MiSeq platform (Figure 8A). Perfect *attP* insertion was achieved in up to 3.50% of alleles (Figure 8B).

In total, six epegRNA pairs were selected for testing knock-in with a large DNA template and eeBxb1 recombinase. To minimize HSPC manipulation down the line, we tested all-in-one electroporation of all eePASSIGE components at once: RNP complex as described above, 2.0 µg of eeBxb1 expression plasmid, and 3.0 µg of donor plasmid (Addgene #182139) per 2.0×10^5 live cells (Figure 9A). As a control condition, we electroporated cells in the same conditions without epegRNA. Cells were recovered for 7 days, during which they were split and passaged once. Reporter expression was higher than control in all edited conditions (Figure 9B). Following selection, cells are sorted to isolate and identify clones with stable knock-in and durable expression.

To our knowledge, this is the first time that eePASSIGE components have been delivered as RNP all-at-once. Further efforts are pursuing bnAb knock-in by eePASSIGE in NHP HSPC using recombinant eeBxb1. If successful, it would be possible to directly compare HDR and eePASSIGE in an NHP model of autologous HSPC transplantation. We hypothesize that long-term engraftment and clonal diversity would be higher in the latter.

Figures and Tables

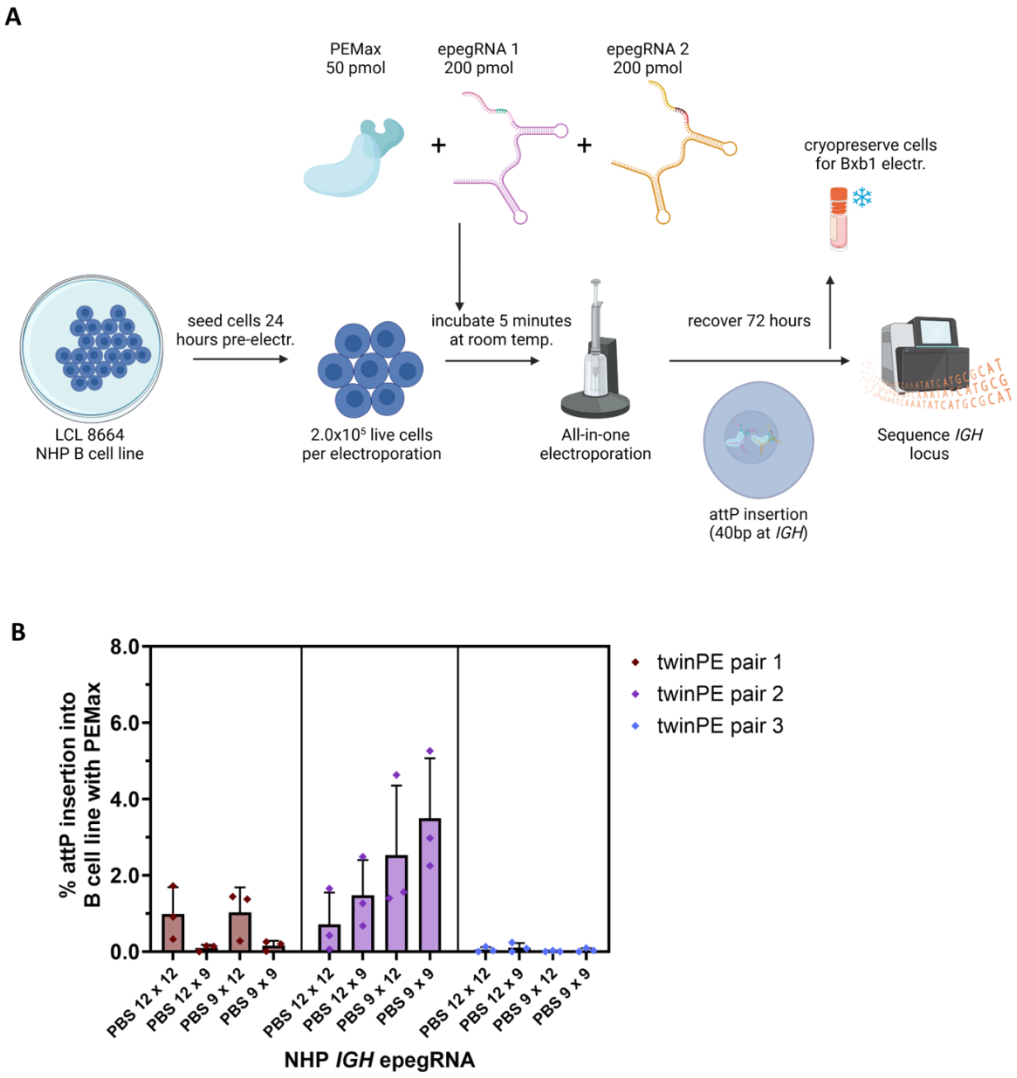

Figure 8. PEmax RNP achieves DNA insertion in NHP cells via electroporation.

(A) LCL 8664 (rhesus macaque) cells were electroporated with PEmax protein and 2 epegRNAs (twinPE pair) using a Neon device. Insertion of the 40 bp *attP* sequence was measured by sequencing of the *IGH* sequence, as described in Chapter 2. (B) Insertion frequency for 3 different twinPE pairs, each with 2 different PBS lengths. n = 3 biological replicates. Error bars represent SD.

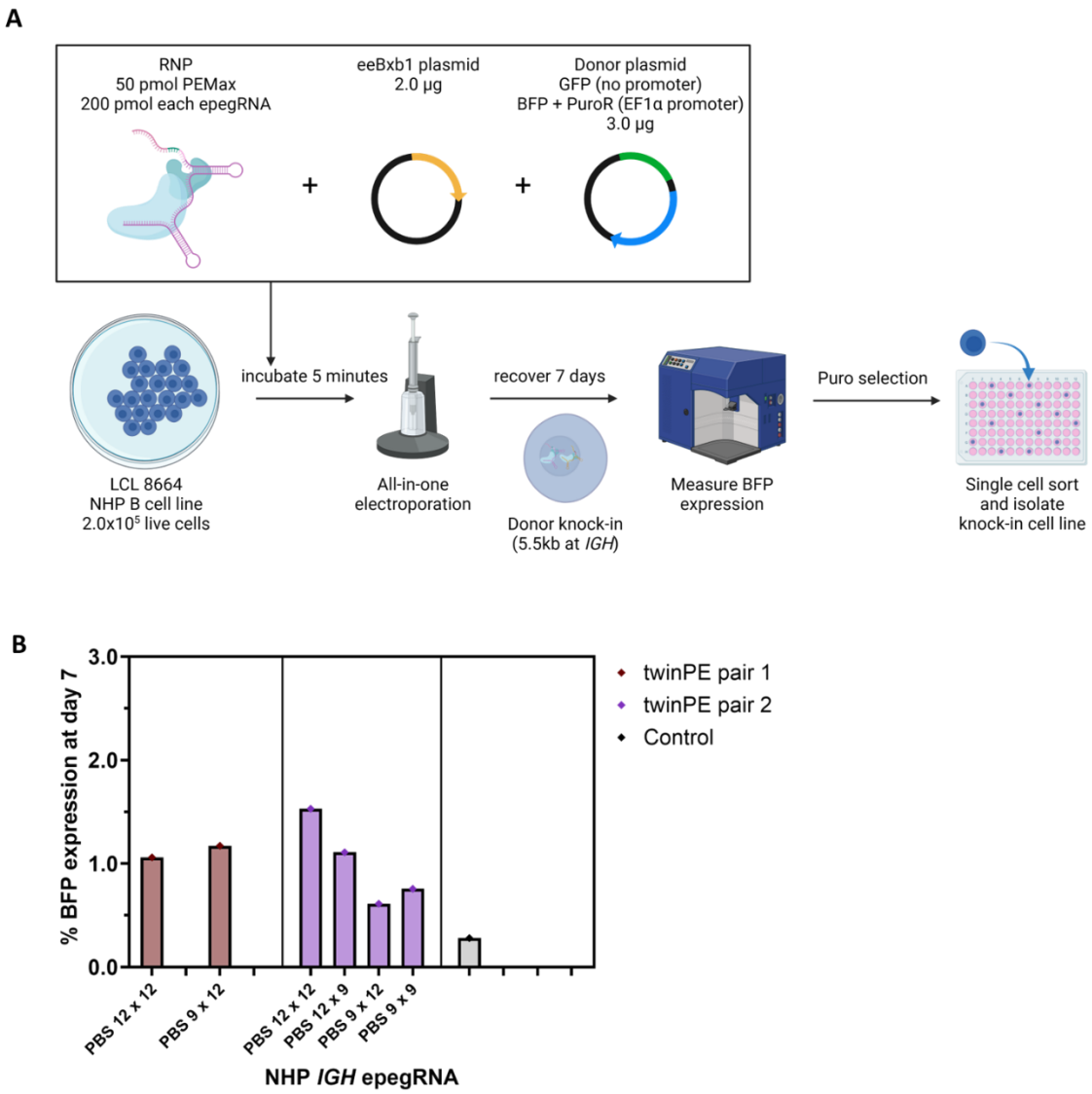

Figure 9. eePASSIGE achieves knock-in of large DNA template at NHP *IGH* locus.

(A) All-in-one electroporation of LCL 8664 using PEmax RNP, eeBxb1 plasmid, and donor plasmid. This DNA template is 5.5 kb long and contains blue fluorescent protein (BFP) and puromycin resistance marker (PuroR), fused by a linker and under the control of a constitutive promoter. Control cells were electroporated in the same conditions without epegRNAs. (B) BFP expression at day 7 as measured by flow cytometry for 6 different twinPE pairs as compared to control.

Table 1. twinPE pairs within NHP *IGH* and predicted scores.

All Cas9 nuclease spacers sequences within a 240 bp window of the PM *IGH* were screened for compatibility as pairs for eePASSIGE, or twinPE pairs. Spacers needed to be located on opposite strands, with proximal PAM sequences, and separated by 60-80 bp from each 5' end. Predicted specificity (MIT) and efficiency (Doench '16) scores were summed between the two spacers. twinPE pairs were sorted by these sums, and the top 5 pairs were synthesized for testing.

Spacer 1 (+) strand	Spacer 2 (-) strand	Predicted specificity + efficiency sum	twinPE pair
GACATGTTCCAAGGGCACCT	CAGAGGCTCCCAGATCCCCA	374	4
ATGTTCCAAGGGCACCTGGG	CAGAGGCTCCCAGATCCCCA	364	5
GTTTTCTGCTATTGCCTGTG	TGCCCTTGGAACATGTCCCG	358	1
CTTAGGTTGGATGTGTCTGA	TCTGGCATCTCGTCCAAATG	355	2
GTTTTCTGCTATTGCCTGTG	CCAGTCCGCCCAGGTGCCCT	348	3
GATGGAGTAACTGAGCCTGG	CTAAGACCCCTGGTTTGCTC	346	
GTCCTCGGGACATGTTCCAA	CAGAGGCTCCCAGATCCCCA	345	
TGTTTTCTGCTATTGCCTGT	TGCCCTTGGAACATGTCCCG	344	
GATGGAGTAACTGAGCCTGG	TCAGCCATCACTAAGACCCC	344	
GGCACCTGGGCGGACTGGCC	AGGCATCGGAAAATCCACAG	344	
TTGTTTTCTGCTATTGCCTG	TGCCCTTGGAACATGTCCCG	341	
GTTTTCTGAGCATTGCAGGC	CCTTCCTGGCCAGTCCGCCC	341	
CTGGGCGGACTGGCCAGGAA	AGGCATCGGAAAATCCACAG	340	
CCTTGGTCTTGATGAGAGCA	GGCCTCCCTAAGCCTCTGTC	340	
CCAGGAAGGGACGGGCACTG	ACCTAAGTCCCATTTTCCAA	338	
GGACATGTTCCAAGGGCACC	CAGAGGCTCCCAGATCCCCA	337	
TCTTGATGAGAGCAGGGTCG	GGCCTCCCTAAGCCTCTGTC	335	
TGGAAAGAGAACTGTCAGAG	CCCTGCTCTCATCAAGACCA	335	
TGTTTTCTGCTATTGCCTGT	CCAGTCCGCCCAGGTGCCCT	334	
TTGGAAAATGGGACTTAGGT	TCTGGCATCTCGTCCAAATG	334	
CTGATGGAGTAACTGAGCCT	CTAAGACCCCTGGTTTGCTC	333	
CCTGGGCGGACTGGCCAGGA	AGGCATCGGAAAATCCACAG	333	
ACGGGCACTGGGGTGCCTTG	ACCTAAGTCCCATTTTCCAA	333	
ATCTTAAATTCTTTGTTGGC	GGCTACGCATCCGTCCTGGC	332	
TGATGGAGTAACTGAGCCTG	CTAAGACCCCTGGTTTGCTC	332	
CTGATGGAGTAACTGAGCCT	TCAGCCATCACTAAGACCCC	331	
TTGTTTTCTGCTATTGCCTG	CCAGTCCGCCCAGGTGCCCT	331	
ATCTTAAATTCTTTGTTGGC	CCAAGGCTACGCATCCGTCC	331	
TGATGGAGTAACTGAGCCTG	TCAGCCATCACTAAGACCCC	330	
GGAAAGAGAACTGTCAGAGT	CCCTGCTCTCATCAAGACCA	329	
TCTGATGGAGTAACTGAGCC	CTAAGACCCCTGGTTTGCTC	329	
CCAGGACGGATGCGTAGCCT	AGGACAGCAGCCACCCTTTC	327	
TCTGATGGAGTAACTGAGCC	TCAGCCATCACTAAGACCCC	327	

Spacer 1 (+) strand	Spacer 2 (-) strand	Predicted specificity + efficiency sum	twinPE pair
TAACTGAGCCTGGGGGCTTG	TCAGCCATCACTAAGACCCC	325	
GCCAGGAAGGGACGGGCACT	ACCTAAGTCCCATTTTCCAA	324	
CCAGGAAGGGACGGGCACTG	GTCCCATTTTCCAAAGGCAT	324	
CGGACTGGCCAGGAAGGGAC	AGGCATCGGAAAATCCACAG	324	
CCAAGGGCACCTGGGCGGAC	CAGAGGCTCCCAGATCCCCA	324	
GGTGGCTGCTGTCCTGACAG	TCTCTTGGAAACCAACTTCA	323	
GGGGCACGGGTAGTCCAGAA	TTCAGGGCACTGAGCTCCTG	322	
GGGCACGGGTAGTCCAGAAA	TTCAGGGCACTGAGCTCCTG	321	
ATGAGAGCAGGGTCGGGGCA	GGCCTCCCTAAGCCTCTGTC	320	
CACGGGTAGTCCAGAAAGGG	TTCAGGGCACTGAGCTCCTG	320	
ACGGGCACTGGGGTGCCTTG	GTCCCATTTTCCAAAGGCAT	319	
GACGGGCACTGGGGTGCCTT	ACCTAAGTCCCATTTTCCAA	319	
GGCCAGGAAGGGACGGGCAC	ACCTAAGTCCCATTTTCCAA	318	
GCGGACTGGCCAGGAAGGGA	AGGCATCGGAAAATCCACAG	318	
GGTCTTGATGAGAGCAGGGT	GGCCTCCCTAAGCCTCTGTC	317	
GGGGCACGGGTAGTCCAGAA	CTTCAGGGCACTGAGCTCCT	317	
GTCCTGACAGAGGCTTAGGG	GATGAACAATCCTTTTCTCT	316	
GGGCACGGGTAGTCCAGAAA	CTTCAGGGCACTGAGCTCCT	316	
CACGGGTAGTCCAGAAAGGG	CTTCAGGGCACTGAGCTCCT	315	
GCCTTGGTCTTGATGAGAGC	GGCCTCCCTAAGCCTCTGTC	314	
GGGGCACGGGTAGTCCAGAA	ACTTCAGGGCACTGAGCTCC	314	
GCCTTTGGAAAATGGGACTT	ATGTGGCTCCCCAAGCCCCC	313	
GGACGGGCACTGGGGTGCCT	ACCTAAGTCCCATTTTCCAA	313	
GTCTTGATGAGAGCAGGGTC	GGCCTCCCTAAGCCTCTGTC	313	
GGTGGCTGCTGTCCTGACAG	GATGAACAATCCTTTTCTCT	312	
GGGCACGGGTAGTCCAGAAA	ACTTCAGGGCACTGAGCTCC	312	
AAAGAATTTAAGATGCAGGT	TGGAAAGAGAACTGTCAGAG	312	
TGGGGTTTTCTGAGCATTGC	CCTTCCTGGCCAGTCCGCCC	312	
CACGGGTAGTCCAGAAAGGG	ACTTCAGGGCACTGAGCTCC	312	
GGTGGCTGCTGTCCTGACAG	TTCTCTTGGAAACCAACTTC	311	
GCCAGGAAGGGACGGGCACT	GTCCCATTTTCCAAAGGCAT	311	
CAACAAAGAATTTAAGATGC	TGGAAAGAGAACTGTCAGAG	309	
CTGCATCTTAAATTCTTTGT	GGCTACGCATCCGTCCTGGC	309	
GCTGTCCTGACAGAGGCTTA	GATGAACAATCCTTTTCTCT	308	
CTGCATCTTAAATTCTTTGT	CCAAGGCTACGCATCCGTCC	308	
TGAGAGCAGGGTCGGGGCAC	GGCCTCCCTAAGCCTCTGTC	308	
GTTTTCTGAGCATTGCAGGC	CCCCAGTGCCCGTCCCTTCC	307	
CGGACTGGCCAGGAAGGGAC	GTCCCATTTTCCAAAGGCAT	305	
GACGGGCACTGGGGTGCCTT	GTCCCATTTTCCAAAGGCAT	305	
GGCCAGGAAGGGACGGGCAC	GTCCCATTTTCCAAAGGCAT	305	
TTGGAAAATGGGACTTAGGT	ATGTGGCTCCCCAAGCCCCC	305	
AGTAACTGAGCCTGGGGGCT	TCAGCCATCACTAAGACCCC	304	
CAACAAAGAATTTAAGATGC	GGAAAGAGAACTGTCAGAGT	304	
AGCATTGCAGGCTGGTCCTC	CCCCAGTGCCCGTCCCTTCC	303	

Spacer 1 (+) strand	Spacer 2 (-) strand	Predicted specificity + efficiency sum	twinPE pair
GTAACTGAGCCTGGGGGCTT	TCAGCCATCACTAAGACCCC	301	
GGACGGGCACTGGGGTGCCT	GTCCCATTTTCCAAAGGCAT	299	
GAGCATTGCAGGCTGGTCCT	CCCCAGTGCCCGTCCCTTCC	294	
TTTCCGATGCCTTTGGAAAA	ATGTGGCTCCCCAAGCCCCC	287	
ACTGGGGTGCCTTGGGGATC	ACCTAAGTCCCATTTTCCAA	284	
GATGAACAATCCTTTTCTCT	CTTATTAAATGTTAAAAGAC	281	
TTCCGATGCCTTTGGAAAAT	ATGTGGCTCCCCAAGCCCCC	281	
CAGAGGCTTAGGGAGGCCCC	GATGAACAATCCTTTTCTCT	280	
TGCTGTCCTGACAGAGGCTT	GATGAACAATCCTTTTCTCT	273	

Table 2. epegRNA sequences synthesized for testing as RNP complex.

epegRNA sequences as synthesized for each twinPE pair. Together, each encodes for the insertion of the *attP* sequence. The 3' end of spacers for twinPE pairs 4 and 5 overlapped with an SNP between PM and RM that precluded targeting in a RM cell line.

twinPE pair	Strand	PBS length	Sequence
1 and 3	(+)	9	mG*U*UUUCUGCUAUUGCCUGUGGUUUUAGAGCUAGAAAUAGCAAGUUAAAA UAAGGCUAGUCCGUUAUCAACUUGAAAAAGUGGCACCGAGUCGGUGCGUACA CCACUGAGACCGCGGUGGUUGACCAGACAAACCUAGGCAAUAGCGCGGUUCU AUCUAGUUACGCGUUAAACCAACUAGAAUUUmU*mU*mU
1 and 3	(+)	12	mG*U*UUUCUGCUAUUGCCUGUGGUUUUAGAGCUAGAAAUAGCAAGUUAAAA UAAGGCUAGUCCGUUAUCAACUUGAAAAAGUGGCACCGAGUCGGUGCGUACA CCACUGAGACCGCGGUGGUUGACCAGACAAACCUAGGCAAUAGCAGCGCGGU UCUAUCUAGUUACGCGUUAAACCAACUAGAAUUUmU*mU*mU
1	(-)	9	mU*G*CCCUUGGAACAUGUCCCGGUUUUAGAGCUAGAAAUAGCAAGUUAAAA UAAGGCUAGUCCGUUAUCAACUUGAAAAAGUGGCACCGAGUCGGUGCGUCAA CCACCGCGGUCUCAGUGGUGUACGGUACAAACCUGACAUGUUCCGCGGUUC UAUCUAGUUACGCGUUAAACCAACUAGAAUUUmU*mU*mU
1	(-)	12	mU*G*CCCUUGGAACAUGUCCCGGUUUUAGAGCUAGAAAUAGCAAGUUAAAA UAAGGCUAGUCCGUUAUCAACUUGAAAAAGUGGCACCGAGUCGGUGCGUCAA CCACCGCGGUCUCAGUGGUGUACGGUACAAACCUGACAUGUUCCAACGCGG UUCUAUCUAGUUACGCGUUAAACCAACUAGAAUUUmU*mU*mU
2	(+)	9	mC*U*UAGGUUGGAUGUGUCUGAGUUUUAGAGCUAGAAAUAGCAAGUUAAAA UAAGGCUAGUCCGUUAUCAACUUGAAAAAGUGGCACCGAGUCGGUGCGUACA CCACUGAGACCGCGGUGGUUGACCAGACAAACCUGACACAUCCCGCGGUUCU AUCUAGUUACGCGUUAAACCAACUAGAAUUUmU*mU*mU
2	(+)	12	mC*U*UAGGUUGGAUGUGUCUGAGUUUUAGAGCUAGAAAUAGCAAGUUAAAA UAAGGCUAGUCCGUUAUCAACUUGAAAAAGUGGCACCGAGUCGGUGCGUACA CCACUGAGACCGCGGUGGUUGACCAGACAAACCUGACACAUCCAACCGCGGU UCUAUCUAGUUACGCGUUAAACCAACUAGAAUUUmU*mU*mU
2	(-)	9	mU*C*UGGCAUCUCGUCCAAAUGGUUUUAGAGCUAGAAAUAGCAAGUUAAAA UAAGGCUAGUCCGUUAUCAACUUGAAAAAGUGGCACCGAGUCGGUGCGUCAA CCACCGCGGUCUCAGUGGUGUACGGUACAAACCUUUGGACGAGCGCGGUUC UAUCUAGUUACGCGUUAAACCAACUAGAAUUUmU*mU*mU
2	(-)	12	mU*C*UGGCAUCUCGUCCAAAUGGUUUUAGAGCUAGAAAUAGCAAGUUAAAA UAAGGCUAGUCCGUUAUCAACUUGAAAAAGUGGCACCGAGUCGGUGCGUCAA CCACCGCGGUCUCAGUGGUGUACGGUACAAACCUUUGGACGAGAUGCGCGG UUCUAUCUAGUUACGCGUUAAACCAACUAGAAUUUmU*mU*mU
3	(-)	9	mC*C*AGUCCGCCCAGGUGCCCUGUUUUAGAGCUAGAAAUAGCAAGUUAAAA UAAGGCUAGUCCGUUAUCAACUUGAAAAAGUGGCACCGAGUCGGUGCGUCAA CCACCGCGGUCUCAGUGGUGUACGGUACAAACCUGCACCUGGGCGCGGUUC UAUCUAGUUACGCGUUAAACCAACUAGAAUUUmU*mU*mU
3	(-)	12	mC*C*AGUCCGCCCAGGUGCCCUGUUUUAGAGCUAGAAAUAGCAAGUUAAAA UAAGGCUAGUCCGUUAUCAACUUGAAAAAGUGGCACCGAGUCGGUGCGUCAA CCACCGCGGUCUCAGUGGUGUACGGUACAAACCUGCACCUGGGCGGCGCGG UUCUAUCUAGUUACGCGUUAAACCAACUAGAAUUUmU*mU*mU

Acknowledgements

This dissertation would not have been possible without the contributions and support of amazing people around me. Any person having been raised in the very same circumstances as mine and exposed to the very same opportunities would have produced this very same body of work. As Robert Sapolsky, neurobiologist and primatologist at Stanford, puts it: "we are nothing more or less than the cumulative biological and environmental luck, over which we had no control, that has brought us to any moment."[201] I owe this achievement to those who have made me the person that I am today.

Jen is without a doubt the most incredible mentor that I could have asked for. Time and time again, she has gone above and beyond to support me as a student. I am forever grateful that she placed her faith in me when I first came to Seattle and granted me the opportunity to pursue a Ph.D. in her lab. It is incredibly inspiring to have a mentor that shares the same visions of pursuing accessible therapies and working on science that is without borders or boundaries. Jen is a uniquely talented scientist who has always provided the right guidance at the right time, while still granting me the independence that I need. Jen and I have both known our ups and downs in research and in life; she has been a beacon of hope in challenging times.

I am deeply indebted to members of the Adair lab and our collaborators for making this project possible. I appreciate Rachel C, Daniel, Karthik, and Patricia, among others, for first welcoming me into the lab and never hesitating to thoughtfully answer my questions. I would like to acknowledge the outstanding amount of work that Molly, Shirley, and Katrina contributed towards this project; their patience knew no end, and so did Mark's, whose coding will never cease to impress me, and Katie's, who made our research possible. I am grateful to Jocelyn and Zach, who trusted me as a first-time mentor. I am grateful to Lois and Rachel K for the opportunity to contribute to their project and to learn from their experience. I am grateful for the days that I worked with Grady and the amount

that I learned about mice thanks to him. I am grateful to Haleema and Onna for making the tail-end of the Adair lab saga even more fun; I hope that the spirit of the lab will continue to live on at UMass.

I am grateful to the Taylor lab, including Matt for sharing his wisdom and contributing crucial pieces to this work, as well as Justin for also being an incredible mentor and for diligently reviewing my work. I am grateful to the Rongvaux lab, including Jon for putting up with my constant requests, as well as Anthony for making research move smoothly. I am grateful to Chris Peterson and his lab for offering me a stimulating environment in which to finish my dissertation. I am also incredibly grateful to all the staff that makes this research at the Fred Hutch and the University of Washington possible. Your work does not go unnoticed.

My committee provided invaluable guidance throughout this journey. I am thankful to Rachel and Jay for reviewing this dissertation. I deeply appreciate Rachel for allowing me into her clinic and for guiding my understanding of the lives and needs of people living with HIV. Her clinical mentorship motivated me to further inform myself about the rich history of advocacy in HIV research. Jay has always been generous in sharing his career advice and impartial opinions. Similarly, I am thankful for the support of Shiu-Lok Hu, whose wisdom has guided my scientific progress at every milestone, and Cynthia Derdeyn, who did not hesitate to jump in before even officially starting at the University of Washington. It has been an honor to bring together such a well accomplished group of researchers. They are without doubt the most brilliant group of people that I have shared a room with.

The friends that I am lucky to have made along this journey have made it all the more enjoyable. I am grateful to those whom I have met along the way, whether it be through graduate school, our shared interest in entrepreneurship, or simply playing soccer in Seattle, mostly in the rain. I am especially grateful to the close friends who have supported me from afar, those who have deeply shaped the person that I am today, and those who have built my confidence up and enabled me to achieve the things that I wanted in life. Namely, I would like to give a special shout-out to my closest

friends Alexis, Haschim, Agustin, Evens, Maxim, Ralph, Dhia, Andrei, Santiago, and Stefan. They are and will always be like brothers to me.

I am consistently reminded of the privilege that I have in being blessed with a large and loving family. How fortunate have I been to never lack support and role models at home. I am grateful to my amazing sisters: Christy for inspiring me to relentlessly push towards new heights and to believe in myself, Roxy for providing me comfort when my heart needs it most and for encouraging me to believe in my values, Alexi for teaching me to overcome adversity and to stand up for myself and others, and Steph for often showing me the way in life and for being my first-ever role model. I am grateful to my one brother, Joe. He likely knows me better than anyone, and I take great comfort in knowing that he will always be there for me, as I will be there for him.

There are no words to describe how grateful I am for my mom, Kathryn, for raising me in such a family and for teaching me how to be grateful. She always encouraged us to pursue what we loved most. As a child, I felt a strong conviction that I was meant to be a scientist and to cure diseases. My mother believed in me. Even when university once seemed an unlikely option, she reminded me to make the most of my situation and to invest in myself. Knowing what I know now about the challenges that she overcome, this message resonates even stronger. She is a true superhero.

Moving away from Montréal and leaving behind those who love me most to pursue a career in science has been a big sacrifice. Nonetheless, it is one that I will never regret because without it, I never would have met my incredible wife, Oyunomin. We found each other at a difficult and dark time in the world. My wife's kindness and loving heart shine right through it all. Her presence is a constant reminder that I need to appreciate life in all its forms. For her, I strive to become not only a more responsible scientist but an overall better person who does what is right. Oyu also keeps me grounded with her cheeky sense of humor. I love her more than anything else in the universe, and I love the person that she makes me.

Lastly, I dedicate this degree to my late grandfather, Chuck. I am grateful for the loving memories, especially those spent at his and my grandmother Lynn's house. Grandpa was an engineer, an immigrant, and a man who gave back to his community. Grandma is a breast cancer survivor and a tenacious woman. They remind me how fortunate that I am to work with brilliant people from around the world who dedicate their careers to saving and improving the lives of others.

References

1 Anderson, W. F. September 14, 1990: the beginning. *Hum Gene Ther* **1**, 371-372 (1990). https://doi.org/10.1089/hum.1990.1.4-371

2 Cring, M. R. & Sheffield, V. C. Gene therapy and gene correction: targets, progress, and challenges for treating human diseases. *Gene Ther*, 1-10 (2020). https://doi.org/10.1038/s41434-020-00197-8

3 Chancellor, D., Barrett, D., Nguyen-Jatkoe, L., Millington, S. & Eckhardt, F. The state of cell and gene therapy in 2023. *Mol Ther* **31**, 3376-3388 (2023). https://doi.org/10.1016/j.ymthe.2023.11.001

4 Palù, G., Bonaguro, R. & Marcello, A. In pursuit of new developments for gene therapy of human diseases. *J Biotechnol* **68**, 1-13 (1999). https://doi.org/10.1016/s0168-1656(98)00134-5

5 Blaese, R. M. *et al*. T lymphocyte-directed gene therapy for ADA- SCID: initial trial results after 4 years. *Science (New York, N.Y.)* **270**, 475-480 (1995). https://doi.org/10.1126/science.270.5235.475

6 McKusick-Nathans Institute of Genetic Medicine. *Online Mendelian Inheritance in Man (OMIM)*, <https://www.omim.org/> (2025).

7 Bulcha, J. T., Wang, Y., Ma, H., Tai, P. W. L. & Gao, G. Viral vector platforms within the gene therapy landscape. *Signal Transduct Target Ther* **6**, 53 (2021). https://doi.org/10.1038/s41392-021-00487-6

8 Arabi, F., Mansouri, V. & Ahmadbeigi, N. Gene therapy clinical trials, where do we go? An overview. *Biomed Pharmacother* **153**, 113324 (2022). https://doi.org/10.1016/j.biopha.2022.113324

9 Cosma, S., Cosma, S., Pennetta, D. & Rimo, G. Overcoming the “valleys of death” in advanced therapies: The role of finance. *Soc Sci Med* **366**, 117639 (2025). https://doi.org/10.1016/j.socscimed.2024.117639

10 Nielsen, L. L. & Maneval, D. C. P53 tumor suppressor gene therapy for cancer. *Cancer Gene Ther* **5**, 52-63 (1998).

11 Rivière, I. & Sadelain, M. Chimeric Antigen Receptors: A Cell and Gene Therapy Perspective. *Mol Ther* **25**, 1117-1124 (2017). https://doi.org/10.1016/j.ymthe.2017.03.034

12 Ylä-Herttuala, S. & Martin, J. F. Cardiovascular gene therapy. *Lancet (London, England)* **355**, 213-222 (2000). https://doi.org/10.1016/S0140-6736(99)04180-X

13 Evans, C. H., Ghivizzani, S. C. & Robbins, P. D. Arthritis gene therapy is becoming a reality. *Nat Rev Rheumatol* **14**, 381-382 (2018). https://doi.org/10.1038/s41584-018-0009-5

14 Meijboom, K. E. *et al*. CRISPR/Cas9-mediated excision of ALS/FTD-causing hexanucleotide repeat expansion in C9ORF72 rescues major disease mechanisms in vivo and in vitro. *Nat Commun* **13**, 6286 (2022). https://doi.org/10.1038/s41467-022-33332-7

15 Elangkovan, N. & Dickson, G. Gene Therapy for Duchenne Muscular Dystrophy. *J Neuromuscul Dis* **8**, S303-S316 (2021). https://doi.org/10.3233/JND-210678

16 Maeder, M. L. & Gersbach, C. A. Genome-editing Technologies for Gene and Cell Therapy. *Mol Ther* **24**, 430-446 (2016). https://doi.org/10.1038/mt.2016.10

17 Jinek, M. *et al*. A programmable dual-RNA-guided DNA endonuclease in adaptive bacterial immunity. *Science (New York, N.Y.)* **337**, 816-821 (2012). https://doi.org/10.1126/science.1225829

18 Gasiunas, G., Barrangou, R., Horvath, P. & Siksnys, V. Cas9-crRNA ribonucleoprotein complex mediates specific DNA cleavage for adaptive immunity in bacteria. *PNAS USA* **109**, E2579-2586 (2012). https://doi.org/10.1073/pnas.1208507109

19 Murray, J. B., Harrison, P. T. & Scholefield, J. Prime editing: therapeutic advances and mechanistic insights. *Gene Ther* (2024). https://doi.org/10.1038/s41434-024-00499-1
20 Leonard, A. & Tisdale, J. F. A new frontier: FDA approvals for gene therapy in sickle cell disease. *Mol Ther* **32**, 264-267 (2024). https://doi.org/10.1016/j.ymthe.2024.01.015
21 Yin, H. *et al*. Therapeutic genome editing by combined viral and non-viral delivery of CRISPR system components in vivo. *Nat Biotechnol* **34**, 328-333 (2016). https://doi.org/10.1038/nbt.3471
22 Pike-Overzet, K., van der Burg, M., Wagemaker, G., van Dongen, J. J. M. & Staal, F. J. T. New insights and unresolved issues regarding insertional mutagenesis in X-linked SCID gene therapy. *Mol Ther* **15**, 1910-1916 (2007). https://doi.org/10.1038/sj.mt.6300297
23 Cornu, T. I., Mussolino, C. & Cathomen, T. Refining strategies to translate genome editing to the clinic. *Nat Med* **23**, 415-423 (2017). https://doi.org/10.1038/nm.4313
24 Kosicki, M., Tomberg, K. & Bradley, A. Repair of double-strand breaks induced by CRISPR-Cas9 leads to large deletions and complex rearrangements. *Nat Biotechnol* **36**, 765-771 (2018). https://doi.org/10.1038/nbt.4192
25 Gillmore, J. D. *et al*. CRISPR-Cas9 In Vivo Gene Editing for Transthyretin Amyloidosis. *N Engl J Med*, NEJMoa2107454 (2021). https://doi.org/10.1056/nejmoa2107454
26 Minikel, E. V. *et al*. Evaluating drug targets through human loss-of-function genetic variation. *Nature* **581**, 459-464 (2020). https://doi.org/10.1038/s41586-020-2267-z
27 Pavani, G. & Amendola, M. Targeted Gene Delivery: Where to Land. *Front Genome Ed* **2**, 609650 (2020). https://doi.org/10.3389/fgeed.2020.609650
28 Papapetrou, E. P. & Schambach, A. Gene Insertion Into Genomic Safe Harbors for Human Gene Therapy. *Mol Ther* **24**, 678-684 (2016). https://doi.org/10.1038/mt.2016.38
29 Banan, M. Recent advances in CRISPR/Cas9-mediated knock-ins in mammalian cells. *J Biotechnol* **308**, 1-9 (2020). https://doi.org/10.1016/j.jbiotec.2019.11.010
30 Azhagiri, M. K. K., Babu, P., Venkatesan, V. & Thangavel, S. Homology-directed gene-editing approaches for hematopoietic stem and progenitor cell gene therapy. *Stem Cell Res Ther* **12**, 500 (2021). https://doi.org/10.1186/s13287-021-02565-6
31 Tabbara, I. A., Zimmerman, K., Morgan, C. & Nahleh, Z. Allogeneic hematopoietic stem cell transplantation: complications and results. *Arch Intern Med* **162**, 1558-1566 (2002). https://doi.org/10.1001/archinte.162.14.1558
32 Jenq, R. R. & van den Brink, M. R. M. Allogeneic haematopoietic stem cell transplantation: individualized stem cell and immune therapy of cancer. *Nat Rev Cancer* **10**, 213-221 (2010). https://doi.org/10.1038/nrc2804
33 Ferrari, G., Thrasher, A. J. & Aiuti, A. Gene therapy using haematopoietic stem and progenitor cells. *Nature Reviews. Genetics* **22**, 216-234 (2021). https://doi.org/10.1038/s41576-020-00298-5
34 Bordignon, C. *et al*. Gene therapy in peripheral blood lymphocytes and bone marrow for ADA-immunodeficient patients. *Science (New York, N.Y.)* **270**, 470-475 (1995). https://doi.org/10.1126/science.270.5235.470
35 Dunbar, C. E. *et al*. Gene therapy comes of age. *Science (New York, N.Y.)* **359**, eaan4672 (2018). https://doi.org/10.1126/science.aan4672
36 Naldini, L. Genetic engineering of hematopoiesis: current stage of clinical translation and future perspectives. *EMBO Mol Med* **11**, e9958 (2019). https://doi.org/10.15252/emmm.201809958
37 Howe, S. J. *et al*. Insertional mutagenesis combined with acquired somatic mutations causes leukemogenesis following gene therapy of SCID-X1 patients. *J Clin Invest* **118**, 3143-3150 (2008). https://doi.org/10.1172/JCI35798

38 Braun, C. J. *et al.* Gene therapy for Wiskott-Aldrich Syndrome—Long-term reconstitution and clinical benefits, but increased risk for leukemogenesis. *Rare Diseases* **2**, e947749 (2014). https://doi.org/10.4161/21675511.2014.947749

39 Hendel, A. *et al.* Chemically modified guide RNAs enhance CRISPR-Cas genome editing in human primary cells. *Nat Biotechnol* **33**, 985-989 (2015). https://doi.org/10.1038/nbt.3290

40 De Ravin, S. S. *et al.* CRISPR-Cas9 gene repair of hematopoietic stem cells from patients with X-linked chronic granulomatous disease. *Sci Transl Med* **9**, eaah3480 (2017). https://doi.org/10.1126/scitranslmed.aah3480

41 Schiroli, G. *et al.* Preclinical modeling highlights the therapeutic potential of hematopoietic stem cell gene editing for correction of SCID-X1. *Sci Transl Med* **9**, eaan0820 (2017). https://doi.org/10.1126/scitranslmed.aan0820

42 Mohrin, M. *et al.* Hematopoietic stem cell quiescence promotes error-prone DNA repair and mutagenesis. *Cell Stem Cell* **7**, 174-185 (2010). https://doi.org/10.1016/j.stem.2010.06.014

43 Kass, E. M. & Jasin, M. Collaboration and competition between DNA double-strand break repair pathways. *FEBS Lett* **584**, 3703-3708 (2010). https://doi.org/10.1016/j.febslet.2010.07.057

44 Bak, R. O., Dever, D. P. & Porteus, M. H. CRISPR/Cas9 genome editing in human hematopoietic stem cells. *Nat Protoc* **13**, 358-376 (2018). https://doi.org/10.1038/nprot.2017.143

45 Daniel-Moreno, A. *et al.* CRISPR/Cas9-modified hematopoietic stem cells-present and future perspectives for stem cell transplantation. *Bone Marrow Transplant* **54**, 1940-1950 (2019). https://doi.org/10.1038/s41409-019-0510-8

46 Signer, R. A. J., Magee, J. A., Salic, A. & Morrison, S. J. Haematopoietic stem cells require a highly regulated protein synthesis rate. *Nature* **509**, 49-54 (2014). https://doi.org/10.1038/nature13035

47 Lee, B.-C., Lozano, R. J. & Dunbar, C. E. Understanding and overcoming adverse consequences of genome editing on hematopoietic stem and progenitor cells. *Mol Ther* **29**, 3205-3218 (2021). https://doi.org/10.1016/j.ymthe.2021.09.001

48 Nasiri, K. *et al.* Spotlight on the impact of viral infections on Hematopoietic Stem Cells (HSCs) with a focus on COVID-19 effects. *Cell Commun Signal* **21**, 103 (2023). https://doi.org/10.1186/s12964-023-01122-3

49 Lattanzi, A. *et al.* Optimization of CRISPR/Cas9 Delivery to Human Hematopoietic Stem and Progenitor Cells for Therapeutic Genomic Rearrangements. *Mol Ther* **27**, 137-150 (2019). https://doi.org/10.1016/j.ymthe.2018.10.008

50 Schiroli, G. *et al.* Precise Gene Editing Preserves Hematopoietic Stem Cell Function following Transient p53-Mediated DNA Damage Response. *Cell Stem Cell* **24**, 551-565.e558 (2019). https://doi.org/10.1016/j.stem.2019.02.019

51 Shin, J. J. *et al.* Controlled Cycling and Quiescence Enables Efficient HDR in Engraftment-Enriched Adult Hematopoietic Stem and Progenitor Cells. *Cell Reports* **32**, 108093 (2020). https:/doi.org/10.1016/j.celrep.2020.108093

52 Locatelli, F. *et al.* Exagamglogene Autotemcel for Transfusion-Dependent β-Thalassemia. *N Engl J Med* **390**, 1663-1676 (2024). https://doi.org/10.1056/NEJMoa2309673

53 Frangoul, H. *et al.* Exagamglogene Autotemcel for Severe Sickle Cell Disease. *N Engl J Med* **390**, 1649-1662 (2024). https://doi.org/10.1056/NEJMoa2309676

54 Kliegman, M. *et al.* A roadmap for affordable genetic medicines. *Nature* **634**, 307-314 (2024). https://doi.org/10.1038/s41586-024-07800-7

55 Stone, D., Wang, X. & Abou-el-Enein, M. Biomanufacturing in gene and cell therapy. *Mol Ther - Methods Clin Dev* **32**, 101261 (2024). https:/doi.org/10.1016/j.omtm.2024.101261

56 Hütter, G. HIV+ patients and HIV eradication - allogeneic transplantation. *Expert Rev Hematol* **9**, 615-616 (2016). https://doi.org/10.1080/17474086.2016.1183478

57 Hütter, G. *et al.* Long-Term Control of HIV by CCR5 Delta32/Delta32 Stem-Cell Transplantation. *N Engl J Med* **360**, 692-698 (2009). https://doi.org/10.1056/NEJMoa0802905

58 Gupta, R. K. *et al.* HIV-1 remission following CCR5Δ32/Δ32 haematopoietic stem-cell transplantation. *Nature* **568**, 244-248 (2019). https://doi.org/10.1038/s41586-019-1027-4

59 Hsu, J. *et al.* HIV-1 remission and possible cure in a woman after haplo-cord blood transplant. *Cell* **186**, 1115-1126.e1118 (2023). https://doi.org/10.1016/j.cell.2023.02.030

60 Jensen, B.-E. O. *et al.* In-depth virological and immunological characterization of HIV-1 cure after CCR5Δ32/Δ32 allogeneic hematopoietic stem cell transplantation. *Nat Med* **29**, 583-587 (2023). https://doi.org/10.1038/s41591-023-02213-x

61 Dickter, J. K. *et al.* HIV-1 Remission after Allogeneic Hematopoietic-Cell Transplantation. *The N Engl J Med* **390**, 669-671 (2024). https://doi.org/10.1056/NEJMc2312556

62 Sáez-Cirión, A. *et al.* Sustained HIV remission after allogeneic hematopoietic stem cell transplantation with wild-type CCR5 donor cells. *Nat Med* **30**, 3544-3554 (2024). https://doi.org/10.1038/s41591-024-03277-z

63 Gaebler, C. *et al.* in *25th International AIDS Conference* (International AIDS Society, Munich, Germany, 2024).

64 Rubinstein, P. G. *et al.* in *Conference on Retroviruses and Opportunistic Infections* (CROI Foundation, San Francisco, CA, 2025).

65 Trøseid, M. *et al.* in *Conference on Retroviruses and Opportunistic Infections* (CROI Foundation, San Francisco, CA, 2025).

66 Henrich, T. J. *et al.* Long-term reduction in peripheral blood HIV type 1 reservoirs following reduced-intensity conditioning allogeneic stem cell transplantation. *J Infect Dis* **207**, 1694-1702 (2013). https://doi.org/10.1093/infdis/jit086

67 Cannon, P. M., Kohn, D. B. & Kiem, H.-P. HIV eradication--from Berlin to Boston. *Nat Biotechnol* **32**, 315-316 (2014). https://doi.org/10.1038/nbt.2868

68 Eberhard, J. M. *et al.* Vulnerability to reservoir reseeding due to high immune activation after allogeneic hematopoietic stem cell transplantation in individuals with HIV-1. *Sci Transl Med* **12**, eaay9355 (2020). https://doi.org/10.1126/scitranslmed.aay9355

69 Liu, R. *et al.* Homozygous defect in HIV-1 coreceptor accounts for resistance of some multiply-exposed individuals to HIV-1 infection. *Cell* **86**, 367-377 (1996). https://doi.org/10.1016/s0092-8674(00)80110-5

70 Libert, F. *et al.* The deltaccr5 mutation conferring protection against HIV-1 in Caucasian populations has a single and recent origin in Northeastern Europe. *Hum Mol Genet* **7**, 399-406 (1998). https://doi.org/10.1093/hmg/7.3.399

71 Xu, L. *et al.* CRISPR/Cas9-Mediated CCR5 Ablation in Human Hematopoietic Stem/Progenitor Cells Confers HIV-1 Resistance In Vivo. *Mol Ther* **25**, 1782-1789 (2017). https://doi.org/10.1016/j.ymthe.2017.04.027

72 Xu, L. *et al.* CRISPR-Edited Stem Cells in a Patient with HIV and Acute Lymphocytic Leukemia. *N Engl J Med* **381**, 1240-1247 (2019). https://doi.org/10.1056/NEJMoa1817426

73 Falcon, A. *et al.* CCR5 deficiency predisposes to fatal outcome in influenza virus infection. *J Gen Virol* **96**, 2074-2078 (2015). https:/doi.org/10.1099/vir.0.000165

74 Glass , W. G. *et al.* CCR5 deficiency increases risk of symptomatic West Nile virus infection. *J Exp Med* **203**, 35-40 (2006). https://doi.org/10.1084/jem.20051970

75 Zolopa, A. R. The evolution of HIV treatment guidelines: current state-of-the-art of ART. *Antiviral Res* **85**, 241-244 (2010). https://doi.org/10.1016/j.antiviral.2009.10.018

76 Freedberg, K. A. *et al*. The cost effectiveness of combination antiretroviral therapy for HIV disease. *N Engl J Med* **344**, 824-831 (2001). https://doi.org/10.1056/NEJM200103153441108
77 Stevens, P. E. & Keigher, S. M. Systemic Barriers to Health Care Access for U.S. Women with HIV: The Role of Cost and insurance. *Int J Health Serv* **39**, 225-243 (2009). https://doi.org/10.2190/HS.39.2.a
78 Johnson, M. *et al*. Barriers to access to care reported by women living with HIV across 27 countries. *AIDS Care* **27**, 1220-1230 (2015). https://doi.org/10.1080/09540121.2015.1046416
79 Margolis, A. M., Heverling, H., Pham, P. A. & Stolbach, A. A review of the toxicity of HIV medications. *J Med Toxicol* **10**, 26-39 (2014). https://doi.org/10.1007/s13181-013-0325-8
80 Langebeek, N. *et al*. Predictors and correlates of adherence to combination antiretroviral therapy (ART) for chronic HIV infection: a meta-analysis. *BMC Med* **12**, 142 (2014). https://doi.org/10.1186/PREACCEPT-1453408941291432
81 Clutter, D. S., Jordan, M. R., Bertagnolio, S. & Shafer, R. W. HIV-1 drug resistance and resistance testing. *Infect Genet Evol* **46**, 292-307 (2016). https://doi.org/10.1016/j.meegid.2016.08.031
82 Davenport, M. P. *et al*. Functional cure of HIV: the scale of the challenge. *Nat Rev Immunol* **19**, 45-54 (2019). https://doi.org/10.1038/s41577-018-0085-4
83 Ogbuagu, O. *et al*. Efficacy and safety of the novel capsid inhibitor lenacapavir to treat multidrug-resistant HIV: week 52 results of a phase 2/3 trial. *Lancet HIV* **10**, e497-e505 (2023). https://doi.org/10.1016/S2352-3018(23)00113-3
84 Byanyima, W., Bekker, L.-G. & Kavanagh, M. M. Long-Acting HIV Medicines and the Pandemic Inequality Cycle - Rethinking Access. *N Engl J Med* **392**, 90-96 (2025). https://doi.org/10.1056/NEJMms2412286
85 Margot, N. A. *et al*. Resistance Analyses in Heavily Treatment-Experienced People with HIV Treated with the Novel HIV Capsid Inhibitor Lenacapavir After 2 years. *J Infect Dis*, jiaf050 (2025). https://doi.org/10.1093/infdis/jiaf050
86 Richman, D. D., Wrin, T., Little, S. J. & Petropoulos, C. J. Rapid evolution of the neutralizing antibody response to HIV type 1 infection. *PNAS USA* **100**, 4144-4149 (2003). https://doi.org/10.1073/pnas.0630530100
87 Overbaugh, J. & Morris, L. The Antibody Response against HIV-1. *Cold Spring Harb perspect med* **2**, a007039 (2012). https://doi.org/10.1101/cshperspect.a007039
88 Korber, B. *et al*. Evolutionary and immunological implications of contemporary HIV-1 variation. *Br med bull* **58**, 19-42 (2001). https://doi.org/10.1093/bmb/58.1.19
89 Burton, D. R. *et al*. HIV vaccine design and the neutralizing antibody problem. *Nat Immunol* **5**, 233-236 (2004). https://doi.org/10.1038/ni0304-233
90 Burton, D. R., Poignard, P., Stanfield, R. L. & Wilson, I. A. Broadly neutralizing antibodies present new prospects to counter highly antigenically diverse viruses. *Science (New York, N.Y.)* **337**, 183-186 (2012). https://doi.org/10.1126/science.1225416
91 Conley, A. J. *et al*. Neutralization of divergent human immunodeficiency virus type 1 variants and primary isolates by IAM-41-2F5, an anti-gp41 human monoclonal antibody. *PNAS USA* **91**, 3348-3352 (1994). https://doi.org/10.1073/pnas.91.8.3348
92 Blankson, J. N. Control of HIV-1 replication in elite suppressors. *Discov Med* **9**, 261-266 (2010).
93 Lambotte, O. *et al*. Heterogeneous neutralizing antibody and antibody-dependent cell cytotoxicity responses in HIV-1 elite controllers. *AIDS* **23**, 897-906 (2009). https://doi.org/10.1097/QAD.0b013e328329f97d

94 Blankson, J. N. Effector mechanisms in HIV-1 infected elite controllers: highly active immune responses? *Antiviral Res* **85**, 295-302 (2010). https://doi.org/10.1016/j.antiviral.2009.08.007
95 Lopez-Galindez, C., Pernas, M., Casado, C., Olivares, I. & Lorenzo-Redondo, R. Elite controllers and lessons learned for HIV-1 cure. *Curr Opin Virol* **38**, 31-36 (2019). https://doi.org/10.1016/j.coviro.2019.05.010
96 Hatziioannou, T. *et al*. A macaque model of HIV-1 infection. *PNAS USA* **106**, 4425-4429 (2009). https://doi.org/10.1073/pnas.0812587106
97 Fouts, T. R. *et al*. Balance of cellular and humoral immunity determines the level of protection by HIV vaccines in rhesus macaque models of HIV infection. *PNAS USA* **112**, E992-999 (2015). https://doi.org/10.1073/pnas.1423669112
98 Del Prete, G. Q. *et al*. Short Communication: Comparative Evaluation of Coformulated Injectable Combination Antiretroviral Therapy Regimens in Simian Immunodeficiency Virus-Infected Rhesus Macaques. *AIDS Res Hum Retroviruses* **32**, 163-168 (2016). https://doi.org/10.1089/AID.2015.0130
99 Gautam, R. *et al*. A single injection of anti-HIV-1 antibodies protects against repeated SHIV challenges. *Nature* **533**, 105-109 (2016). https://doi.org/10.1038/nature17677
100 Haigwood, N. L. & Zolla-Pazner, S. Humoral immunity to HIV, SIV, and SHIV. *AIDS* **12 Suppl A**, S121-132 (1998).
101 Shepherd, B. E. *et al*. Hematopoietic stem-cell behavior in nonhuman primates. *Blood* **110**, 1806-1813 (2007). https://doi.org/10.1182/blood-2007-02-075382
102 Peterson, C. W. *et al*. Long-term multilineage engraftment of autologous genome-edited hematopoietic stem cells in nonhuman primates. *Blood* **127**, 2416-2426 (2016). https://doi.org/10.1182/blood-2015-09-672337
103 Radtke, S. *et al*. A distinct hematopoietic stem cell population for rapid multilineage engraftment in nonhuman primates. *Sci Transl Med* **9** (2017). https://doi.org/10.1126/scitranslmed.aan1145
104 Radtke, S. *et al*. Stochastic fate decisions of HSCs after transplantation: early contribution, symmetric expansion, and pool formation. *Blood* **142**, 33-43 (2023). https://doi.org/10.1182/blood.2022018564
105 Donahue, R. E. & Dunbar, C. E. Update on the use of nonhuman primate models for preclinical testing of gene therapy approaches targeting hematopoietic cells. *Hum Gene Ther* **12**, 607-617 (2001). https://doi.org/10.1089/104303401300057289
106 Berry, N., Mee, E. T., Almond, N. & Rose, N. J. The Impact and Effects of Host Immunogenetics on Infectious Disease Studies Using Non-Human Primates in Biomedical Research. *Microorganisms* **12**, 155 (2024). https://doi.org/10.3390/microorganisms12010155
107 Maynard, L. H., Humbert, O., Peterson, C. W. & Kiem, H.-P. Genome editing in large animal models. *Mol Ther* **29**, 3140-3152 (2021). https://doi.org/10.1016/j.ymthe.2021.09.026
108 Rongvaux, A. *et al*. Development and function of human innate immune cells in a humanized mouse model. *Nat Biotechnol* **32**, 364-372 (2014). https://doi.org/10.1038/nbt.2858
109 Radtke, S., Chan, Y. Y., Sippel, T. R., Kiem, H. P. & Rongvaux, A. MISTRG mice support engraftment and assessment of nonhuman primate hematopoietic stem and progenitor cells. *Exp Hematol* **70**, 31-41.e31 (2019). https://doi.org/10.1016/j.exphem.2018.12.003
110 Castelli, J. M. P. *et al*. *In vivo* production of an anti-HIV antibody from primate hematopoietic cells by non-viral knock-in. *bioRxiv* (2025). https://doi.org/10.1101/2025.05.02.651933
111 Binley, J. M. *et al*. Comprehensive cross-clade neutralization analysis of a panel of anti-human immunodeficiency virus type 1 monoclonal antibodies. *J Virol* **78**, 13232-13252 (2004). https://doi.org/10.1128/jvi.78.23.13232-13252.2004

112 Julg, B. *et al.* Safety and antiviral activity of triple combination broadly neutralizing monoclonal antibody therapy against HIV-1: a phase 1 clinical trial. *Nat Med* **28**, 1288-1296 (2022). https://doi.org/10.1038/s41591-022-01815-1
113 Lewin, S. R. *et al.* Multi-stakeholder consensus on a target product profile for an HIV cure. *Lancet HIV* **8**, e42-e50 (2021). https://doi.org/10.1016/s2352-3018(20)30234-4
114 Lewis, A. D., Chen, R., Montefiori, D. C., Johnson, P. R. & Clark, K. R. Generation of neutralizing activity against human immunodeficiency virus type 1 in serum by antibody gene transfer. *J Virol* **76**, 8769-8775 (2002). https://doi.org/10.1128/jvi.76.17.8769-8775.2002
115 Horwitz, J. A. *et al.* HIV-1 suppression and durable control by combining single broadly neutralizing antibodies and antiretroviral drugs in humanized mice. *PNAS USA* **110**, 16538-16543 (2013). https://doi.org/10.1073/pnas.1315295110
116 Balazs, A. B. *et al.* Antibody-based protection against HIV infection by vectored immunoprophylaxis. *Nature* **481**, 81-84 (2011). https://doi.org/10.1038/nature10660
117 Balazs, A. B. *et al.* Vectored immunoprophylaxis protects humanized mice from mucosal HIV transmission. *Nat Med* **20**, 296-300 (2014). https://doi.org/10.1038/nm.3471
118 Saunders, K. O. *et al.* Sustained delivery of a broadly neutralizing antibody in nonhuman primates confers long-term protection against simian/human immunodeficiency virus infection. *J Virol* **89**, 5895-5903 (2015). https://doi.org/10.1128/jvi.00210-15
119 Saunders, K. O. *et al.* Broadly neutralizing human immunodeficiency virus type 1 antibody gene transfer protects nonhuman primates from mucosal simian-human immunodeficiency virus infection. *J Virol* **89**, 8334-8345 (2015). https://doi.org/10.1128/jvi.00908-15
120 Martinez-Navio, J. M. *et al.* Host anti-antibody responses following adeno-associated virus-mediated delivery of antibodies against HIV and SIV in rhesus monkeys. *Mol Ther* **24**, 76-86 (2016). https://doi.org/10.1038/mt.2015.191
121 Jardine, J. *et al.* Rational HIV immunogen design to target specific germline B cell receptors. *Science* **340**, 711-716 (2013). https://doi.org/10.1126/science.1234150
122 Jardine, J. G. *et al.* HIV-1 VACCINES. Priming a broadly neutralizing antibody response to HIV-1 using a germline-targeting immunogen. *Science* **349**, 156-161 (2015). https://doi.org/10.1126/science.aac5894
123 Jardine, J. G. *et al.* HIV-1 broadly neutralizing antibody precursor B cells revealed by germline-targeting immunogen. *Science* **351**, 1458-1463 (2016). https://doi.org/10.1126/science.aad9195
124 Leggat, D. J. *et al.* Vaccination induces HIV broadly neutralizing antibody precursors in humans. *Science* **378**, eadd6502 (2022). https://doi.org/10.1126/science.add6502
125 Hartweger, H. *et al.* HIV-specific humoral immune responses by CRISPR/Cas9-edited B cells. *J Exp Med* **216**, 1301-1310 (2019). https://doi.org/10.1084/jem.20190287
126 Moffett, H. F. *et al.* B cells engineered to express pathogen-specific antibodies protect against infection. *Sci Immunol* **4**, eaax0644 (2019). https://doi.org/10.1126/sciimmunol.aax0644
127 Voss, J. E. *et al.* Reprogramming the antigen specificity of B cells using genome-editing technologies. *Elife* **8**, e42995 (2019). https://doi.org/10.7554/eLife.42995
128 Nahmad, A. D. *et al.* Engineered B cells expressing an anti-HIV antibody enable memory retention, isotype switching and clonal expansion. *Nat Commun* **11**, 5851 (2020). https://doi.org/10.1038/s41467-020-19649-1
129 Huang, D. *et al.* Vaccine elicitation of HIV broadly neutralizing antibodies from engineered B cells. *Nat Commun* **11**, 5850 (2020). https://doi.org/10.1038/s41467-020-19650-8
130 Ou, T. *et al.* Reprogramming of the heavy-chain CDR3 regions of a human antibody repertoire. *Mol Ther* **30**, 184-197 (2022). https://doi.org/10.1016/j.ymthe.2021.10.027

131 Nahmad, A. D. *et al.* In vivo engineered B cells secrete high titers of broadly neutralizing anti-HIV antibodies in mice. *Nat Biotechnol* **40**, 1241-1249 (2022). https://doi.org/10.1038/s41587-022-01328-9

132 Rogers, G. L. *et al.* Reprogramming human B cells with custom heavy-chain antibodies. *Nat Biomed Eng* **8**, 1700-1714 (2024). https://doi.org/10.1038/s41551-024-01240-4

133 Luo, X. M. *et al.* Engineering human hematopoietic stem/progenitor cells to produce a broadly neutralizing anti-HIV antibody after in vitro maturation to human B lymphocytes. *Blood* **113**, 1422-1431 (2009). https://doi.org/10.1182/blood-2008-09-177139

134 Moffett, H. F. *et al.* B cells engineered to express pathogen-specific antibodies protect against infection. *Sci Immunol* **4** (2019). https://doi.org/10.1126/sciimmunol.aax0644

135 Swarts, D. C. & Jinek, M. Cas9 versus Cas12a/Cpf1: Structure-function comparisons and implications for genome editing. *Wiley Interdiscip Rev RNA* **9**, e1481 (2018). https://doi.org/10.1002/wrna.1481

136 Chen, W. *et al.* Massively parallel profiling and predictive modeling of the outcomes of CRISPR/Cas9-mediated double-strand break repair. *Nucleic Acids Res* **47**, 7989-8003 (2019). https://doi.org/10.1093/nar/gkz487

137 Tatiossian, K. J. *et al.* Rational selection of CRISPR-Cas9 guide RNAs for homology-directed genome editing. *Mol Ther* **29**, 1057-1069 (2021). https://doi.org/10.1016/j.ymthe.2020.10.006

138 Concordet, J. P. & Haeussler, M. CRISPOR: intuitive guide selection for CRISPR/Cas9 genome editing experiments and screens. *Nucleic Acids Res* **46**, W242-w245 (2018). https://doi.org/10.1093/nar/gky354

139 Zetsche, B. *et al.* Cpf1 is a single RNA-guided endonuclease of a class 2 CRISPR-Cas system. *Cell* **163**, 759-771 (2015). https://doi.org/10.1016/j.cell.2015.09.038

140 Schubert, M. S. *et al.* Optimized design parameters for CRISPR Cas9 and Cas12a homology-directed repair. *Sci Rep* **11**, 19482 (2021). https://doi.org/10.1038/s41598-021-98965-y

141 Brochu, H. N. *et al.* Systematic profiling of full-length Ig and TCR repertoire diversity in rhesus macaque through long read transcriptome sequencing. *J Immunol* **204**, 3434-3444 (2020). https://doi.org/10.4049/jimmunol.1901256

142 Yu, H. *et al.* A novel humanized mouse model with significant improvement of class-switched, antigen-specific antibody production. *Blood* **129**, 959-969 (2017). https://doi.org/10.1182/blood-2016-04-709584

143 Romero, Z. *et al.* Editing the sickle cell disease mutation in human hematopoietic stem cells: Comparison of endonucleases and homologous donor templates. *Mol Ther* **27**, 1389-1406 (2019). https://doi.org/10.1016/j.ymthe.2019.05.014

144 Pattabhi, S. *et al.* In vivo outcome of homology-directed repair at the HBB gene in HSC using alternative donor template delivery methods. *Mol Ther Nucleic Acids* **17**, 277-288 (2019). https://doi.org/10.1016/j.omtn.2019.05.025

145 Ferrari, S. *et al.* Choice of template delivery mitigates the genotoxic risk and adverse impact of editing in human hematopoietic stem cells. *Cell Stem Cell* **29**, 1428-1444.e1429 (2022). https://doi.org/10.1016/j.stem.2022.09.001

146 Feist, W. N. *et al.* Multilayered HIV-1 resistance in HSPCs through CCR5 Knockout and B cell secretion of HIV-inhibiting antibodies. *Nat Commun* **16**, 3103 (2025). https://doi.org/10.1038/s41467-025-58371-8

147 Haworth, K. G. *et al.* In vivo murine-matured human CD3(+) cells as a preclinical model for T cell-based immunotherapies. *Mol Ther Methods Clin Dev* **6**, 17-30 (2017). https://doi.org/10.1016/j.omtm.2017.05.004

148 Lee, B. C. *et al*. Impact of CRISPR/HDR editing versus lentiviral transduction on long-term engraftment and clonal dynamics of HSPCs in rhesus macaques. *Cell Stem Cell* **31**, 455-466.e454 (2024). https://doi.org/10.1016/j.stem.2024.02.010
149 Pandey, S. *et al*. Efficient site-specific integration of large genes in mammalian cells via continuously evolved recombinases and prime editing. *Nat Biomed Eng* **9**, 22-39 (2025). https://doi.org/10.1038/s41551-024-01227-1
150 Garber, D. A. *et al*. Durable protection against repeated penile exposures to simian-human immunodeficiency virus by broadly neutralizing antibodies. *Nat Commun* **11**, 3195 (2020). https://doi.org/10.1038/s41467-020-16928-9
151 Das, R. *et al*. Microenvironment-dependent growth of preneoplastic and malignant plasma cells in humanized mice. *Nat Med* **22**, 1351-1357 (2016). https://doi.org/10.1038/nm.4202
152 Hashwah, H. *et al*. The IL-6 signaling complex is a critical driver, negative prognostic factor, and therapeutic target in diffuse large B-cell lymphoma. *EMBO Mol Med* **11**, e10576 (2019). https://doi.org/10.15252/emmm.201910576
153 Radtke, S. *et al*. Preparation and gene modification of nonhuman primate hematopoietic stem and progenitor cells. *J Vis Exp* (2019). https://doi.org/10.3791/58933
154 Adair, J. E. *et al*. Semi-automated closed system manufacturing of lentivirus gene-modified haematopoietic stem cells for gene therapy. *Nat Commun* **7**, 13173 (2016). https://doi.org/10.1038/ncomms13173
155 Katoh, K. & Standley, D. M. MAFFT multiple sequence alignment software version 7: improvements in performance and usability. *Mol Biol Evol* **30**, 772-780 (2013). https://doi.org/10.1093/molbev/mst010
156 Rangan, S. R., Martin, L. N., Bozelka, B. E., Wang, N. & Gormus, B. J. Epstein-Barr virus-related herpesvirus from a rhesus monkey (Macaca mulatta) with malignant lymphoma. *Int J Cancer* **38**, 425-432 (1986). https://doi.org/10.1002/ijc.2910380319
157 Johari, Y. B. *et al*. Engineering of the CMV promoter for controlled expression of recombinant genes in HEK293 cells. *Biotechnol J* **17**, e2200062 (2022). https://doi.org/10.1002/biot.202200062
158 Shahbazi, R. *et al*. Targeted homology-directed repair in blood stem and progenitor cells with CRISPR nanoformulations. *Nat Mater* **18**, 1124-1132 (2019). https://doi.org/10.1038/s41563-019-0385-5
159 Chatterjee, S., Sivanandam, V. & Wong Kk, Jr. Adeno-associated virus and hematopoietic stem cells: The potential of adeno-associated virus hematopoietic stem cells in genetic medicines. *Hum Gene Ther* **31**, 542-552 (2020). https://doi.org/10.1089/hum.2020.049
160 Durocher, Y., Perret, S. & Kamen, A. High-level and high-throughput recombinant protein production by transient transfection of suspension-growing human 293-EBNA1 cells. *Nucleic Acids Res* **30**, E9 (2002). https://doi.org/10.1093/nar/30.2.e9
161 Swindells, S. *et al*. Long-Acting Cabotegravir and Rilpivirine for Maintenance of HIV-1 Suppression. *N Engl J Med* **382**, 1112-1123 (2020). https://doi.org/10.1056/NEJMoa1904398
162 Nachega, J. B. *et al*. Long-acting antiretrovirals and HIV treatment adherence. *Lancet HIV* **10**, e332-e342 (2023). https://doi.org/10.1016/S2352-3018(23)00051-6
163 Chen, X. *et al*. Recent advances in CRISPR-Cas9-based genome insertion technologies. *Mol Ther Nucleic Acids* **35** (2024). https://doi.org/10.1016/j.omtn.2024.102138
164 Julg, B. *et al*. Protection against a mixed SHIV challenge by a broadly neutralizing antibody cocktail. *Sci Transl Med* **9**, eaao4235 (2017). https://doi.org/10.1126/scitranslmed.aao4235
165 Julg, B. *et al*. Safety and antiviral activity of triple combination broadly neutralizing monoclonal antibody therapy against HIV-1: a phase 1 clinical trial. *Nat Med* **28**, 1288-1296 (2022). https://doi.org/10.1038/s41591-022-01815-1

166 Campa, C. C., Weisbach, N. R., Santinha, A. J., Incarnato, D. & Platt, R. J. Multiplexed genome engineering by Cas12a and CRISPR arrays encoded on single transcripts. *Nat Methods* **16**, 887-893 (2019). https://doi.org/10.1038/s41592-019-0508-6
167 Liu, Z. *et al.* Genome editing of CCR5 by AsCpf1 renders CD4+T cells resistance to HIV-1 infection. *Cell & Bioscience* **10**, 85 (2020). https://doi.org/10.1186/s13578-020-00444-w
168 Qi, J., Ding, C., Jiang, X. & Gao, Y. Advances in Developing CAR T-Cell Therapy for HIV Cure. *Front Immunol* **11** (2020). https://doi.org/10.3389/fimmu.2020.00361
169 Carvalho, T. First two patients receive CAR T cell therapy for HIV. *Nat Med* **29**, 1290-1291 (2023). https://doi.org/10.1038/d41591-023-00042-6
170 Gratwohl, A. *et al.* Hematopoietic stem cell transplantation: a global perspective. *JAMA* **303**, 1617-1624 (2010). https://doi.org/10.1001/jama.2010.491
171 Pandey, A. & Galvani, A. P. The global burden of HIV and prospects for control. *The Lancet HIV* **6**, e809-e811 (2019). https://doi.org/10.1016/S2352-3018(19)30230-9
172 Carvalho, M., Sepodes, B. & Martins, A. P. Patient access to gene therapy medicinal products: a comprehensive review. *BMJ Innovations* **7**, 123 (2021). https://doi.org/10.1136/bmjinnov-2020-000425
173 Adair, J. E. *et al.* Towards access for all: 1st Working Group Report for the Global Gene Therapy Initiative (GGTI). *Gene Ther*, 1-6 (2021). https://doi.org/10.1038/s41434-021-00284-4
174 Lewin, S. R. *et al.* Multi-stakeholder consensus on a target product profile for an HIV cure. *The Lancet HIV* **8**, e42-e50 (2021). https://doi.org/10.1016/S2352-3018(20)30234-4
175 Lieber, A. & Kiem, H.-P. Prospects and challenges of *in vivo* hematopoietic stem cell genome editing for hemoglobinopathies. *Mol Ther* **31**, 2823-2825 (2023). https://doi.org/10.1016/j.ymthe.2023.09.006
176 An, M. *et al.* Engineered virus-like particles for transient delivery of prime editor ribonucleoprotein complexes in vivo. *Nat Biotechnol* (2024). https://doi.org/10.1038/s41587-023-02078-y
177 Breda, L. *et al.* In vivo hematopoietic stem cell modification by mRNA delivery. *Science (New York, N.Y.)* **381**, 436-443 (2023). https://doi.org/10.1126/science.ade6967
178 U.S. Food and Drug Administration. Drug Products, Including Biological Products, that Contain Nanomaterials. (2022). https:/www.fda.gov/media/157812/download
179 European Medicines Agency. Scientific Guidelines on Nanomedicines. (2016). https:/www.ema.europa.eu/en/human-regulatory-overview/research-and-development/scientific-guidelines/multidisciplinary-guidelines/multidisciplinary-nanomedicines
180 Dudek, A. M. & Porteus, M. H. Answered and Unanswered Questions in Early-Stage Viral Vector Transduction Biology and Innate Primary Cell Toxicity for Ex-Vivo Gene Editing. *Front Immunol* **12**, 660302 (2021). https://doi.org/10.3389/fimmu.2021.660302
181 Lin, Y., Wagner, E. & Lächelt, U. Non-viral delivery of the CRISPR/Cas system: DNA versus RNA versus RNP. *Biomater Sci* **10**, 1166-1192 (2022). https://doi.org/10.1039/d1bm01658j
182 Chen, Y. & Ping, Y. Development of CRISPR/Cas Delivery Systems for In Vivo Precision Genome Editing. *Acc Chem Res* **56**, 2185-2196 (2023). https://doi.org/10.1021/acs.accounts.3c00279
183 Benedict, C. A. *et al.* Targeting retroviral vectors to CD34-expressing cells: binding to CD34 does not catalyze virus-cell fusion. *Hum Gene Ther* **10**, 545-557 (1999). https://doi.org/10.1089/10430349950018625
184 Berckmueller, K. *et al.* CD90-targeted lentiviral vectors for HSC gene therapy. *Mol Ther* **31**, 2901-2913 (2023). https://doi.org/10.1016/j.ymthe.2023.08.003

185 Barosi, G. Essential thrombocythemia vs. early/prefibrotic myelofibrosis: Why does it matter. *Best Pract Res Clin Haematol* **27**, 129-140 (2014). https://doi.org/10.1016/j.beha.2014.07.004

186 Radtke, S. *et al*. Purification of Human CD34^{+}CD90^{+} HSCs Reduces Target Cell Population and Improves Lentiviral Transduction for Gene Therapy. *Mol Ther Methods Clin Devel* **18**, 679-691 (2020). https://doi.org/10.1016/j.omtm.2020.07.010

187 Ban, Q. *et al*. Intraosseous injection of SMNP vectors enables CRISPR/Cas9-mediated knock-in of HBB gene into hematopoietic stem and progenitor cells. *Nano Today* **47**, 101659 (2022). https://doi.org/10.1016/j.nantod.2022.101659

188 Tyler, J. A., Perkins, Z. & De'Ath, H. D. Intraosseous access in the resuscitation of trauma patients: a literature review. *Eur J Trauma Emerg Surg* **47**, 47-55 (2021). https://doi.org/10.1007/s00068-020-01327-y

189 Nervi, B., Link, D. C. & DiPersio, J. F. Cytokines and hematopoietic stem cell mobilization. *J Cell Biochem* **99**, 690-705 (2006). https://doi.org/10.1002/jcb.21043

190 Chang, H.-H., Liou, Y.-S. & Sun, D.-S. Hematopoietic stem cell mobilization. *Tzu Chi Medical Journal* **34** (2022).

191 Mercadante, C. *et al*. Single Dose of Tgroβ (EN-145)/Plerixafor Safely and Effectively Mobilizes Primitive HSCs in Mouse Models for In Vivo Gene Therapy of Sickle Cell Disease. *Blood* **144**, 4770-4770 (2024). https://doi.org/10.1182/blood-2024-208459

192 Haynes, B. F. *et al*. Strategies for HIV-1 vaccines that induce broadly neutralizing antibodies. *Nat Rev Immunol* **23**, 142-158 (2023). https://doi.org/10.1038/s41577-022-00753-w

193 Ishikawa, F. Modeling normal and malignant human hematopoiesis in vivo through newborn NSG xenotransplantation. *Int J Hematol* **98**, 634-640 (2013). https://doi.org/10.1007/s12185-013-1467-9

194 Ishikawa, F. *et al*. Development of functional human blood and immune systems in NOD/SCID/IL2 receptor γ chain^{null} mice. *Blood* **106**, 1565-1573 (2005). https://doi.org/10.1182/blood-2005-02-0516

195 McIntosh, B. E. *et al*. Nonirradiated NOD,B6.SCID Il2rγ-/- Kit(W41/W41) (NBSGW) mice support multilineage engraftment of human hematopoietic cells. *Stem Cell Reports* **4**, 171-180 (2015). https://doi.org/10.1016/j.stemcr.2014.12.005

196 Joo, J. H. *et al*. Intraosseous delivery of platelet-targeted factor VIII lentiviral vector in humanized NBSGW mice. *Blood Advances* **6**, 5556-5569 (2022). https://doi.org/10.1182/bloodadvances.2022008079

197 Little, C. J. *et al*. Robust engraftment of fetal nonhuman primate CD34-positive cells in immune-deficient mice. *J Leukoc Biol* (2022). https://doi.org/10.1002/JLB.5TA0921-481RR

198 Gaudelli, N. M. *et al*. Programmable base editing of A•T to G•C in genomic DNA without DNA cleavage. *Nature* **551**, 464-471 (2017). https://doi.org/10.1038/nature24644

199 Anzalone, A. V. *et al*. Programmable deletion, replacement, integration and inversion of large DNA sequences with twin prime editing. *Nat Biotechnol* **40**, 731-740 (2022). https://doi.org/10.1038/s41587-021-01133-w

200 Levesque, S., Cosentino, A., Verma, A., Genovese, P. & Bauer, D. E. Enhancing prime editing in hematopoietic stem and progenitor cells by modulating nucleotide metabolism. *Nat Biotechnol* (2024). https://doi.org/10.1038/s41587-024-02266-4

201 Sapolsky, R. M. *Determined: A Science of Life Without Free Will*. (Penguin Press, 2023).